Ph. D.
Thesis

VIBRATION, BUCKLING AND PARAMETRIC RESONANCE CHARACTERISTICS OF DELAMINATED COMPOSITE PLATES SUBJECTED TO IN-PLANE PERIODIC LOADING

VIBRATION, BUCKLING AND PARAMETRIC RESONANCE CHARACTERISTICS OF DELAMINATED COMPOSITE PLATES SUBJECTED TO IN-PLANE PERIODIC LOADING

Jayaram Mohanty

DEPARTMENT OF CIVIL ENGINEERING
NATIONAL INSTITUTE OF TECHNOLOGY
ROURKELA-769008, ODISHA, INDIA
DECEMBER 2012

NIT ROURKELA
2012

Vibration, Buckling and Parametric Resonance Characteristics of Delaminated Composite Plates Subjected to In-plane Periodic Loading

A thesis submitted to

National Institute of Technology, Rourkela

for the award of degree of

Doctor of Philosophy
in

Engineering

by

Jayaram Mohanty

Under the supervision of

Prof Shishir Kumar Sahu
National Institute of Technology
Rourkela-769008

&

Prof Pravat Kumar Parhi
College of Engineering & Technology
BPUT, Bhubaneswar-751003

Department of Civil Engineering
National Institute of Technology
Rourkela-769008, Odisha, India
December 2012

Dedicated

to my

Beloved Parents &

Spouse

Certificate

This is to certify that the thesis entitled "**Vibration, buckling and Parametric Resonance Characteristics of Delaminated Composite Plates Subjected to In-plane Periodic Loading"** being submitted to the National Institute of Technology, Rourkela (India) by Jayaram Mohanty for the award of the degree of **Doctor of Philosophy in Engineering** is a record of bonafide research work carried out by him under my supervision and guidance. Jayaram Mohanty has worked for more than three years and the thesis fulfills the requirements of the regulations of the degree. The results embodied in this thesis have not been submitted to any other university or institute for the award of any degree or diploma.

Date: December, 21, 2012

Prof. Shishir Kumar Sahu
Supervisor
Department of Civil Engineering
National Institute of Technology
Rourkela-769008
Odisha, India

Certificate

This is to certify that the thesis entitled "**Vibration, buckling and Parametric Resonance Characteristics of Delaminated Composite Plates Subjected to In-plane Periodic Loading"** being submitted to the National Institute of Technology, Rourkela (India) by Jayaram Mohanty for the award of the degree of Doctor of Philosophy in Engineering is a record of bonafide research work carried out by him under my supervision and guidance. Jayaram Mohanty has worked for more than three years and the thesis fulfills the requirements of the regulations of the degree. The results embodied in this thesis have not been submitted to any other university or institute for the award of any degree or diploma.

Date: December, 21, 2012

Prof. Pravat Kumar Parhi
Co-Supervisor
Department of Civil Engineering
College of Engineering & Technology
BPUT, Bhubaneswar-751003
Odisha, India

Acknowledgement

I avail this unique opportunity to express my deep sense of gratitude and heartfelt reverence to Dr. Shishir Kumar Sahu, Professor, Department of Civil Engineering, National Institute of Technology, Rourkela for his valuable guidance, keen interest, constructive criticism, painstaking effort and meticulous supervision during the entire course of the investigation and preparation of the manuscript.

I acknowledge gratefully my indebtedness to Dr. Pravat Kumar Parhi, Professor and Head, Department of Civil Engineering, College of Engineering and Technology, Bhubaneswar for his constant support, generous advice, constructive suggestions, and unstinted help in preparation of my manuscript.

I am highly obliged to Prof. S.K. Sarangi, Director, National Institute of Technology, Rourkela for providing me in time support and facilities during my Ph.D. programme.

I express my sincere gratitude to Prof. B.C. Ray, Head of the Metallurgy and Materials Engineering, for extending the laboratory facility of the Department and his suggestions at various stages of the work.

I express my gratefulness to Professor K.C. Patra, Prof. M. Panda and Prof. J.K. Pani, Ex-Head of the Civil Engineering Department and Prof. N. Roy, Head of the Department for their cooperation, valuable suggestions and inspiration during my Ph.D. programme.

It is my fathomless pleasure to express my infinite gratitude to Prof. S. K. Das, Department of Civil Engineering and Prof. K. K. Mohapatra, Department of Electronics & Communication Engineering, National Institute of Technology, Rourkela for their valuable advice, constant inspiration and unstinted help during the course of the investigation.

I express my sincere gratitude to Professor Dr. O.N. Mohanty, Ex Vice-Chancellor, BPUT, Prof. Dr. J.K. Satpathy, Vice-Chancellor, BPUT; Prof. S.C. Mishra, Ex Dean, Prof. S.K. Mishra, Ex Principal and Prof. P.K. Hota, Principal of CET and Prof. P.K. Sahoo, Prof. A.C. Ray, Ex- Head of Civil Engineering Department for their valuable advice and inspiration during the Ph.D. programme.

I would also like to thank Prof. M.R.Barik, Prof. K.C. Biswal , Prof. C.R. Patra, Prof. S.P. Singh, Prof. A.V. Asha and Prof. U.K. Mishra of Civil Engineering Department for their whole hearted suggestions at various stages of the work.

I acknowledge with thanks the help rendered to me by the staff members of the Structural Engineering Laboratory and Metallurgy & Material Engineering department Laboratory and other staffs of Civil Engineering department for their continuous encouragement during the progress of my work.

The author is also thankful to Department of Science & Technology, Govt. of India for their financial support through the R & D Project No. SR/S3/MERC/0009/2008 for the material and facility during the testing of composites.

I record my deep sense of appreciation of adjustment of my son Sipun and daughter Sikha and other family members for their love and affection despite the difficulties they faced during my study due to insufficient attention.

I fall short of words to express my feeling to my wife Dr. Swarnalata Das for her selfless sacrifice, inspiration, unstinting moral support and wholehearted cooperation in achieving my goal.

At the nib but not neap, I bow my head before my late father, late mother, late father-in-law, mother-in-law and Lord Jagannath who had shown a beam of spiritual light in the darkness.

Date: December 21, 2012 **(Jayaram Mohanty)**

ABSTRACT

The composite materials have significant applications over metallic materials in different fields of structural engineering. Structural elements subjected to in-plane periodic forces may lead to parametric or dynamic instability under certain combination of load parameters which caused resonant transverse vibrations. The spectrum of values of parameters causing unstable motion is referred to as the regions of dynamic instability or parametric resonance. Delamination is a very serious concern to composite applications and it arises as a consequence of impact loading, stress concentration near geometrical or material discontinuity or manufacturing defects. The study of dynamic stability itself requires a special investigation of basic problems of vibration and static stability. So the present investigation deals with the study of vibration, static and dynamic stability of delaminated composite plates. However, some studies on static analysis of delaminated composites involving the effects of different parameters on interlaminar shear strength (ILSS) are studied for completeness. The influence of various parameters on the free vibration and static stability (buckling) behavior of delaminated composite plates are investigated both experimentally and numerically. The parametric instability behaviour of delaminated composite plates is examined using finite element method.

For numerical analysis, a finite element model is developed with an eight noded two dimensional quadratic isoparametric element having five degrees of freedom per node based on first order shear deformation theory (FSDT). Element elastic stiffness, geometric stiffness and mass matrices are derived using the principle of Stationery potential energy. A simple two dimensional single delamination model proposed earlier for vibration is extended in the present analysis for the vibration, static and dynamic stability analysis of delaminated composite panels under in-plane uniaxial periodic forces by multiple delamination modelling. A general formulation for parametric resonance characteristics of delaminated composite plates under in-plane periodic loading is presented.

Experimental investigations are conducted for ILSS, vibration and buckling analysis of delaminated composite plates. Materials used for fabrication of laminates are woven roving glass fiber as reinforcement, epoxy as resin, hardener, polyvinyl

alcohol as a releasing agent and Teflon foil for introduction of artificial delamination. Fiber and matrix are used in 50:50 proportion by weight. Material constants are determined from the tensile test as per relevant ASTM standards. The FFT analyzer B&K–3560 is used for modal testing of composite plates. To obtain the buckling result, INSTRON 1195 machine of 100 KN capacities is used.

There is a very good agreement between numerical result and experimental result in case of natural frequency and critical buckling loads of woven fiber composite plates with delaminations. Both the results revealed that the fundamental natural frequency and critical buckling load of delaminated composite plates decrease with the increase in area of delaminations and fiber orientations. The instability studies showed a good agreement with the results available in the open literature. The onset of instability occurs at lower exciting frequency with the increase in delamination size and static load factor. It is also observed that with the increase in number of layers, aspect ratio and degree of orthotropy of delaminated plates, the dynamic instability occurs at higher excitation frequency.

Thus the instability behavior of delaminated plates is influenced by the geometry, material, ply lay-up, ply orientation and size of delamination. This can be used to the advantage of tailoring during the design of delaminated composite structure. This study can be used as a tool for structural health monitoring for identification of delamination, its location and extent of damage in composites and helps in assessment of structural integrity of composite structures.

Key words: **Delamination, dynamic stability, woven fiber, composite plate, in-plane periodic loading, critical buckling load, natural frequency, excitation frequency.**

CONTENTS

LIST OF TABLES

LIST OF FIGURE

Nomenclature

The principal symbols used in this thesis are presented for easy reference. A single symbol is used for different meanings depending on the context and defined in the text as they occur.

English

a, b	Dimensions of plate along X and Y axis respectively
h	Thickness of the plate
[B]	Strain-displacement matrix of the element
[Bp]	Strain-displacement matrix of the element for plane stress
[D]	Flexural rigidity / elasticity matrix of plate
[Dp]	Flexural rigidity / elasticity matrix of plate for plane stress
dx, dy	Element length in x and y direction
dv	Volume of the element
E_{11}, E_{22}	Modulii of elasticity of lamina in both 1 & 2 direction respectively
G_{12}, $G_{13,}$ G_{23}	Shear modulii of rigidity
$\| J \|$	Jacobian
[K]	Global elastic stiffness matrix
[Kp]	Plane stiffness matrix
[Kg]	Global geometric stiffness matrix
k_x, k_y, k_{xy}	Curvatures of the plate
[M]	Global consistent mass matrix
N_x, $N_{y,}$ N_{xy}	In plane internal stress resultants of the plate
M_x, $M_{y,}$ M_{xy}	Moment resultants of the plate
N(t)	In-plane harmonic load
Ns	Static portion of the load N(t)
Nt	Amplitude of dynamic portion of load N(t)
n	Number of layers of laminated panel
Q_x , Q_y	Transverse shearing forces

q	Vector of degrees of freedom
N_{cr}	Critical buckling load
{P}	Global load vector
T	Transformation matrix
u, v, w	Displacements in X, Y & Z direction
u^0, v^0, w^0	Mid-plane displacements in X, Y & Z direction
U_0	Strain energy due to initial in-plane stresses
U_1	Strain energy associated with bending with transverse shear
U_2	work done by the initial in-plane stresses and the nonlinear strain
X, Y, Z	Global coordinate axis system

Greek

σ_{xx}, σ_{yy}, σ_{xy}	Stresses at a point
ε_{xx}, ε_{yy}, γ_{xy}	Bending strains
ν	Poisson's ratio
θ_x , θ_y	Slopes with respect to Y and X axes
ω	Natural frequency
Ω	Excitation frequency
α	Static load factor
β	Dynamic load factor

Mathematical Operators

$[\ ]^{-1}$	Inverse of a matrix
$[\ ]^{T}$	Transpose of a matrix

LIST OF PUBLICATIONS OUT OF THIS WORK

Papers in International Journals

1. **J. Mohanty, S. K. Sahu and P.K. Parhi** (2012): Numerical and experimental study on free vibration of delaminated woven fiber glass/epoxy composite plates, *International Journal of Structural Stability and Dynamics*, Vol.**12**(2), pp.377-394.

2. **J. Mohanty, S. K. Sahu and P.K. Parhi** (2011): Numerical and experimental study on buckling behaviour of multiple delaminated composite plates, *International Journal of Structural Integrity*, (Accepted for publication).

3. **J. Mohanty, S. K. Sahu and P.K. Parhi** (2012): Parametric instability of delaminated composite plates subjected to periodic in-plane loading, *International Journal of vibration and control.* (Recommended for publication)

Papers Presented in International Conferences

1. **S. K. Sahu and J. Mohanty** (2012): Dynamic stability of delaminated composite plates subjected to in-plane harmonic loading, *International Conference on Civil Engineering and Architecture (ICCEA 2012),*August 03-04 at Hong-Kong.

2. **J. Mohanty, S. K. Sahu and P.K. Parhi** (2011): Effect of delamination on interlaminar shear strength of laminated woven fiber glass/epoxy composite plates, *Proceedings of 5th International Conference on Advances in Mechanical Engineering (ICAME-2011),* June 06-08 at Sardar Vallabhbhai National Institute of Technology, Surat, Gujarat, India, pp:114-118.

3. **J. Mohanty, S. K. Sahu , P.K. Parhi and B.C. Ray** (2010): Vibration analysis of delaminated woven fiber glass/epoxy composite plates, *Proceedings of International Conference on Challenges and Application of Mathematics in Science & Technology* (CAMIST) at NIT, Rourkela, India, pp: 168-176.

4. **J. Mohanty, S. K. Sahu, L Sinha and P.K. Parhi** (2010): Buckling behaviour of delaminated woven fiber glass/epoxy composite plates, *Proceedings of 5th International Conference on Theoretical, Applied, Computational & Experimental Mechanics,* Dec. 27-29 at IIT, Kharagpur, India, pp: 320-322.

5. **P. Nayak**, **J. Mohanty and S. K. Sahu** (2009): Vibration analysis of woven fiber glass/epoxy composite plates, *Proceedings of 9th International Conference on Vibration Problems*, January-2009 at IIT, Kharagpur, India, pp: 31

BIO-DATA

1	**Name in Full**	:	**JAYARAM MOHANTY**
2	**Date of Birth**	:	29.04.1967
3	**Permanent Address**	:	Jayaram mohanty, Plot No. 333, Barabari (Jagamara), PO: Khandagiri Bhubaneswar-751030, Odisha
4	**Educational Qualifications**	:	Bachelor Degree in Civil Engineering from Institution of Engineers (India) M.Tech in Civil Engineering with specialisation in Structural Engg. from Biju Pattanaik University of Technology Rourkela, Odisha, India
5	**Research Experience**	:	Five Years
6	**Professional Experience**	:	Twenty four years in Civil Engineering Department, College of Engineering & Technology, BPUT, Bhubaneswar, Odisha
7	**Publications**	:	International Journal 3 Nos National Journal 3 Nos Reports 3 Nos
8	**Book Published**	:	Design of Rigid Pavement using High Volume Fly Ash Concrete **Publisher :** VDM, Verlag Dr. Muller GmbH & Co. KG, Germany

CHAPTER 1
INTRODUCTION

1.1 Introduction

Laminated composite structures are widely used in aircraft, automobile, marine, nuclear, civil engineering structures and other industrial fields because of the higher value of specific strength and stiffness. These can be tailored through the variation of fiber orientation, number of layers, aspect ratio and stacking sequence to obtain an efficient design. The optimum design of laminated structures demands an effective analytical procedure. But the presence of varying coupling stiffness and anisotropy complicates the problems of dynamic stability of laminated plates in addition to inherent problems due to the diverse loading and boundary conditions encountered for obtaining a suitable theoretical solution.

As the demand for composite materials increases, the defect problems in composite structures become an important concern. Among them, delamination is one of the common defects, which is induced due to improper handling in the process of manufacturing, low velocity impact or excessive interlaminar stresses at the free edges under loading. Delaminations may not be visible or barely visible on the surface, since they are embedded inside the body of the composite structures. However, the presence of delamination in composite laminates may adversely affect the design parameters like interlaminar shear strength, vibration characteristics, buckling strength of the structure, dynamic stability characteristics, safety and durability of structures etc. Therefore, a comprehensive functional understanding in respect of vibration, static and dynamic stability characteristics of delaminated plates is very much essential.

1.2 Importance of the structural stability studies of delaminated composite plates

The structural elements like beams, plates and shells are sometimes subjected to periodic in-plane loading and become dynamically unstable with increase in transverse vibration without bounds for certain combination of load amplitude and disturbing frequency. The above phenomenon is called dynamic instability or parametric resonance. Again the presence of delamination may increase the complications associated with the parametric resonance of the laminated plates. The dynamic instability of delaminated plates may occur below the critical buckling load of the structure under compressive loading over a range or ranges of excitation frequencies. Several methods used for combating parametric resonance such as damping and vibration isolation may be insufficient and sometimes produce dangerous effects. The parametric instability may arise not merely at a single expectation frequency but even for small excitation amplitudes and combinations of frequencies.

Presence of one or more delaminations in a composite laminate structure may lead to a premature collapse of the structure due to buckling at a lower level of compressive loading. So the effect of delamination on stability of composite structures needs attention and thus constitutes a problem of current interest. The location of dynamic instability region (DIR) is quite essential for the study of dynamic stability. The calculation of dynamic instability region (DIR) spectra is often provided in terms of the spectrum of natural frequencies and the static buckling loads. Furthermore, composite plates with delamination may result in significant changes of these characteristics. Therefore it is an important task to calculate both of them with sufficiently high precision. Thus, the study of dynamic stability itself requires a special investigation on basic problems of vibration and static stability. Thus, the parametric instability characteristics are of great technical importance for understanding the dynamic system of delaminated plates under periodic loading.

1.3 Objectives of present study

The present investigation mainly focuses on the study of vibration, static and dynamic stability of industry driven woven fiber glass/epoxy delaminated composite plates. A study of variation of interlaminar shear strength (ILSS) of composites with delamination is also studied for the sake of completeness. A first order shear deformation theory based on finite element model is developed for studying the free vibration, critical buckling load and parametric instability characteristics of mid-plane delaminated composite plates. The effect of delamination size on ILSS is studied experimentally. The influence of delamination size, boundary conditions, number of layers, fiber orientations and aspect ratio on the free vibration and static stability (buckling) behavior of delaminated cross ply and angle ply laminates are investigated experimentally and numerically. The effect of delamination size, number of layers, aspect ratio, degree of orthotropy and static load factors on the parametric instability behaviour of delaminated cross ply plates are also examined numerically.

This thesis contains six chapters. In Chapter 1, a brief introduction of the importance of the study has been outlined.

In Chapter 2, a detailed review of the literature pertinent to the previous research works made in this field has been listed. A critical discussion of the earlier investigations is done. The aim and scope of the present study is also outlined in this chapter.

In Chapter 3, a description of the theory and formulation of the problem and the finite element procedure used to analyse the vibration, buckling and parametric instability characteristics of homogeneous and delaminated composite plates is explained in detail. The computer programme used to implement the formulation is briefly described.

In Chapter 4, the experimental investigation for ILSS, free vibration and static stability are described in detail. This chapter includes fabrication procedures

for samples, test set-up, apparatus required for different tests and determination of material constants.

In Chapter 5, the results and discussions obtained in the study have been presented in detail. The effect of delamination size on ILSS, is studied experimentally; the influence of delamination size, boundary conditions, number of layers, fiber orientations and aspect ratio on the free vibration and static stability (buckling) behavior of delaminated cross ply and angle ply plates are investigated experimentally and numerically; the effect of delamination size, number of layers, aspect ratio, degree of orthotropy and static load factors on the parametric instability behaviour of delaminated cross ply plates are also examined numerically.

Finally, in Chapter 6, the conclusions drawn from the above studies are described. There is also a brief note on the scope for further investigation in this field.

CHAPTER 2

REVIEW OF LITERATURE

2.1 Introduction

The presence of delamination in composite laminates may adversely affect the safety and durability of structures. Therefore a comprehensive understanding of the delamination behavior is of fundamental importance in the assessment of structural performance of laminated composites. In structural mechanics, dynamic stability has received considerable attention over the years which encompasses many class of problems. Thus the dynamic stability characteristics are of great technical importance for understanding the dynamic systems under periodic loads. Though the present investigation is mainly focused on dynamic stability of delaminated composite plates, some relevant researches on free vibration and static stability or buckling of plates are also studied for the sake of its relevance and completeness. The studies in this chapter are grouped as follows:

- **Vibration**
- **Static stability/buckling**
- **Dynamic stability**

However, some studies on static analysis of delaminated composites involving effects of different parameters on inter laminar shear strength (ILSS) are also studied for completeness.

2.2 Static analysis of delaminated composites

Some experimental studies involving effects of different parameters on the static analysis i.e. interlaminar shear strength of laminated composites are studied. Ruiz and Xia (1991) reported that relatively high values of interlaminar shear strength (ILSS) appear under impact loading causing debonding. The interlaminar shear strength is one of the most important parameter in determining the ability of a composite material to resist delamination damage in laminates (Hallet *et al*.,1999). Costa *et al*. (2001) studied the effect of porosity on interlaminar shear strength of

carbon/epoxy composite laminates. Kotek *et al.* (2001) examined the interlaminar shear strength of textile reinforced carbon-carbon composite. Okutan (2002) discussed the effects of geometric parameters on the failure strength for pin loaded fiberglass reinforced epoxy laminates. Zhang *et al.* (2002) investigated the effect of fiber orientation on the ILSS of graphite/epoxy laminated composites and showed that ILSS depends on the fiber orientation of the neighboring plies around the interfaces. Abadi and Poro (2003) measured interlaminar shear strength (ILSS) of fiber reinforced carbon-carbon composites (CCC). Christensen and Teresa (2003) studied the effect of transverse pressure on ILSS of a quasi isotropic laminate T300/F584. They noted significant increase in ILSS of T300 carbon fiber and F584 epoxy matrix with the increase in transverse pressure. Ray (2004) investigated the effects of thermal and moist environments (hygrothermal) on ILSS of glass fibre/epoxy composites. Teresa *et al*. (2004) examined the effect of through-thickness compression on the interlaminar shear strength of laminated fiber composites. For both glass and carbon fiber composites, through-thickness compression resulted in a significant enhancement in the interlaminar shear strength. Agrawal and Prasad (2005) discussed the influence of environment (cathodic exposure) on inter laminar shear strength of carbon/epoxy composite laminates and observed a significant reduction in the interlaminar shear strength after cathodic exposure. Chakrabarti and Sheikh (2005) made an analysis of laminated sandwich plates based on interlaminar shear stress continuous plate theory. Nancy *et al*. (2005) used double notch shear (DNS) test to characterize the ILSS of ceramic matrix woven composites. Pinho *et al*. (2005) proposed that LaRC04 failure criteria can predict with accuracy interlaminar damage in composite laminates and can be a good choice. Ray (2005) evaluated the ILSS of glass fiber reinforced unsaturated polyster and epoxy resin composites by exposing the composites to 75°C temperature gradient thermal shock, using 3-point bend test. Yokoyama and Nakai (2006) studied the effects of deformation rate and specimen thickness on the ILSS and failure mode. They found that the ILSS is independent on the deformation rate up to nearly 1.6m/s, but depends on the specimen thickness. Khashaba and Seif (2006) investigated on the effect of different loading conditions on the mechanical behaviour of $(0/+45/90)_s$ woven composites and reported that the woven composites performed better under bending loading than under tension

loading. Das *et al*. (2007) examined the effects of cross head velocities on ILSS of woven FRP composites and found that the variation of ILSS of laminates of FRP composites is significant for low loading speed and not so prominent for high speed loading. Lopes et al. (2008) discussed the influence of porosity on interlaminar shear strength of fiber-metal laminates both numerically and experimentally. They reported that the interlaminar shear strength of fibre-metal laminates decreases considerably due to porosity. Cox and Wilson (2008) evaluated ILSS of a graphite/epoxy composite with carbon nanofiber reinforcement (CNF) and found that non-reinforced specimens exhibited 20% higher lap-shear strengths than CNF-reinforced specimens. Hong-yan *et al*. (2009) investigated on the effects of voids (void content, void shape and size) on the ILSS of $[(+/-45)(4)/(0,90)/(+/-45)(2)]_S$ and $[(+/-45)/0(4)/(0,90)/0(2)]_S$ composite laminates. Kong and Wang (2009) examined the role of nano clays in the enhancement of interlaminar shear strength (ILSS) of glass fiber reinforced diallyl phthalate (GFR-DAP) composites and observed that only 2.5 wt% clay loading in DAP matrix increased the ILSS of resulting GFR-DAP laminates by 7.64%. Aslan and Alnak (2010) performed experimental and numerical analysis to study the interlaminar shear strength of laminated woven E-glass/epoxy composites by four point bend shear test. Walter *et al*. (2010) conducted monotonic, multi-step and cyclic short beam shear tests on 2D and 3D woven composites. The test results were used to determine the effect of z- yarns on interlaminar shear strength. The results showed that with the increase in z-yarns percentage there is decrease in interlaminar shear strength. Jaeschke *et al.* (2011) reported that the magnitude of heat affected zone at the cutting edge of the CF-PPS composite plate is correlated with the interlaminar shear strength of the plate.

The above studies deals with static analysis of composites without considering delamination. However studies involving delaminated composites are scarce in literature. Kim and Donaldson (2006) made an experimental and analytical study on the damage initiation in the form of interlaminar delamination of carbon fiber reinforced polymer composite under thermal and mechanical loadings. Piotrowski *et al*. (2006) studied the delamination behavior of a laminated E-glass reinforced polymer matrix composite versus changes in the processing of the polymer matrix; changes in the resin matrix rheology and in the e-glass finish chemistry and concentration. The ILSS of a laminated polymer matrix composite was examined as functions of matrix phase

additions, the matrix mixing procedure, the glass fiber finish chemistry and concentration, and the matrix rheology. Matrix phase additions, mixing, and glass finish were found to significantly affect the ILSS, while the matrix rheology had less of an impact.

2.3 Vibration of delaminated composite plates

A considerable amount of investigations are available in the open literature on vibration of laminated composite beams, plates and shells without delamination. However, studies addressing delamination in composite laminates are very limited. The delamination problem is generally more complex involving geometrical and material discontinuity. Della and Shu (2007) reviewed the available mathematical models for the vibration of delaminated composite laminates. As per the study, the earliest reported model for the vibration analysis of composite beams was reported by Ramkumar *et al.* (1979)**.** Ostachowicz and Krawczuk (1994) analyzed the natural frequency of composite beams with delamination using finite element method (FEM). Lee *et al*. (2003) performed an analytical solution for multiple delaminated beams. Brandinelli and Massabo (2003) developed an analytical model to investigate the effect of bridging mechanisms between the delaminated interfaces on the vibration of a delaminated composite beam. Park *et al.* (2004) developed a recurrent single delaminated beam model for vibration analysis of multi-delaminated beams. Kim and Hwang (2002) presented an analytical solution using the "constrained mode" assumption for delaminated honey-comb sandwich beams. Shu and Della (2004) investigated the vibration of sandwich beams with two delaminations at identical span wise locations. Othman and Barton (2008) studied failure initiation and propagation characteristics of honeycomb sandwich composites. Zhu *et al*. (2005) formulated the reference surface element and its applications in dynamic analysis of delaminated composite beams. Yuan *et al*. (2008) calculated the reflection and transmission coefficients for time harmonic flexural waves in a semi-infinite delaminated beam following analytical approach.

The above studies are based on one dimensional models. Two dimensional models are also developed to predict the behaviour of delaminated composites in a more realistic way. Ju *et al*. (1995) presented finite element formulation for the analysis of free vibration of composite plates with multiple delaminations.

Parhi *et al.* (2000) investigated the dynamic behavior in the presence of single and multiple delaminations of laminated composite plates. Zak *et al.* (2001) studied the influence of the delamination length and position on changes in natural frequencies and modes of vibration of the unidirectional composite plates by using finite element method. Yam *et al.* (2004) proposed a finite element model to predict dynamic behavior of multi-layer composite plates with internal delamination at arbitrary locations. Oh *et al.* (2005) developed a four-noded finite element formulation based on the efficient high-order zig-zag plate theory of laminated composite plates with multiple delaminations to predict the natural frequencies, mode shape and time response. Olsson *et al.* (2006) developed a model to predict delamination threshold loads for dynamic impact on plates.

However, very few studies involving experimental investigations on vibration of delaminated composite plates are available in literature. Champanelli and Engblom (1995) presented limited vibration data of three numbers of delaminated graphite/PEEK composite plates with delamination location at mid edge and corner of the plate and compared with modeling results. Luo and Hangud (1996) conducted modal analysis experiments on glass fiber/epoxy cantilever composite plates with fixed size of strip delamination. Kessler *et al.* (2002) studied damage detection in composite panels using frequency response method. Azouaoui *et al.* (2007) made an experimental investigation to study the delamination behaviour of glass/polyester composite plates subjected to low-energy compact fatigue.

Krawezuk *et al.* (1997) developed a finite element model to study the dynamics of cracked composite material structures. Chang *et al.* (1998) studied vibration of delaminated composite plates under axial load. Hou and Jeronimidis (1999) made an experimental investigation on circular composite plates with an impact induced delamination**.** Chattopadhyay *et al.* (2000) formulated a high order theory for dynamic stability analysis of delaminated composite plates. Thornburgh and Chattopadhyay (2003) used finite element method to study the vibration of composite laminates with delamination and transverse matrix cracks. Suzuki *et al.* (2004) used multilayered finite element numerical analysis for non-linear vibration and damping characterization of delaminated CFRP composite laminates.

Sancho and Miravete (2006) developed a design for delaminated composite structure considering the three dimensional stress field in the vicinity of free edges, holes and changes in number of layers. Karmkar *et al.* (2006) investigated the effect of delamination on free vibration characteristics of graphite-epoxy composite pretwisted cylindrical shallow shells of various stacking sequences considering length of delamination as a parameter. Hein (2006) performed free vibration analysis for multiple delaminated beams and investigated the influences of delamination size and position on the natural frequencies of the stepped beam numerically. Acharya *et al.* (2007) studied free vibration of delaminated composite cylindrical shell roofs. Roy and Chakraborty (2008) proposed three dimensional finite element analysis to evaluate the response of graphite/epoxy laminates subjected to impact loading.

Shiau and Zeng (2010) investigated on the effect of delamination on free vibration of a simply supported rectangular homogeneous plate with through-width delamination by the finite strip method. Results showed that the delamination has considerable effect on the natural frequencies of the plate. The aspect ratio of the plate is also having significant effect on the natural frequency of the plate, especially on the mode 2 frequency of the plate. Zhang *et al.* (2010) developed a Structural Health Monitoring (SHM) system based on vibration monitoring to detect, locate and assess delamination damage in laminated composite structures. Towards this end, finite element modelling is employed to simulate the dynamic response of composite laminates (beams and plates) with delamination and extract their vibration parameters. Hadi and Ameen (2011) characterized the embedded delamination on the dynamic response of composite laminated structures. A finite element model for geometrically nonlinear large amplitude vibration of shallow cylindrical and delamination shell analysis was presented using higher order shear deformation theory where the nonlinearity was introduced in the Green-Lagrange sense.

2.4 Static stability of delaminated composite plates

Several theoretical studies involving analytical models and numerical analysis were developed to study buckling behavior of delaminated structures. Use of theoretical analysis in predicting buckling load of delaminated plate was difficult. Therefore, numerical and experimental methods have become important in solving the

buckling problem of a laminated composite plate having delamination. The problem of delamination buckling and growth was addressed by Chai *et al.* (1981) for a laminated plate. They presented a one-dimensional model to describe the failure mechanism. Sallam and Simitses (1985) investigated on the delamination buckling and growth of flat cross-ply laminates using a one-dimensional model. Bruno and Grimaldi (1989) analyzed delamination failure of layered composite plates loaded in compression. Compression failure of carbon fiber-reinforced coupons containing central delaminations was studied by Pavier and Chester (1990). An analytical and experimental investigation on unidirectional graphite/epoxy composites was performed by Kutlu and Chang (1992) to study the compression response of composites containing multiple delaminations. Compressive buckling stability of composite panels with through-width, equally spaced multiple delaminations were investigated experimentally and analytically using Rayleigh-Ritz approximation technique by Suemasu (1993).

Yeh and Tan (1994) studied the buckling behaviour of laminated plates with elliptical delamination under uniaxial compressive loading experimentally and analytically. Kim and Hong (1997) presented a finite element model for buckling and post buckling behavior of composite laminates with an embedded circular delamination using degenerated shell elements. Gu and Chattopadhyay (1999) investigated experimentally delamination buckling and postbuckling of composite laminates. A buckling analysis of laminates with an embedded delamination was conducted by Hu *et al*. (1999) by employing a finite-element method based on the Mindlin plate theory. Hwang and Mao (2001) predicted the buckling loads of delaminated unidirectional carbon/epoxy composites with strip delamination. The buckling and postbuckling behaviors of carbon/epoxy composite laminates with multiple delaminations were experimentally and numerically studied by Hwang and Liu (2002). The effect of the strip delamination width on the buckling loads of the simply supported carbon/epoxy woven laminated composite plates was investigated by Zor (2003) following 3D finite element models. Kucuk (2004) established a three-dimensional finite element model of the square laminated plates to study the effects of the lateral strip delamination width on the buckling loads. Zor *et al.* (2005) developed a three-dimensional finite element model to study the effects of the square delamination on the buckling loads. Experimental measurements and numerical solutions using ANSYS on

the buckling of single centered strip delaminated woven glass-fiber composite laminates were carried out on rectangular plates by Pekbey and Sayman (2006). Capello and Tumino (2006) examined the buckling and post buckling behaviour of unidirectional and cross-ply composite laminated plates with multiple delaminations.

Lee and Park (2007) investigated on the buckling behaviors of laminated composite structures with a delamination using the enhanced assumed strain (EAS) solid element three-dimensional finite element (FE) formulation. In particular, new results reported in this paper are focused on the significant effects of the local buckling for various parameters, such as size of delamination, aspect ratio, width-to-thickness ratio, stacking sequences, and location of delamination and multiple delaminations. Tumino *et al.* (2007) studied the role of delamination length, angle of ply and stacking sequence on the buckling load of multidelaminated composite specimens following finite element method with linear and nonlinear analysis. The compressive behavior of composite laminates with through-the-width delaminations was investigated analytically by Kharazi and Ovesy (2008).

Aran *et al.* (2009) examined the effect of delamination length, position through thickness and stacking sequence of the plies on the buckling and postbuckling of laminates with a single delamination using a three dimensional finite element model. It was found that significant decrease occurs in the critical buckling load after a certain value of the delamination length. The position of delamination and the fiber orientation also affects the loads. Aslan and Sahin (2009) investigated the effects of the delamination size on the critical buckling load and compressive failure load of unidirectional E-glass/epoxy composite laminates with multiple large triangular delaminations. Obdrzalek and Vrbka (2010) studied the buckling behavior of a small delaminated plate subjected to compression loading by means of the finite element analysis. Esfahani *et al.* (2010) made experimental and numerical analysis of delaminated hybrid composite beam structures. Mohsen and Amin (2010) examined numerically the buckling and post buckling analysis of composite laminated structures with delaminations by using the generalized differential quadrature method. Kang *et al.* (2011) followed numerical analysis to study the compressive buckling of composite laminates with a delamination. Damghani *et al.* (2011) predicted the critical buckling load of composite plates with through-the-length delaminations using

exact stiffness analysis. Chattopadhyay and Murthy (2011) investigated the elastic buckling and postbuckling analysis of an axially loaded beam-plate with an across-the-width delamination, located at a given depth below the upper surface of the plate. Tsouvalis and Garganidis (2011) made the buckling strength parametric study of composite laminated plates with delaminations .

A critical review of above works show that most of the previous works deal with numerical analysis of one dimensional delaminated unidirectional laminates using a numerical technique including FEM based package. However, the numerical and experimental investigations on buckling analysis of delaminated bidirectional industry driven woven roving glass/epoxy composite plates are scarce in literature. Zhang and Fu (2000) made a micro mechanical model of woven fabric for the analysis of buckling under uniaxial tension. Xu *et al*. (2006) investigated on the buckling analysis of triaxial woven fabric composite structures and parametric study-uniaxial loading.

2.5 Dynamic stability of delaminated composite plates

In modeling delamination, both, analytical as well as numerical methods have been used in studying the dynamic and buckling behaviour of composite laminates. A lot of studies are available on the use of numerical methods to predict the natural frequencies and critical buckling load of delaminated composite plates using different approaches. However studies involving dynamic stability of delaminated plates are much less in literature. The earlier works on dynamic stability of structures are reviewed by Simites (1987) and Sahu and Datta (2007). The dynamic stability of rectangular isotropic plates under various in-plane forces has been studied by Bolotin (1964) , Jagdish (1974), Hutt and Salam (1971). Deolasi and Datta (1995) used finite element method based on first order shear deformation theory (FSDT) to study the parametric instability characteristics of thin isotropic plates.

A number of researchers have investigated the dynamic stability characteristics of rectangular composite plates.The dynamic stability of rectangular laminated composite plate due to periodic in-plane load is studied by Srinivasan and Chellapandi (1986) using finite strip method (FSM). Bert and Birman (1987) investigated the dynamic instability of shear deformable antisymmetric angle ply plates. Yamaki and Nagai (1975) examined the dynamic stability of rectangular plates under periodic

compressive forces. Dynamic stability of laminated composite plates due to periodic in-plane loads is investigated by Chen and Yang (1990) using FSDT. Moorthy *et al*. (1990) and Chattopadhyay and Radu (2000) predicted the dynamic instability boundaries of rectangular composite plates. Kwon (1991) investigated the dynamic instability of composite laminates following finite element method. Wang and Dawe (2002) examined the dynamic instability of composite laminated rectangular plate and prismatic plate structures. Liao and Cheng (1994) studied the dynamic instability characteristics of stiffened isotropic and composite square plate. Srivastava *et al.* (2003) investigated the dynamic instability of stiffened plates subjected to non-uniform harmonic edge loading. Patel *et al*. (2009) performed the parametric study on dynamic instability behaviour of laminated composite stiffened plate by using the FSDT. Lee (2010) studied the finite element dynamic stability of laminated composite skew plates containing cutouts based on higher order shear deformation theory (HSDT). Dey and Singha (2006) investigated the dynamic stability characteristics of simply supported composite skew plates subjected to a periodic in-plane load. The principal and second instability regions are identified for different parameters such as skew angle, thickness- to- span ratio, fiber orientation and static in-plane load. Dynamic instability behaviour of composite and sandwich laminates with interfacial slips has examined by Chakrabarti and Sheikh (2010) by using RHSDT (refined higher order shear deformation theory). Dynamic instability analysis of composite laminated thin walled structures was carried out by Fazilati and Ovesy (2010) by using two versions of FSM (finite strip method). Biswas *et al.* (2011) studied the static and dynamic instability characteristics of curved laminates with internal damage subjected to follower loading.

Park and Lee (2009) examined parametric instability of delaminated composite spherical shells subjected to in-plane pulsating forces. Radu and Chattopadhyay (2002) analyzed the dynamic stability of composite plates including delamination using higher order theory and transformation matrix. They analyzed composite plates with various thickness, delamination length and placement and observed that delamination affects the instability regions by shifting them to lower parametric resonance frequencies. Yeh and Tung (2006) investigated the dynamic instability behavior of delaminated composite plates under transverse excitation experimentally and analytically.

2.6 Critical discussion

The present review indicates that more studies are conducted on laminated composite plate, beams and shells without delamination. However studies involving delamination in composite laminates are very limited. As regards to methodology, the researchers are more interested to use numerical methods instead of analytical methods. With the advent of high speed computers, more studies are made using finite element method. From the present review of literature, the lacunae of the earlier investigations which need further attention of future researchers are presented below.

2.6.1 Vibration of delaminated composite plates

The review of the present work as cited in the literature indicated that a considerable amount of analytical models and numerical analysis was reported for the vibration analysis of unidirectional composite laminates with delaminations. Many researchers followed one dimensional model for vibration behavior of delaminated composites (Zhu *et al.*, 2005; Othman & Barton, 2008). Two dimensional models were also developed to predict the behaviour of delaminated composites in a more realistic way. Ju *et al*.(1995), Zak *et al*.(2001) and Yam *et al*.(2004) studied the free vibration of delaminated composites by using the finite element formulation. The natural frequencies of composite plates with multiple delaminations were predicted by Oh *et al*. (2005) following a four-noded finite element formulation based on the efficient high-order zig-zag plate theory.

Experimental investigations on vibration of delaminated composite plates are very scarce in literature. Campanelli and Engblom (1995), Luo and Hangud (1996) and Azouaoui *et al.* (2007) made experimental investigation to study natural frequency of delaminated graphite/PEEK, glass fiber/epoxy and glass/polyester composite plates. Hou and Jeronimidis (1999) made an experimental investigation on circular composite plates with an impact induced delamination.

The vibration of composite laminates with delamination and transverse matrix cracks using finite element method was studied by Thornburgh and Chattopadhyay(2003). The effect of delamination on free vibration characteristics of

graphite-epoxy composite pretwisted cylindrical shallow shells of various stacking sequences involving length of delamination as a parameter was investigated by Karmkar *et al.*(2006).

2.6.2 Static stability of delaminated composite plates

The studies involving behavior of delaminated composite plates subjected to in plane load are much less in literature. Several theoretical studies involving analytical models and numerical analysis were developed to study buckling behavior of delaminated structures. Numerical and experimental methods were attempted by various researchers for predicting the buckling load of delaminated composite plates (Yeh and Tan, 1994; Gu and Chattopadhyay 1999). Chai *et al.* (1981) and Sallam and Simitses (1985) followed one one-dimensional model to describe the buckling problem of delaminated composites.

Kutlu and Chang (1992) studied the compression response of unidirectional graphite/epoxy composites containing multiple delaminations by using analytical and experimental investigation. A three-dimensional FEM model was developed by Kucuk (2004) and Zor *et al.* (2005) to study the effects of delamination on the buckling loads. Tumino *et al.* (2007) studied the role of delamination length, angle of ply and stacking sequence on the buckling load of multi-delaminated composite specimens following finite element method with linear and nonlinear analysis.

2.6.3 Dynamic stability of delaminated composite plates

Most of the researchers followed analytical and numerical methods to predict the natural frequencies and critical buckling load of delaminated composite plates. Investigations on dynamic stability of delaminated plates are very scarce in literatures. The parametric instability characteristics of thin isotropic plates was investigated by Hutt and Salam (1971) and Deolasi and Datta (1995).

The dynamic stability characteristics of rectangular composite plates was investigated by a number of researchers (Jagdish, 1974; Yamaki and Nagai,1975; Srinivasan and Chellapandi, 1986; Wang and Dawe, 2002). Bert and Birman (1987) investigated the dynamic instability of shear deformable antisymmetric angle ply plates. Dynamic stability of laminated composite plates due to periodic in-plane loads is

investigated by Chen and Yang (1990). Liao and Cheng (1994) studied the dynamic instability characteristics of stiffened isotropic and composite square plate. Srivastava *et al.* (2003) examined the dynamic instability of stiffened plates subjected to non-uniform harmonic edge loading. The parametric study on dynamic instability behaviour of laminated composite plate was performed by using FEM (Patel *et al.*, 2009; Lee, 2010). However the study of instability behavior of composite plates subjected to delamination is scarce in literature. Radu and Chattopadhyay (2002), Park and Lee **(**2009) and Yeh and Tung (2006) investigated the dynamic instability behavior of delaminated composite plates under transverse excitation experimentally and analytically.

2.7 Scope of the present study

An extensive review of the literature shows that a lot of work was done on the vibration and static stability of delaminated composite plates. The woven composite is a new class of textile composite and has many industrial applications. Very little work has been done on dynamic stability of delaminated composite plates. The present study is mainly aimed at filling some of the lacunae that exist in the proper understanding of the dynamic stability of industry driven woven fiber delaminated plates. Based on the review of literature, the different problems identified for the present investigation are presented as follows.

- Interlaminar shear strength of delaminated composites
- Free vibration of delaminated composite plates
- Buckling/ static stability of delaminated composite plates
- Dynamic stability of delaminated composite plates

The present study mainly focuses on the parametric resonance characteristics of homogeneous and delaminated composite plates. The influence of various parameters such as delamination size, aspect ratio, number of layers, degree of orthotropy and static load factor on the instability behaviour of delaminated plates are examined numerically using Bolotin's approach and finite element method. A special investigation of vibration and buckling of delaminated industry driven composite plates are also conducted both numerically and experimentally.

CHAPTER 3

THEORY AND FORMULATION

3.1 The basic problem

This chapter represents the theory and finite element formulation (FEM) for free vibration, static stability and dynamic stability analysis of the composite plate of various geometry with and without delamination. The basic configuration of the problem considered here is a composite laminated plate with mid-plane single delamination subjected to in plane periodic load as shown in Figure 3.1. The boundary conditions are incorporated in the most general manner. The details of delamination is shown in Figure 8.1 through 8.7 of Appendix-I.

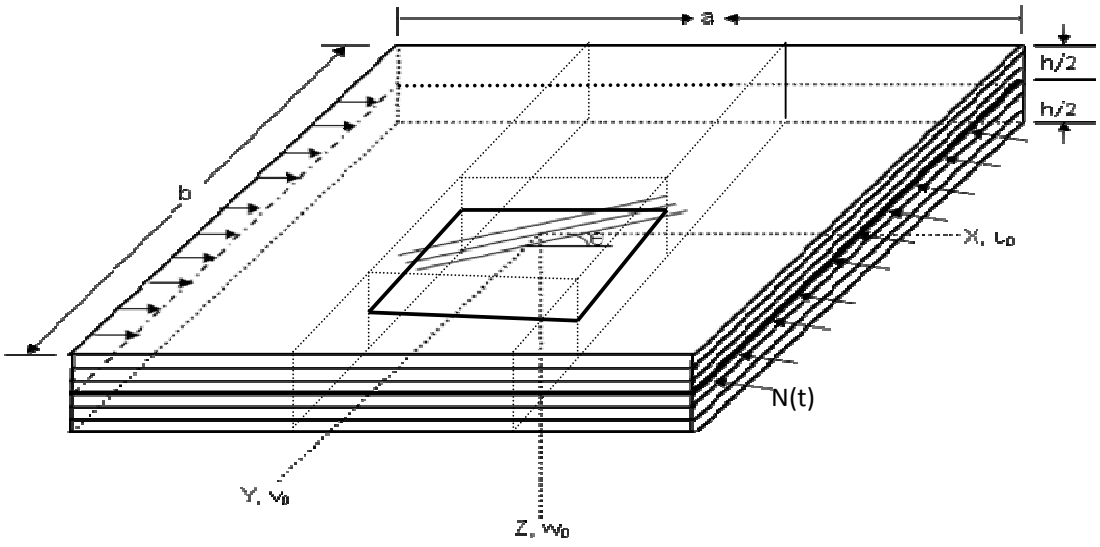

Figure 3.1: Delaminated composite plate under in-plane periodic load

3.2 Proposed analysis

The governing equations for the dynamic stability of delaminated composite plates subjected to in-plane periodic loading are developed. The presence of external in-plane loads induces a stress field in the structure. This necessitates the determination of the stress field as a prerequisite for the solution of problems like vibration, buckling and dynamic stability behaviour of plates. As the thickness of the

structure is relatively smaller, the determination of stress field reduces to the solution of a plane stress problem. The governing differential equations have been developed using the first order shear deformation theory (FSDT). The assumptions made in the analysis are given below.

3.2.1 Assumptions of the analysis

1. The analysis is linear, in line with previous studies on the dynamic stability of panels (Bert and Birman, 1988; Sahu and Datta, 2003) with a few exceptions. This implies both linear constitutive relations (generalized Hooke's law for the material and linear kinematics) and small displacements to accommodate small deformation theory.
2. The delaminated panels are of various shapes with no initial imperfections. The consideration for imperfections is less important for dynamic loading and is consistent with the work of Bert and Birman (1988).
3. The straight line that is perpendicular to the neutral surface before deformation remains straight but not normal after deformation (FSDT). Normal stress in the Z-direction is neglected.
4. The loading on the delaminated panel is considered as axial with a simple harmonic fluctuation with respect to time.
5. All damping effects are neglected.

3.3 Governing equations

The Governing differential equations, the strain energy due to loads, kinetic energy and formulation of vibration, buckling and dynamic stability problems are derived on the basis of principle of Potential Energy and Lagrange's equation and are presented as follows.

3.3.1 Governing differential equations

The equation of motion is obtained by taking a differential element of plate as shown in Figure 3.2(a) & (b). The figure 3.2(a) shows an element with internal forces like membrane forces ($N_x, N_y, and N_{xy}$) .The Figure 3.2(b) shows shearing forces (Q_x and Q_y) and the moment resultants (M_x, M_y and M_{xy}).

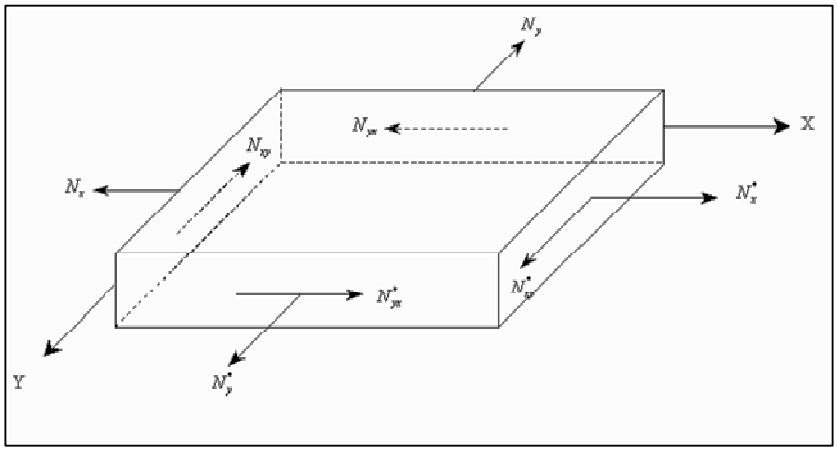

Figure 3.2 (a): Force resultants

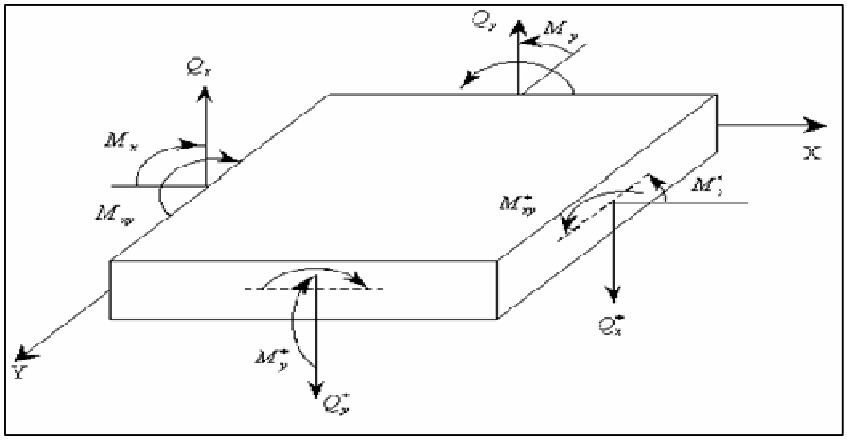

Figure 3.2 (b): Moment resultants

The governing differential equations of equilibrium for free vibration of a shear deformable laminated plate subjected to external in-plane loading can be expressed as (Chandrashekhara,1989; Sahu and Datta**,** 2003):

$$\frac{\partial N_x}{\partial x}+\frac{\partial N_{xy}}{\partial y}=P_1\frac{\partial^2 u}{\partial t^2}+P_2\frac{\partial^2 \theta_x}{\partial t^2}$$

$$\frac{\partial N_{xy}}{\partial x}+\frac{\partial N_y}{\partial y}=P_1\frac{\partial^2 v}{\partial t^2}+P_2\frac{\partial^2 \theta_y}{\partial t^2}$$

$$\frac{\partial Q_x}{\partial x}+\frac{\partial Q_y}{\partial y}+N_x^0\frac{\partial^2 w}{\partial x^2}+N_y^0\frac{\partial^2 w}{\partial y^2}=P_1\frac{\partial^2 w}{\partial t^2} \qquad (3.3.1)$$

$$\frac{\partial M_x}{\partial x}+\frac{\partial M_{xy}}{\partial y}-Q_x=P_3\frac{\partial^2\theta_x}{\partial t^2}+P_2\frac{\partial^2 u}{\partial t^2}$$

$$\frac{\partial M_{xy}}{\partial x}+\frac{\partial M_y}{\partial y}-Q_y=P_3\frac{\partial^2\theta_y}{\partial t^2}+P_2\frac{\partial^2 v}{\partial t^2}$$

where N_x^0 and N_y^0 are the external loading in the X and Y directions respectively. $(P_1,P_2,P_3)=\sum_{k=1}^{n}\int_{z_{k-1}}^{z_k}(\rho)_k(1,z,z^2)dz$

where n = number of layers of the laminated composite panel, $(\rho)_k$ = mass density of k_{th} layer from the mid-plane.

3.3.2 Energy expressions

The delaminated composite plate is subjected to initial in-plane edge loads N_x^0, N_y^0 and N_{xy}^0. These in-plane loads cause in-plane stresses of σ_x^0, σ_y^0 and σ_{xy}^0inducing a plane stress problem. The delaminated composite plates with the initial stresses undergo small lateral deformations. The total stress at any layer is the sum of the initial stresses plus the stresses due to bending and shear deformation. The strain energy U_o due to initial in-plane stresses is written as

$$U_0 = U_0 = \frac{1}{2}\iiint\{\varepsilon^0\}^T\{\sigma^0\}dV \qquad (3.3.2)$$

where

$$\{\varepsilon^0\}^T=\{\varepsilon_x^{.0}\varepsilon_y^{.0}\gamma_{xy}^{.0}\}^T=\left[\frac{\partial u^0}{\partial x}\frac{\partial v^0}{\partial y}\frac{\partial u^0}{\partial y}+\frac{\partial v^0}{\partial x}\right]^T \qquad (3.3.3)$$

and the stresses are

$$\{\sigma^0\}=[D_p]\{\varepsilon^0\} \qquad (3.3.4)$$

The strains can be expressed in terms of initial in-plane deformations u^0, v^0 as

$$\{\varepsilon^0\} = [B_P]\{q^0\} \tag{3.3.5}$$

Substituting the values of stress and strain in the equation (3.3.2), we get

$$U_0 = \frac{1}{2}\iint \{q^0\}^T [B_P]^T [D_P][B_P]\{q^0\} dA \tag{3.3.6}$$

The strain energy is expressed as

$$U_0 = \frac{1}{2}\{q^0\}^T [K_P]\{q^0\} \tag{3.3.7}$$

where

$$[K_P] = \iint [B_P]^T [D_P][B_P] dA \tag{3.3.8}$$

Considering the prestressed state as the initial state, the strain energy stored due to bending and shear deformation in the presence of initial stresses (neglecting higher order terms) is given by

$$U = U_1 + U_2 \tag{3.3.9}$$

where U_1 = Strain energy associated with bending with transverse shear,

U_2 = Work done by the initial in-plane stresses and the nonlinear strain

$$U_1 = \frac{1}{2}\iiint [\{\varepsilon_l\}^T [D]\{\varepsilon_l\}] dV \tag{3.3.10}$$

where the strains can be expressed in terms of deformations as

$$\{\varepsilon_l\} = [B]\{q^0\} \tag{3.3.11}$$

and $$U_2 = \frac{1}{2}\iiint [\{\sigma^0\}^T \{\varepsilon_{nl}\}] dV \tag{3.3.12}$$

The method of explicit integration is performed through the thickness of the panel and thus the generalized force and moment resultants can directly be related to

the strain components through the laminate stiffness. The kinetic energy V of the plate can be derived as

$$V = \iint \left[\frac{h}{2} \left\{ \frac{\partial \overline{u}^2}{\partial t} + \frac{\partial \overline{v}^2}{\partial t} + \frac{\partial \overline{w}^2}{\partial t} \right\} + \frac{h^3}{12} \left\{ \frac{\partial \theta_x^{\ 2}}{\partial t} + \frac{\partial \theta_y^{\ 2}}{\partial t} \right\} \right] dxdy \qquad (3.3.13)$$

Now, the various energies can be expressed in matrix form as

$$U_0 = \frac{1}{2}\{q\}^T [K_P]\{q\}$$

$$U_1 = \frac{1}{2}\{q\}^T [K]\{q\} \qquad (3.3.14)$$

$$U_2 = \frac{1}{2}\{q\}^T [K_g]\{q\}$$

$$V = \frac{1}{2}\{\dot{q}\}^T [M]\{\dot{q}\}$$

where $[K_p]$ = Plane stiffness matrix

$[K]$ = Bending stiffness matrix with shear deformation

$[K_g]$ = Geometric stiffness or stress stiffness matrix

$[M]$ = Consistent mass matrix

3.3.3 Formulation of static and dynamic problems

The equation of motion for vibration of a delaminated composite panel, subjected to in-plane loads can be expressed as:

$$[M]\{\ddot{q}\} + [[K] - N(t)[K_g]]\{q\} = 0 \qquad (3.3.15)$$

Here,'q' is the vector of degrees of freedom u, v, w, θ_x and θ_y. The in-plane load

'N (t)' may be harmonic and can be expressed in the form:

$$N(t) = N_s + N_t Cos\Omega t \qquad (3.3.16)$$

where N_s is the static portion of the load N(t), N_t is the amplitude of the dynamic portion of N(t) and Ω is the frequency of the excitation. Considering the static and dynamic components of load as a function of the critical load,

$$N_s = \alpha N_{cr}, \quad N_t = \beta N_{cr} \tag{3.3.17}$$

where α and β are the static and dynamic load factors respectively. Using equation (3.3.16), the equation of motion under periodic loads in matrix form may be obtained as:

$$[M]\{\ddot{q}\} + [[K] - \alpha N_{cr}[K_g] - \beta N_{cr}[K_g] Cos\,\Omega t]\{q\} = 0 \tag{3.3.18}$$

The above equation (3.3.18) represents a system of differential equations with periodic coefficients of the Mathieu-Hill type. The development of regions of instability arises from Floquet's theory which establishes the existence of periodic solutions of periods T and 2T. The boundaries of the primary instability regions with period 2T, where T = 2 π/Ω are of practical importance [Bolotin, 1964] and the solution can be achieved in the form of the trigonometric series:

$$q(t) = \sum_{k=1,3,5,..}^{\infty} [\{a_k\} Sin(k\Omega t/2) + \{b_k\} Cos(k\Omega t/2)] \tag{3.3.19}$$

Putting this in equation (3.3.18) and if only the first term of the series i.e., k = 1 is considered, and equating coefficients of Sin Ωt/2 and Cos Ωt/2, the equation (3.3.19) reduces to

$$[[K] - \alpha N_{cr}[K_g] \pm \frac{1}{2}\beta N_{cr}[K_g] - \frac{\Omega^2}{4}[M]]\{q\} = 0 \tag{3.3.20}$$

Equation (3.3.20) represents an eigenvalue problem for known values of α, β and N_{cr}. The two conditions under the plus and minus sign correspond to the two boundaries of the dynamic instability region. The eigen values are Ω, which give the boundary frequencies of the instability regions for given values of α and β. In this analysis, the computed static buckling load of the panel is considered as the reference load in line with many previous investigations (Ganapati *et al.*, 1994;

Moorthy *et al.* 1990). This equation (3.3.20) represents a solution to a number of related problems as follows,

(1) **Free vibration**: $\alpha = 0$, $\beta = 0$ and $\omega = \Omega/2$

$$[[K] - \omega^2 [M]]\{q\}=0 \quad (3.3.21)$$

(2) **Vibration with static axial load:** $\beta = 0$ and $\omega = \Omega/2$

$$[[K] - \alpha N_{cr} [K_g] - \omega^2 [M]]\{q\}=0 \quad (3.3.22)$$

(3) **Static stability:** $\alpha = 1$, $\beta = 0$, $\Omega = 0$

$$[[K] - N_{cr} [K_g]] \{q\}=0 \quad (3.3.23)$$

3.4 Finite element formulation

A delaminated composite plate of length *a*, width *b* and thickness *h* consisting of *n* arbitrary number of anisotropic layers is considered as shown in Figure 3.1. The layer details of the plate are shown in Figure 3.3. The global coordinate system is considered with respect to the mid-plane of the plate with the Z-axis perpendicular to the X-Y plane and θ is the angle of fiber orientation, measured anticlockwise with respect to X-axis. In the present investigation, the delaminated composite plate is discretised in to a mesh of 8×8 with total 64 elements. An eight noded two dimensional quadratic isoparametric element having five degrees of freedom (u^0, v^0,w, θ_x, ,θ_y) per node is chosen.

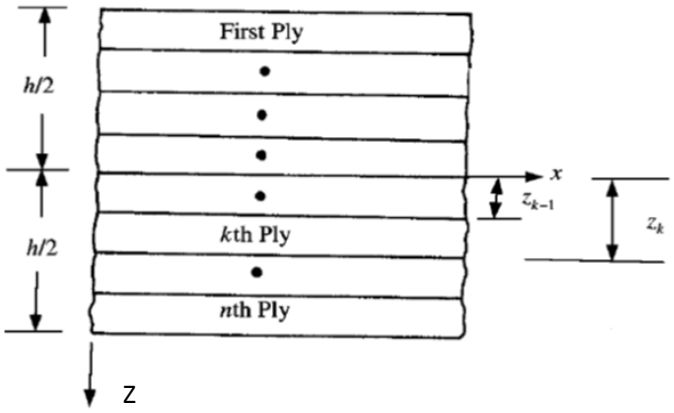

Figure3.3: Layer details of the plate

3.4.1 Displacement field and shape functions

The displacement field of any point at a distance z from the mid surface is assumed to be in the form of

$$u(x,y,z) = u^0(x,y) + z\theta x(x,y) \quad (3.4.1)$$

$$v(x,y,z) = v^0(x,y) + z\theta y(x,y) \quad (3.4.2)$$

$$w(x,y,z) = w^0(x,y) \quad (3.4.3)$$

where u, v, w are displacements in the X, Y, Zdirections respectively for any point, u^0,v^0 , w^0 are those at the middle plane of the plate. θ_x, θ_y are the rotations of the cross section normal to the Y and X axis respectively. The middle plane of the plate is considered as the reference plane of the plate. The mid plane strains of the laminate are given by

$$\varepsilon_{xx}{}^0 = u^0{}_{,x};\ \varepsilon_{yy}{}^0 = v^0{}_{,y};\ \gamma_{xy}{}^0 = u^0{}_{,y} + v^0{}_{,x};\ \gamma_{xz}{}^0 = \theta_x + w_{,x};, \gamma_{yz}{}^0 = \theta_y + w_{,y} \quad (3.4.4)$$

Assuming small deformations, the generalized linear in-plane strains of the laminate at a distance z from the mid-surface are expressed as

$$\{\varepsilon_{xx}\varepsilon_{yy}\gamma_{xy}\gamma_{xz}\gamma_{yz}\}^T=\{\varepsilon^0{}_{xx}\ \ \varepsilon^0{}_{yy}\gamma^0{}_{xy}\,\gamma^0{}_{xz,}\ \gamma^0{}_{yz}\}^T+z\{\,k_{xx}\ \ k_{yy}\ \ k_{xy}\ \ k_{xz}\,k_{yz}\}^T \quad (3.4.5)$$

where $\begin{Bmatrix} \in^0_{xx} \\ \in^0_{yy} \\ \gamma^0_{xy} \\ \gamma^0_{xz} \\ \gamma^0_{yz} \end{Bmatrix} = \begin{Bmatrix} \dfrac{\partial u^0}{\partial x} \\ \dfrac{\partial v^0}{\partial y} \\ \dfrac{\partial u^0}{\partial y} + \dfrac{\partial v^0}{\partial x} \\ \theta_x + \dfrac{\partial \omega}{\partial x} \\ \theta_y + \dfrac{\partial \omega}{\partial y} \end{Bmatrix}$

$$\text{and} \begin{Bmatrix} k_{xx} \\ k_{yy} \\ k_{xy} \\ k_{xz} \\ k_{yz} \end{Bmatrix} = \begin{Bmatrix} \dfrac{\partial \theta_x}{\partial x} \\ \dfrac{\partial \theta_y}{\partial y} \\ \dfrac{\partial \theta_x}{\partial x} + \dfrac{\partial \theta_y}{\partial y} \\ 0 \\ 0 \end{Bmatrix}$$

where ε^0_{xx}, ε^0_{yy}, γ^0_{xy} are the mid-plane strains and k_{xx} k_{yy} k_{xy} are the curvatures of the laminated plate .

The element has 4 corner nodes and 4 mid side nodes. In the displacement model, simple functions are assumed to approximate the displacements for each element. For the present isoparametric element, the shape functions which are used to represent the geometry as well as the displacements within the element are expressed by the shape functions N_i.

$$x = \sum_{i=1}^{8} N_i x_i \quad , \quad y = \sum_{i=1}^{8} N_i y_i \quad , \quad u^0 = \sum_{i=1}^{8} N_i u_i^0 \quad , \quad v^0 = \sum_{i=1}^{8} N_i v_i^0$$

$$w = \sum_{i=1}^{8} N_i w_i \quad , \quad \theta_x = \sum_{i=1}^{8} N_i \theta_{xi} \quad , \quad \theta_y = \sum_{i=1}^{8} N_i \theta_{yi} \qquad (3.4.6)$$

where x_i , y_i ,are the co-ordinates of the i^{th} node and u_i^0, v_i^0,w_i , θ_{xi}, θ_{yi} are the displacement functions for different nodes .

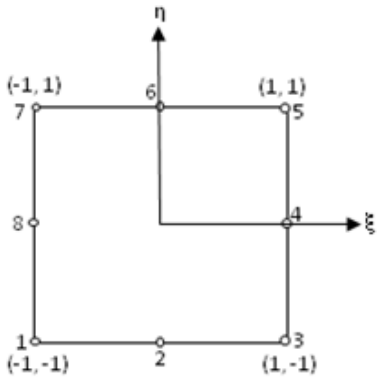

Figure 3.4: The element in isoparametric co-ordinates

N_i for different nodes as shown in Figure 3.4 is defined as,

At corner nodes (i.e. for node 1, 3, 5, 7)

$$N_i = \frac{1}{4}(1+\xi\xi_i)(1+\eta\eta_i)(\xi\xi_i + \eta\eta_i - 1)$$

At middle nodes (i.e. for nodes 2, 6)

$$N_i = \frac{1}{2}(1-\xi^2)(1+\eta\eta_i)$$

At middle nodes (i.e. for nodes 4, 8)

$$N_i = \frac{1}{2}(1+\xi\xi_i)(1-\eta^2) \qquad (3.4.7)$$

where ξ and η are the local isoparametric co-ordinates of the element and ξ_i and η_i are the respective values at node i. The correctness of the shape function N_i is checked from the relations

$$\sum N_i = 1 \quad \sum N_i,\xi = 0 \; \sum N_i,\eta = 0 \qquad (3.4.8)$$

The derivatives of the shape functions N_i with respect to x and y are expressed in terms of their partial derivatives with respect to ξ and η by the relationships:

$$\frac{\partial N_i}{\partial x} = \frac{\partial N_i}{\partial \xi}\frac{\partial \xi}{\partial x} + \frac{\partial N_i}{\partial \eta}\frac{\partial \eta}{\partial x}$$

$$\frac{\partial N_i}{\partial y} = \frac{\partial N_i}{\partial \xi}\frac{\partial \xi}{\partial y} + \frac{\partial N_i}{\partial \eta}\frac{\partial \eta}{\partial y}$$

$$\begin{Bmatrix} \frac{\partial N_i}{\partial x} \\ \frac{\partial N_i}{\partial y} \end{Bmatrix} = \begin{bmatrix} \frac{\partial \xi}{\partial x} & \frac{\partial \eta}{\partial x} \\ \frac{\partial \xi}{\partial y} & \frac{\partial \eta}{\partial y} \end{bmatrix} \begin{Bmatrix} \frac{\partial N_i}{\partial \xi} \\ \frac{\partial N_i}{\partial \eta} \end{Bmatrix}$$

$$\begin{bmatrix} N_{i,x} \\ N_{i,y} \end{bmatrix} = [J]^{-1} \begin{bmatrix} N_{i,\xi} \\ N_{i,\eta} \end{bmatrix} \tag{3.4.9}$$

where $[J] = \begin{bmatrix} x,_{\xi} & y,_{\xi} \\ x,_{\eta} & y,_{\eta} \end{bmatrix} = \begin{bmatrix} \sum N_{i,\xi} x_i & \sum N_{i,\xi} y_i \\ \sum N_{i,\eta} x_i & \sum N_{i,\eta} y_i \end{bmatrix}$ is the Jacobian matrix.

3.4.2 Stress strain relations

A macromechanical analysis is carried out to establish the relationship between the forces and strains of a laminate. The elastic behavior of each lamina is essentially two dimensional and orthotropic in nature. So the elastic constants for the composite lamina are given below.

E_{11} = Modulus of elasticity of lamina along 1-direction

E_{22} = Modulus of elasticity of lamina along 2-direction

G_{12} = Shear modulus

ν_{12} = Major Poisson's ratio

ν_{21} = Minor Poisson's ratio

The on-axis elastic constant matrix $[Q_{ij}]_k$ corresponding to material axes 1-2 for k^{th} layer is given by

$$\left[Q_{ij}\right]_k = \begin{bmatrix} Q_{11} & Q_{12} & 0 \\ Q_{12} & Q_{22} & 0 \\ 0 & 0 & Q_{66} \end{bmatrix} \text{ for i, j = 1, 2, 6} \tag{3.4.10}$$

$$\text{and } [Q_{ij}]_k = \begin{bmatrix} Q_{44} & 0 \\ 0 & Q_{55} \end{bmatrix} \text{ for i,j =4,5} \tag{3.4.11}$$

For obtaining the off-axis elastic constant matrix, $[\overline{Q}_{ij}]_k$ corresponding to any arbitrarily oriented reference X-Y axes for the k^{th} layer ,appropriate transformation is required.

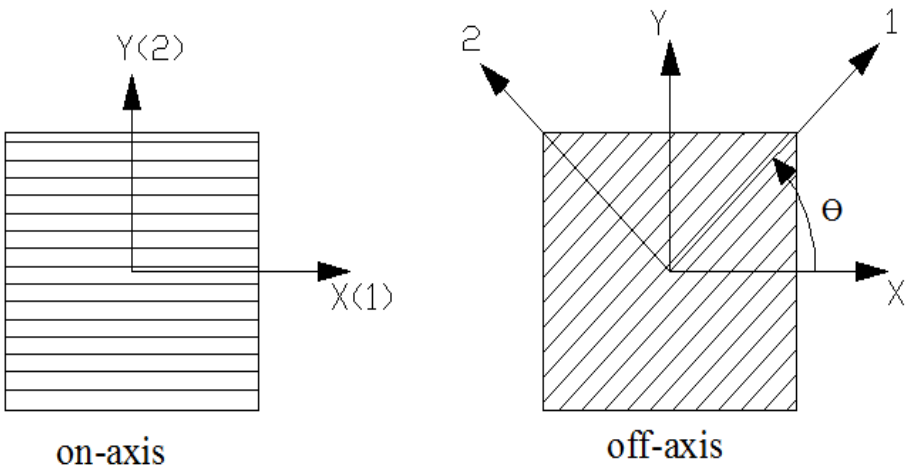

Figure 3.5: O**n-axis and off-axis configurations of lamina**

Hence as shown in Figure 3.5, the off-axis elastic constant matrix is obtained from the on axis elastic constant matrix by the relation

$$\left[\overline{Q}_{ij}\right]_k = \begin{bmatrix} \overline{Q}_{11} & \overline{Q}_{12} & \overline{Q}_{16} \\ \overline{Q}_{12} & \overline{Q}_{22} & \overline{Q}_{26} \\ \overline{Q}_{16} & \overline{Q}_{26} & \overline{Q}_{66} \end{bmatrix} \qquad \text{for i ,j =1,2,6}$$

$$[Q_{ij}]_k = [T]^{-1}[Q_{ij}]_k[T]^T$$

$$= \begin{bmatrix} m^2 & n^2 & -2mn \\ n^2 & m^2 & 2mn \\ mn & -mn & m^2-n^2 \end{bmatrix}_k [Q_{ij}]_k \begin{bmatrix} m^2 & n^2 & mn \\ n^2 & m^2 & -mn \\ -2mn & 2mn & m^2-n^2 \end{bmatrix}_k$$

(3.4.12)

where [T] = Transformation matrix $= \begin{bmatrix} m^2 & n^2 & 2mn \\ n^2 & m^2 & -2mn \\ -mn & mn & m^2-n^2 \end{bmatrix}_k$

$$Q_{11} = \frac{E_{11}}{1-v_{12}v_{21}}; \qquad Q_{12} = \frac{E_{11}v_{21}}{1-v_{12}v_{21}}; \quad Q_{21} = \frac{E_{22}v_{12}}{1-v_{12}v_{21}}; Q_{22} = \frac{E_{22}}{1-v_{12}v_{21}}$$

$Q_{66} = G_{12}$; $Q_{44} = G_{13}$; $Q_{55} = G_{23}$

For i ,j =4,5

$$\left[\overline{Q}_{ij}\right]_k = \left[\begin{matrix} \overline{Q}_{44} & \overline{Q}_{45} \\ Q_{45} & Q_{55} \end{matrix}\right]_k$$

$$= \begin{bmatrix} m & -n \\ n & m \end{bmatrix}_k \begin{bmatrix} Q_{44} & 0 \\ 0 & Q_{55} \end{bmatrix}_k \begin{bmatrix} m & n \\ -n & m \end{bmatrix}_k \qquad (3.4.13)$$

where m = cosθ, n = sinθ , θ is the angle from the X-axis to the 1-axis measured anticlockwise.

The stress strain relationship for a laminate at a distance z is given by

$$\begin{Bmatrix} \sigma_{xx} \\ \sigma_{yy} \\ \tau_{xy} \end{Bmatrix}_z = \begin{bmatrix} \overline{Q}_{11} & \overline{Q}_{12} & \overline{Q}_{16} \\ \overline{Q}_{12} & \overline{Q}_{22} & \overline{Q}_{26} \\ \overline{Q}_{16} & \overline{Q}_{26} & \overline{Q}_{66} \end{bmatrix}_z \begin{Bmatrix} \varepsilon_{xx} \\ \varepsilon_{yy} \\ \gamma_{xy} \end{Bmatrix}_z$$

$$= \begin{bmatrix} \overline{Q}_{11} & \overline{Q}_{12} & \overline{Q}_{16} \\ \overline{Q}_{12} & \overline{Q}_{22} & \overline{Q}_{26} \\ \overline{Q}_{16} & \overline{Q}_{26} & \overline{Q}_{66} \end{bmatrix}_z \left\{ \begin{Bmatrix} \varepsilon^0_{xx} \\ \varepsilon^0_{yy} \\ \gamma^0_{xy} \end{Bmatrix} + z \begin{Bmatrix} k_{xx} \\ k_{yy} \\ k_{xy} \end{Bmatrix} \right\} \qquad (3.4.14)$$

and $$\begin{Bmatrix} \tau_{xz} \\ \tau_{yz} \end{Bmatrix}_z = \begin{bmatrix} \overline{Q}_{44} & \overline{Q}_{45} \\ \overline{Q}_{45} & \overline{Q}_{55} \end{bmatrix}_z \begin{Bmatrix} \gamma_{xz} \\ \gamma_{yz} \end{Bmatrix} \qquad (3.4.15)$$

Here σ_{xx} and σ_{yy} are the normal stresses along X and Y directions respectively and τ_{xz} and τ_{yz} are the shear stresses in xz, yz planes respectively.

The force and moment resultants are obtained by integrating the stresses and their moments through the laminate thickness as given by

$$\begin{Bmatrix} N_{xx} \\ N_{yy} \\ N_{xy} \end{Bmatrix}_z = \sum_{k=1}^{n} \left[\overline{Q}_{ij}\right] \left\{ \int_{z_{k-1}}^{z_k} \begin{Bmatrix} \varepsilon^0_{xx} \\ \varepsilon^0_{yy} \\ \gamma^0_{xy} \end{Bmatrix} dz + \int_{z_{k-1}}^{z_k} \begin{Bmatrix} k_{xx} \\ k_{yy} \\ k_{xy} \end{Bmatrix} z dz \right\} \qquad (3.4.16)$$

$$\begin{Bmatrix} M_{xx} \\ M_{yy} \\ M_{xy} \end{Bmatrix}_z = \sum_{k=1}^{n} \left[\overline{Q}_{ij}\right] \left\{ \int_{z_{k-1}}^{z_k} \begin{Bmatrix} \varepsilon^0_{xx} \\ \varepsilon^0_{yy} \\ \gamma^0_{xy} \end{Bmatrix} z dz + \int_{z_{k-1}}^{z_k} \begin{Bmatrix} k_{xx} \\ k_{yy} \\ k_{xy} \end{Bmatrix} z^2 dz \right\} \qquad (3.4.17)$$

$$\begin{Bmatrix} Q_{xz} \\ Q_{yz} \end{Bmatrix}_z = \sum_{k=1}^{n} \left[\overline{Q}_{ij}\right] \left\{ \int_{z_{k-1}}^{z_k} \begin{Bmatrix} \gamma_{xz}^0 \\ \gamma_{yz}^0 \end{Bmatrix} dz \right\} i, j = 4,5 \qquad (3.4.18)$$

The above 3 equations are combined together to obtain the force, moment and transverse shear resultants.

The relationship among stress resultants and the deformations are given by

$$\begin{Bmatrix} N_{xx} \\ N_{yy} \\ N_{xy} \\ M_{xx} \\ M_{yy} \\ M_{xy} \\ Q_{xz} \\ Q_{yz} \end{Bmatrix} = \begin{bmatrix} A_{11} & A_{12} & A_{16} & B_{11} & B_{12} & B_{16} & 0 & 0 \\ A_{12} & A_{22} & A_{26} & B_{12} & B_{22} & B_{26} & 0 & 0 \\ A_{16} & A_{26} & A_{66} & B_{16} & B_{26} & B_{66} & 0 & 0 \\ B_{11} & B_{12} & B_{16} & D_{11} & D_{12} & D_{16} & 0 & 0 \\ B_{12} & B_{22} & B_{26} & D_{12} & D_{22} & D_{26} & 0 & 0 \\ B_{16} & B_{26} & B_{66} & D_{16} & D_{26} & D_{66} & 0 & 0 \\ 0 & 0 & 0 & 0 & 0 & 0 & S_{44} & S_{45} \\ 0 & 0 & 0 & 0 & 0 & 0 & S_{45} & S_{55} \end{bmatrix} \begin{Bmatrix} \varepsilon_{xx}^0 \\ \varepsilon_{yy}^0 \\ \gamma_{xy}^0 \\ K_{xx} \\ K_{yy} \\ K_{xy} \\ \gamma_{xz}^0 \\ \gamma_{yz}^0 \end{Bmatrix} \qquad (3.4.19)$$

where $\mathbf{A_{ij}} = \sum^{n}_{k=1} (\overline{Q}_{ij})_k (z_k - z_{k-1})$

$$\mathbf{B_{ij}} = \frac{1}{2} \sum^{n}_{k=1} (\overline{Q}_{ij})_k (z^2_k - z^2_{k-1})$$

$$\mathbf{D_{ij}} = \frac{1}{3} \sum^{n}_{k=1} (\overline{Q}_{ij})_k (z^3_k - z^3_{k-1}) \quad \text{for i ,j=1,2,6}$$

$$\mathbf{S_{ij}} = \kappa \sum^{n}_{k=1} (\overline{Q}_{ij})_k (z_k - z_{k-1}) \qquad \text{for i,j=4,5} \qquad (3.4.20)$$

$\mathbf{A_{ij}}$ = inplane stiffness terms relating the in-plane forces with inplane strains.

$\mathbf{B_{ij}}$= Coupling stiffness terms relating the in-plane forces with curvature and moments with in-plane strains.

$\mathbf{D_{ij}}$ = bending stiffness terms relating moments with curvature.

Here, $[\ \overline{Q}_{ij}\ ]_k$ is the off axis elastic constant matrix for the k^{th} lamina and the shear correction factor κ is assumed as 5/6. It accounts for the non-uniform distribution of transverse shear strain across the thickness of the laminate.

$\mathbf{A_{ij}}$, $\mathbf{B_{ij}}$, $\mathbf{D_{ij}}$are the extension, bending stretching coupling and bending stiffness respectively. $\mathbf{S_{ij}}$ is the transverse shear stiffness of the laminate. The elastic properties of each lamina are generally assumed to be constant through its thickness as these laminae are considered to be thin.

3.5 Delamination modeling

A simple two dimensional single delamination model proposed by Gim (1994)is extended by Parhi *et al*. (2000) for the vibration of delaminated composite panels. In the present analysis, it is further extended for static and dynamic stability analysis under in-plane uniaxial periodic forces by multiple delamination modelling. In order to satisfy the compatibility and equilibrium requirements at the common delamination boundary, it is assumed that the in-plane displacement, transverse displacement and rotation at a common node for all the three sublaminates including the original one are identical applying multiple constraint condition at any arbitrary delamination boundary. It can be applicable to any general case of a laminated composite plate having multiple delaminations at any arbitrary location. Here, the delaminated area is assumed as the interface of two separate sub laminates bonded together along the delamination surface.

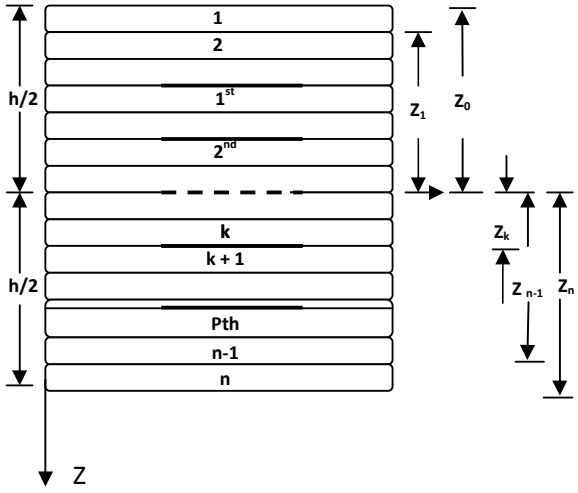

Figure 3.6: **Laminate geometry with multiple delaminations**

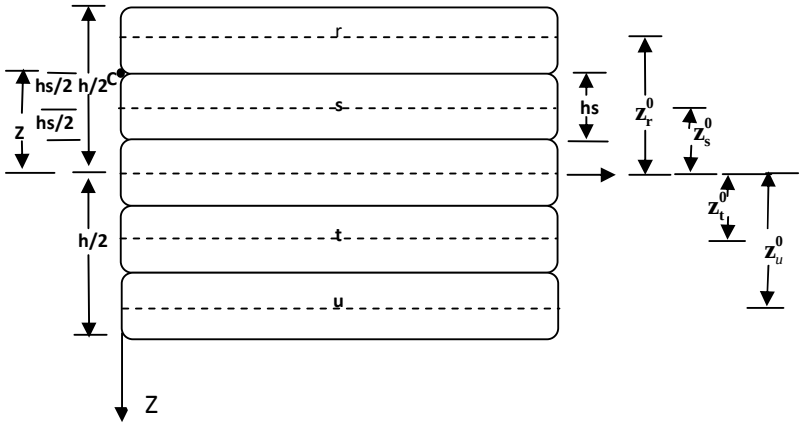

Figure 3.7: Three arbitrary delaminations leading to four sub-laminates

Typical composite plate of uniform thickness '*h'* with '*n'* number of layers and '*p'* number of arbitrarily located delaminations is considered for the analysis as shown in Figure 3.6. The principal material axes of each layer are arbitrarily oriented with respect to the mid-plane of the plate. Let z^0_sbe the distance between the mid-plane of the original laminate and the mid-plane of the arbitrary s^{th} sub-laminate as shown in Figure 3.7.

Considering the sub-laminates as a separate plate, the displacement field within it is expressed as:

$$u_s = u_s^0 + \left(z - z_s^0\right)\theta_{xs} \ , \quad v_s = v_s^0 + \left(z - z_s^0\right)\theta_{ys} \tag{3.5.1}$$

where u^0_s and v^0_s are the mid-plane displacements of the s^{th} sub-laminate along X and Y direction and z_s^0 is distance between mid-plane of s^{th} sub-laminate and the mid-plane of the laminate in Z direction

The mid-plane strains of the sub-laminate are

$$\left\{\varepsilon_{xx}^0 \quad \varepsilon_{yy}^0 \quad \gamma_{xy}^0\right\}_s^T = \left\{\frac{\partial u_s^0}{\partial x} \quad \frac{\partial v_s^0}{\partial y} \quad \frac{\partial u_s^0}{\partial y} + \frac{\partial v_s^0}{\partial x}\right\}^T \tag{3.5.2}$$

where ε^0_{xx} ε^0_{yy} γ^0_{xy} are mid-plane strains.

From equation (3.5.2) the strain components within the sub-laminate *s* can be

expressed as $\left\{\varepsilon_{xx}^{0} \quad \varepsilon_{yy}^{0} \quad \gamma_{xy}^{0}\right\}_{s}^{T} = \left\{\frac{\partial u_s}{\partial x} \quad \frac{\partial v_s}{\partial y} \quad \frac{\partial u_s}{\partial y}+\frac{\partial v_s}{\partial x}\right\}^{T}$

$$=\left\{\frac{\partial u_s^0}{\partial x} \quad \frac{\partial v_s^0}{\partial y} \quad \frac{\partial u_s^0}{\partial y}+\frac{\partial v_s^0}{\partial x}\right\}^{T}+(z-z_s^0)\left\{\frac{\partial \theta_x}{\partial x} \quad \frac{\partial \theta_y}{\partial y} \quad \frac{\partial \theta_x}{\partial y}+\frac{\partial \theta y}{\partial x}\right\}^{T}$$

$$=\left\{\varepsilon_{xx}^{0} \quad \varepsilon_{yy}^{0} \quad \gamma_{xy}^{0}\right\}_{s}^{T}+(z-z_s^0)\left\{k_{xx} \quad k_{yy} \quad k_{xy}\right\}_{s}^{T} \qquad (3.5.3)$$

where k_{xx} k_{yy} k_{xy} are curvatures of the laminated plate.

In order to satisfy the compatibility and equilibrium requirements at the common delamination boundary, it is assumed that the in-plane displacements, transverse displacement and rotations at a common node for all the three sub-laminates including the original one are identical. Applying multiple constraint condition at any arbitrary delamination boundary *c*, the in-plane displacements at '*c'* at a distance '*z'* from the mid-plane of the laminate can be written as

$u_c = u^0 + z\theta_x$, $v_c = v^0 + z\theta_y$

From equation (3.5.1), the displacement at any point, *c* is given by

$u_{sc} = u_s^0 + (z-z_s^0)\theta_x$, $v_{sc} = v_s^0 + (z-z_s^0)\theta_y$

Equating u_c with u_{sc} and v_c with v_{sc} , the mid-plane displacements of the sub-laminate can be expressed in the form of the mid-plane displacements(u^0, v^0) of the original un-delaminated laminate as,

$$u_s^0 = u^0 + z_s^0\theta_x,\ v_s^0 = v^0 + z_s^0\theta_y \qquad (3.5.4)$$

From equation (3.5.4), the mid-plane strain components of the s^{th} sub-laminate can be derived as:

$$\left\{\varepsilon_{xx}^0 \varepsilon_{yy}^0 \gamma_{xy}^0\right\}_s^T = \left\{\varepsilon_{xx}^0 \varepsilon_{yy}^0 \gamma_{xy}^0\right\}^T + z_s^0 \left\{k_{xx} k_{yy} k_{xy}\right\}^T \tag{3.5.5}$$

The strain components within the sub-laminate can be written as

$$\left\{\varepsilon_{xx} \varepsilon_{yy} \gamma_{xy}\right\}_s^T = \left\{\varepsilon_{xx}^0 \varepsilon_{yy}^0 \gamma_{xy}^0\right\}_s^T + (z - z_s^0)\left\{k_{xx} k_{yy} k_{xy}\right\}^T$$

$$= \left\{\varepsilon_{xx}^0 \varepsilon_{yy}^0 \gamma_{xy}^0\right\}^T + z_s^0 \left\{k_{xx} k_{yy} k_{xy}\right\}^T + (z - z_s^0)\left\{k_{xx} k_{yy} k_{xy}\right\}^T \tag{3.5.6}$$

For any lamina of s^{th} sub-laminate, the in-plane and shear stresses are found from the relation

$$\left\{\sigma_{xx} \sigma_{yy} \tau_{xy}\right\}^T = \begin{bmatrix} \overline{Q}_{11} & \overline{Q}_{12} & \overline{Q}_{16} \\ \overline{Q}_{12} & \overline{Q}_{22} & \overline{Q}_{26} \\ \overline{Q}_{16} & \overline{Q}_{26} & \overline{Q}_{66} \end{bmatrix} \left\{\varepsilon_{xx} \varepsilon_{yy} \gamma_{xy}\right\}_s^T \tag{3.5.7}$$

$$\left\{\tau_{xz} \tau_{yz}\right\}^T = \begin{bmatrix} \overline{Q}_{44} & \overline{Q}_{45} \\ \overline{Q}_{45} & \overline{Q}_{5} \end{bmatrix} \left\{\gamma_{xz} \gamma_{yz}\right\}_s^T \tag{3.5.8}$$

where σ_{xx} and σ_{yy} are the normal stresses along X and Y directions respectively and τ_{xz} and τ_{yz} are the shear stresses in XZ, YZ planes respectively.

Integrating these stresses over the thickness of the sub -laminate, the stress and moment resultants of the sub- laminate are derived which lead to the elasticity matrix of the s^{th} sub-laminate $[D]_s$ in the form

$$\left[D\right]_s = \begin{bmatrix} A_{ij} & z_s^0 A_{ij} + B_{ij} & 0 \\ B_{ij} & z_s^0 B_{ij} + D_{ij} & 0 \\ 0 & 0 & S_{ij} \end{bmatrix} \tag{3.5.9}$$

$[D]_s$ is the elasticity matrix of the s^{th} sub-laminate

where, $$\left[A_{ij}\right]_s = \int_{-\frac{h_s}{2}+z_s^0}^{\frac{h_s}{2}+z_s^0} \left[\overline{Q}_{ij}\right]_s dz \quad ,$$

$$\left[B_{ij}\right]_s = \int_{-\frac{h_s}{2}+z_s^0}^{\frac{h_s}{2}+z_s^0} \left[\overline{Q}_{ij}\right]_s \left(z - z_s^0\right) dz = \int_{\frac{-h_s}{2}+z_s^0}^{\frac{h_s}{2}+z_s^0} \left[\overline{Q}_{ij}\right]_s z dz - z_s^0 \left[A_{ij}\right]_s$$

$$\left[D_{ij}\right]_s = \int_{-\frac{h_s}{2}+z_s^0}^{\frac{h_s}{2}+z_s^0} \left[\overline{Q}_{ij}\right]_s \left(z - z_s^0\right)^2 dz = \int_{\frac{-h_s}{2}+z_s^0}^{\frac{h_s}{2}+z_s^0} \left[\overline{Q}_{ij}\right]_s \left[z^2 + \left(z_s^0\right)^2 - 2zz_s^2\right] dz = \int_{\frac{-h_s}{2}+z_s^0}^{\frac{h_s}{2}+z_s^0} \left[\overline{Q}_{ij}\right]_s z^2 dz$$

$$- 2z_s^2 \left[\int_{\frac{-h_s}{2}+z_s^0}^{\frac{h_s}{2}+z_s^0} \left[\overline{Q}_{ij}\right]_s z dz\right] + \left(z_s^0\right)^2 \left[A_{ij}\right]_s \qquad \text{for i, j = 1, 2, 6}$$

$$\left[S_{ij}\right]_s = \int_{-\frac{h_s}{2}+z_s^0}^{\frac{h_s}{2}+z_s^0} \left[\overline{Q}_{ij}\right] dz \qquad \text{for i,j =4,5} \qquad (3.5.10)$$

The in-plane stress and moment resultants for the s[th] sub-laminate can be expressed in a generalized manner as:

$$\begin{Bmatrix} N_{xx} \\ N_{yy} \\ N_{xy} \\ N_{xx} \\ N_{yy} \\ N_{xy} \end{Bmatrix} = \begin{bmatrix} A_{11} & A_{12} & A_{16} & z_s^0 A_{11} + B_{11} & z_s^0 A_{12} + B_{12} & z_s^0 A_{16} + B_{16} \\ A_{12} & A_{22} & A_{26} & z_s^0 A_{12} + B_{12} & z_s^0 A_{22} + B_{22} & z_s^0 A_{26} + B_{26} \\ A_{16} & A_{26} & A_{66} & z_s^0 A_{16} + B_{16} & z_s^0 A_{26} + B_{26} & z_s^0 A_{66} + B_{66} \\ A_{11} & A_{12} & A_{16} & z_s^0 A_{11} + B_{11} & z_s^0 A_{12} + B_{12} & z_s^0 A_{16} + B_{16} \\ A_{12} & A_{22} & A_{26} & z_s^0 A_{12} + B_{12} & z_s^0 A_{22} + B_{22} & z_s^0 A_{26} + B_{26} \\ A_{16} & A_{26} & A_{66} & z_s^0 A_{16} + B_{16} & z_s^0 A_{26} + B_{26} & z_s^0 A_{66} + B_{66} \end{bmatrix}_s \begin{Bmatrix} \varepsilon_{xx}^0 \\ \varepsilon_{yy}^0 \\ \gamma_{xy}^0 \\ k_{xx} \\ k_{yy} \\ k_{xy} \end{Bmatrix}_s \qquad (3.5.11)$$

Similarly, the transverse shear resultants for the s[th] sub-laminate are presented as

$$\begin{Bmatrix} Q_{xz} \\ Q_{yz} \end{Bmatrix}_s = \begin{bmatrix} S_{44} & S_{45} \\ S_{45} & S_{55} \end{bmatrix}_s \begin{Bmatrix} \gamma_{xz} \\ \gamma_{yz} \end{Bmatrix} \qquad (3.5.12)$$

After finding the elastic stiffness matrices separately for different sub-laminates along the thickness, the sum of all the sub-laminate stiffnesses represents the resultant stiffness matrix.

3.6 Strain displacement relations

Green-Lagrange's strain displacement is used throughout the structural analysis. The linear part of the strain is used to derive the elastic stiffness matrix and non-linear part of the strain is used to derive the geometrical stiffness matrix.

$$\{\varepsilon\}=\{\varepsilon_l\}+\{\varepsilon_{nl}\} \tag{3.6.1}$$

The linear strains are defined as

$$\varepsilon_{xl} = \frac{\partial u}{\partial x} + Zk_x$$

$$\varepsilon_{yl} = \frac{\partial u}{\partial y} + Zk_y$$

$$\gamma_{xyl} = \frac{\partial u}{\partial y} + \frac{\partial v}{\partial x} + Zk_{xy} \tag{3.6.2}$$

$$\gamma_{xz} = \frac{\partial u}{\partial z} + \frac{\partial w}{\partial x}$$

$$\gamma_{yz} = \frac{\partial w}{\partial y} + \frac{\partial v}{\partial z}$$

where the bending strains k_j are expressed as

$$K_x = \frac{\partial \theta_x}{\partial x}$$

$$K_y = \frac{\partial \theta_y}{\partial y}$$

$$K_{xy} = \frac{\partial \theta_x}{\partial y} - \frac{\partial \theta_y}{\partial x} \tag{3.6.3}$$

Assuming that *w* does not vary with *Z*, the non-linear strains of the plate are expressed as

$\varepsilon_{xnl}= [(\partial u/\partial x)^2 +(\partial v/\partial x)^2 + (\partial w/\partial x)^2]/2,$

ε_{ynl}= [$(\partial v/\partial y)^2$ +$(\partial u/\partial y)^2$ + $(\partial w/\partial y)^2$]/2,

γ_{xynl} = [$(\partial u/\partial x)$ $(\partial u/\partial y)$ + (($\partial v/\partial x$) ($\partial v/\partial y$) + ($\partial w/\partial x$)($\partial w/\partial y$)],

γ_{xznl} = [$(\partial u/\partial x)$ $(\partial u/\partial z)$ + $(\partial v/\partial x)$ $(\partial v/\partial z)$ + $(\partial w/\partial x)$ $(\partial w/\partial z)$],

γ_{xznl}= [$(\partial u/\partial y)$ $(\partial u/\partial z)$ + $(\partial v/\partial y)$ $(\partial v/\partial z)$ + $(\partial w/\partial y)$ $(\partial w/\partial z)$],

The linear strain can be described in term of displacements as

$$\{\varepsilon\} = [B]\{de\} \tag{3.6.4}$$

where $\{de\} = [u_1\ v_1\ w_1\theta_{x1}\theta_{y1}\ u_2\ v_2\ \ldots\ldots\ldots\ldots\ u_8\ v_8\ w_8\theta_{x8}\theta_{y8}]^T$

$[B] = [[B_1]\ \ldots\ldots\ [B_7]\ [B_8]]$

$$[B_i] = \begin{bmatrix} \frac{\partial Ni}{\partial x} & 0 & 0 & 0 & 0 \\ 0 & \frac{\partial Ni}{\partial y} & 0 & 0 & 0 \\ \frac{\partial Ni}{\partial y} & \frac{\partial Ni}{\partial x} & 0 & \frac{\partial Ni}{\partial x} & 0 \\ 0 & 0 & 0 & 0 & \frac{\partial Ni}{\partial y} \\ 0 & 0 & \frac{\partial Ni}{\partial x} & \frac{\partial Ni}{\partial y} & \frac{\partial Ni}{\partial x} \\ 0 & 0 & \frac{\partial Ni}{\partial x} & Ni & 0 \\ 0 & 0 & \frac{\partial Ni}{\partial x} & 0 & Ni \end{bmatrix}_{i=1to8} \tag{3.6.5}$$

3.7 Derivation of element matrices

3.7.1 Elastic stiffness matrix

The potential energy of deformation for the element is given by

$$U_e = \frac{1}{2}\iint\{\varepsilon\}^T[\sigma]dA \tag{3.7.1}$$

$$\{\varepsilon\} = \{\varepsilon^0_{xx}\ \varepsilon^0_{yy}\ \gamma^0_{xy}\ k_{xx}\ k_{yy}\ k_{xy}\ \gamma_{xz}\ \gamma_{yz}\}^T \tag{3.7.2}$$

where $\{\varepsilon\} = [B]\{d_e\} = [\ [B_1]\ \ldots\ldots\ldots\ldots\ [B_8]\ ]\{d_e\}$ (3.7.3)

with $\{d_e\} = \left\{u_1^0 v_1^0 w_1 \theta_x^1 \theta_y^1 \ldots\ldots\ldots\ldots\ldots u_\varepsilon^0 v_\varepsilon^0 w_\varepsilon \theta_x^\varepsilon \theta_y^\varepsilon\right\}^T$ (3.7.4)

Then $U_e = \frac{1}{2} \iint \{d_e\}^T [B]^T [D][B] \{d_e\} dxdy = \frac{1}{2} \{d_e\}^T [K_e] \{d_e\}$ (3.7.5)

where the element stiffness matrix

$$[K_e] = \int_{-1}^{1} \int_{-1}^{1} [B]^T [D][B] \left| J \right| d\xi d\eta \quad (3.7.6)$$

[B] is called the strain displacement matrix.

In equation (3.7.6) $[B_i] = \sum_{i=1}^{8} \begin{bmatrix} N_{i,x} & 0 & 0 & 0 & 0 \\ 0 & N_{i,y} & 0 & 0 & 0 \\ N_{i,y} & N_{i,x} & 0 & 0 & 0 \\ 0 & 0 & 0 & N_{i,x} & 0 \\ 0 & 0 & 0 & 0 & N_{i,y} \\ 0 & 0 & 0 & N_{i,y} & N_{i,x} \\ 0 & 0 & N_{i,x} & N_i & 0 \\ 0 & 0 & N_{i,y} & 0 & N_i \end{bmatrix}$

$\left| J \right| d\xi d\eta$, is the determinant of the jacobian matrix. The element stiffness matrix can be expressed in local natural co-ordinates of the element. The integration of equation (3.7.6) is carried out using the Gauss quadrature method.

3.7.2 Geometric stiffness matrix

The element geometric stiffness matrix is derived using the non-linear in-plane Green's strains. The strain energy due to initial stresses is

$$U_2 = \int_v \left[\sigma^0\right]^T \{\varepsilon_{n1}\} dV \quad (3.7.7)$$

Using non-linear strains, the strain energy can be written in matrix form as

$$U_2 = \frac{1}{2} \int_v [f]^T [S][f] dV \quad (3.7.8)$$

$$\{f\} = \left[\frac{\partial u}{\partial x}, \frac{\partial u}{\partial y}, \frac{\partial v}{\partial x}, \frac{\partial v}{\partial y}, \frac{\partial w}{\partial x}, \frac{\partial w}{\partial y}, \frac{\partial \theta_x}{\partial x}, \frac{\partial \theta_x}{\partial y}, \frac{\partial \theta_y}{\partial x}, \frac{\partial \theta_y}{\partial y} \right]^T \quad (3.7.9)$$

$$[S] = \begin{bmatrix} s & 0 & 0 & 0 & 0 \\ 0 & s & 0 & 0 & 0 \\ 0 & 0 & s & 0 & 0 \\ 0 & 0 & 0 & s & 0 \\ 0 & 0 & 0 & 0 & s \end{bmatrix}$$

$$[s] = \begin{bmatrix} \sigma_x & \tau_{xy} \\ \tau_{xy} & \sigma_y \end{bmatrix} = \frac{1}{h} \begin{bmatrix} N_x & N_{xy} \\ N_{xy} & N_y \end{bmatrix}$$

The in-plane stress resultants N_x , N_y, N_{xy} at each Gauss point are obtained by applying uniaxial stress in X-direction and the geometric stiffness matrix is formed for these stress resultants.

$$[f] = [G]\,[\delta_e] \tag{3.7.10}$$

where, $[\delta_e] = [u, v, w, \theta_x, \theta_y]^T$

The strain energy, U_2 becomes

$$U_2 = \frac{1}{2}\int \{\delta_e\}^T [G]^T [S][G]\{\delta_e\} dV = \frac{1}{2}\{\delta_e\}^T [K_g]\{\delta_e\} \tag{3.7.11}$$

where element geometric stiffness matrix

$$[K_g] = \int_{-1}^{1} \int_{-1}^{1} [G]^T [S]\,[G] \left| J \right| d\xi d\eta \tag{3.7.12}$$

$$[G] = \begin{bmatrix} N_{i,x} & 0 & 0 & 0 & 0 \\ N_{i,y} & 0 & 0 & 0 & 0 \\ 0 & N_{i,x} & 0 & 0 & 0 \\ 0 & N_{i,y} & 0 & 0 & 0 \\ 0 & 0 & N_{i,x} & 0 & 0 \\ 0 & 0 & N_{i,y} & 0 & 0 \\ 0 & 0 & 0 & N_{i,x} & 0 \\ 0 & 0 & 0 & N_{i,y} & 0 \\ 0 & 0 & 0 & 0 & N_{i,x} \\ 0 & 0 & 0 & 0 & N_{i,y} \end{bmatrix} \tag{3.7.13}$$

3.7.3 Consistent mass matrix

The consistent element mass matrix $[M_e]$ is expressed as

$$[M_e] = \int_{-1}^{1} \int_{-1}^{1} [N]^T [P] [N] \left| J \right| d\xi d\eta \qquad (3.7.14)$$

where [N], the shape function matrix and [P], the inertia matrix

$$[N] = \begin{bmatrix} Ni & 0 & 0 & 0 & 0 \\ 0 & Ni & 0 & 0 & 0 \\ 0 & 0 & Ni & 0 & 0 \\ 0 & 0 & 0 & Ni & 0 \\ 0 & 0 & 0 & 0 & Ni \end{bmatrix} \quad i = 1 \ to \ 8$$

$$[P] = \begin{bmatrix} P_1 & 0 & 0 & P_2 & 0 \\ 0 & P_1 & 0 & 0 & P_2 \\ 0 & 0 & P_1 & 0 & 0 \\ P_2 & 0 & 0 & P_3 & 0 \\ 0 & P_2 & 0 & 0 & P_3 \end{bmatrix}$$

where,

$$(P_1, P_2, P_3) = \sum_{k=1}^{n} \int_{z_{k-1}}^{z_k} (\rho)_k (1, z, z^2) dz$$

The derivatives of the shape function N_i with respect to x,y are expressed in term of their derivatives with respect to ξ and η by the following relationship

$$\begin{bmatrix} N_{i,x} \\ N_{i,y} \end{bmatrix} = [J]^{-1} \begin{bmatrix} N_{i,\zeta} \\ N_{i,\eta} \end{bmatrix} \qquad (3.7.15)$$

where $[J] = \begin{bmatrix} \frac{\partial x}{\partial \zeta} & \frac{\partial y}{\partial \xi} \\ \frac{\partial x}{\partial \eta} & \frac{\partial y}{\partial \eta} \end{bmatrix}$

3.8 Computer program

A computer program is developed by using MATLAB environment to perform all the necessary computations. The element stiffness, geometric stiffness and mass matrices are derived using the formulation. Numerical integration technique by Gaussian quadrature is adopted for the element matrices. The overall matrices [K], [K_g], and [M] are obtained by assembling the corresponding element matrices. Reduced integration is used to avoid possible shear locking. The boundary conditions are imposed restraining the generalized displacements in different nodes of the discretized structure. The further details of program features and flow charts, used in this study are presented in Appendix II.

CHAPTER 4

EXPERIMENTAL PROGRAMME

4.1 Introduction

This chapter deals with the details of the experimental works conducted on the static analysis involving interlaminar shear strength (ILSS), free vibration and buckling of industry driven woven roving delaminated composite plates. Therefore composite plates are fabricated for the aforementioned experimental work and the material properties are found out by tensile test as per ASTM D3039/ D3039M (2008) guidelines to characterize the delaminated composite plates. The experimental results are compared with the analytical or numerical predictions. The experimental work performed is categorized in four sections as follows:

- **Static analysis**
- **Determination of material constants**
- **Vibration study**
- **Buckling study**

4.2 Experimental programme for static analysis

4.2.1 Materials

The following constituent materials were used for fabricating the laminate:

- Woven roving glass fiber as reinforcement
- Epoxy as resin
- Hardener
- Polyvinyl alcohol as a releasing agent
- Teflon foil for artificial introduction of delamination

4.2.2 Fabrication of specimens

In the present investigation, the glass:epoxy laminate was fabricated in a proportion of 50:50 by weight fractions of fiber: matrix. Araldite LY-556, an unmodified epoxy resin based on Bisphenol-A and hardener (Ciba-Geig, India) HY-951, aliphatic primary amine were used with woven roving E-glass fibers treated with silane based sizing system (Saint-Gobain Vetrotex) to fabricate the laminated composite. Woven roving glass fibers were cut into required shape and size for fabrication. Epoxy resin matrix was prepared by using 8% hardeners. Contact moulding in an open mould by hand lay-up was used to combine plies of woven roving (WR) in the prescribed sequence. A flat plywood rigid platform was selected. A plastic sheet i.e. a mould releasing sheet was kept on the plywood platform and a thin film of polyvinyl alcohol was applied as a releasing agent. Laminating starts with the application of a gel coat (epoxy and hardener) deposited on the mould by brush, whose main purpose was to provide a smooth external surface and to protect the fibers from direct exposure to the environment. Subsequent plies were placed one upon another with the matrix in each layer to obtain sixteen stacking plies. The laminate consisted of 16 layers of identically 0-90^{o} oriented woven fibers as per ASTM D2344/ D2344M (2006) specifications. Delaminations were introduced at 1, 2.5 and 3.5 cm lengths by providing Teflon film at the mid plane of the laminates through full width and equidistant from both ends of the specimen. The mould and lay up were covered with a release film to prevent the lay up from bonding with the mould surface. Then the resin impregnated fibers were placed in the mould for curing. The laminates were cured at normal room temperature under a pressure of 0.2 MPa for three days. After proper curing of the delaminated plates, the release films were detached. From the laminates the specimens were cut for three-point bend test (Figure 4.1a & 4.1b) by brick cutting machine into 45 x 6mm (Length x Breadth) size as per ASTM D2344/ D2344 specification and the thickness was taken as per the actual measurement. The average thickness of specimens for bend test is 4.8mm.

4.2.3 Bending test

The most commonly used test for ILSS is the short beam strength (SBS) test under three point bending. The SBS test was done as per ASTM D 2344/ D 2344 M (2006) by using the INSTRON 1195 material testing machine. The specimens were tested at 2, 50, 100, 200 and 500 mm/minute cross head velocities with a constant span of 34 mm to obtain interlaminar shear strength (ILSS) of intact and delaminated samples.

Before testing, the thickness and width of the specimens were measured accurately. The test specimen was placed on the test fixtures and aligned so that its midpoint was centered and it's long axis was perpendicular to the loading nose. The load was applied to the specimen at a specified cross head velocity. Breaking load of the sample was recorded. About five samples were tested at each level of experiment and their average value along with standard deviation (SD) and coefficient of variation (CV) were reported in result part.

The interlaminar shear strength was calculated using the formula,

$S = (0.75P_b)/bd$ as per ASTM D 2344

Where P_b is the breaking load in kg; b is the width in mm and d is the thickness in mm.

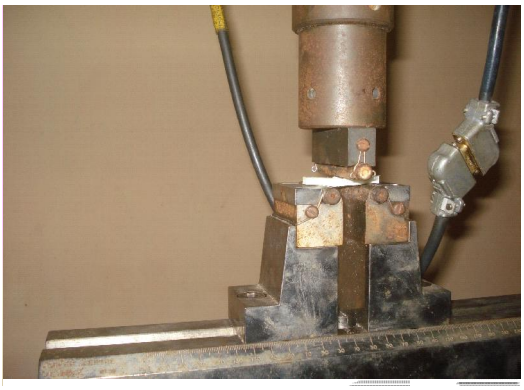

Figure 4.1 (a): Three point bend test setup and fixture

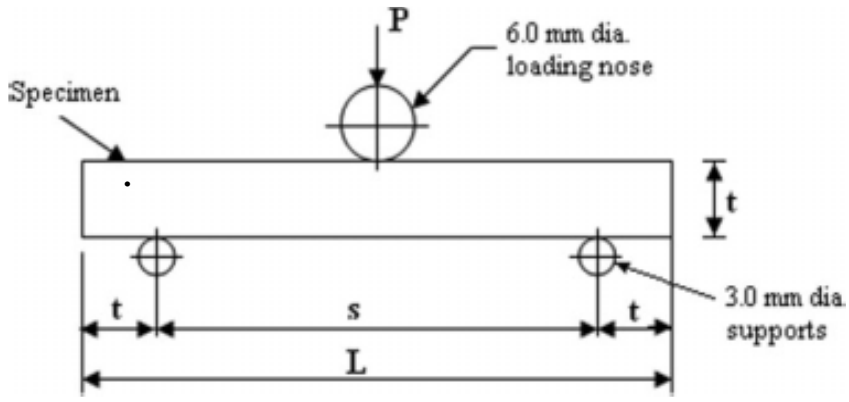

Figure 4.1 (b): Schematic diagram of three point bend test

4.2.4 Scanning electron microscope (SEM) test

After failure in bending test, 14 samples were selected for S.E.M. test. The test was conducted by Scanning electron microscope (JEOL-JSM-6480 LV) for each

selected sample at 3 different magnifications i.e., X700, X500 and X300 to study the crack pattern at the interface.

4.3 Determination of material constants

Laminated composite plates behave like orthotropic lamina, the characteristics of which can be defined completely by four material constants i.e. E_1, E_2, G_{12}, and υ_{12} where the suffixes 1 and 2 indicate principal material directions. For material characterization of composites, laminate having eight layers was fabricated to evaluate the material constants.

The constants are determined experimentally by performing unidirectional tensile tests on specimens cut in longitudinal and transverse directions, and at 45° to the longitudinal direction, as described in ASTM standard: D 3039/D 3039 M (2008). The tensile test specimens are having a constant rectangular cross section in all the cases. The dimensions of the specimen are mentioned below in Table 4.1.

Table 4.1: Size of the specimen for tensile test

Length(mm)	Width(mm)	Thickness(mm)
200	25	3

The specimens were cut from the plates themselves by diamond cutter or by hex saw as per requirement as shown in Figure 4.2 (a). Four replicate sample specimens were tested and mean values were adopted. The test specimens are shown in Figure 4.2. (b) to Figure 4.2(d).

Figure 4.2(a)

Figure 4.2(b)

Figure 4.2(c)

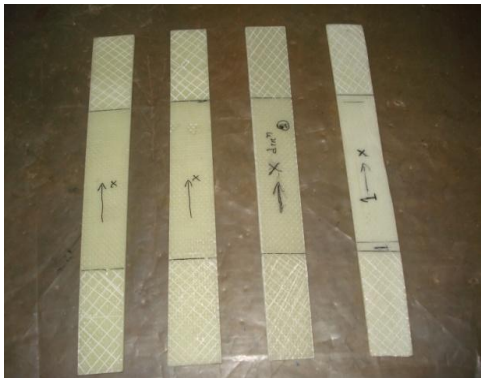

Figure 4.2(d)

Figure 4.2(a): Diamond cutter for cutting specimens, (b) Specimens in "Y" direction, (c) Specimens in "45^0" direction, (d) Specimens in "X" direction.

Coupons were machined carefully to minimize any residual stresses after they were cut from the plate and the minor variations in dimensions of different specimens are carefully measured. For measuring the Young's modulus, the specimen was loaded in INSTRON 1195 universal testing machine (as shown in Figure 4.3) monotonically to failure with a recommended rate of extension (rate of loading) of 0.2 mm/minute. Specimens were fixed in the upper jaw first and then gripped in the movable jaw (lower jaw). Gripping of the specimen should be as much as possible to prevent the slippage. Here, it was taken as 50mm in each side for gripping. Initially strain was kept at zero. The load, as well as the extension, was recorded digitally with the help of a load cell and an extensometer respectively. Failure pattern of woven fiber glass/epoxy composite specimen is shown in Figure 4.4. From these data, engineering stress vs. strain curve was plotted; the initial slope of which gives the

Young's modulus. The ratio of transverse to longitudinal strain directly gives the Poisson's ratio by using two strain gauges in longitudinal and transverse direction. But here Poisson's ratio is taken as 0.17.

The shear modulus was determined using the following formula from Jones [1975]as:

$$G_{12} = \frac{1}{\frac{4}{E_{45}} - \frac{1}{E_1} - \frac{1}{E_2} + \frac{2\vartheta_{12}}{E_1}}$$

The values of material constants finally obtained experimentally for vibration and buckling are presented in Chapter-5.

Figure 4.3: Tensile test of woven fiber glass/epoxy composite specimens

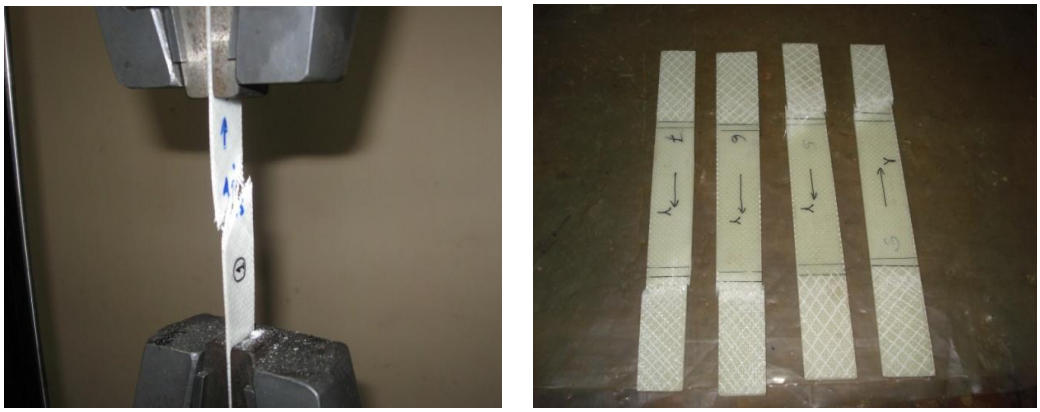

Figure 4.4: Failure pattern of woven fiber glass/epoxy composite specimen

4.4 Experimental programme for vibration study

4.4.1 Fabrication of specimens

The fabrication procedure for preparation of the plate in case of vibration study was same as in ILSS. Specimens are fabricated by hand layup technique and cured under room temperature. The laminate consisted of eight layers of identically 0-90^o oriented woven fibers. The artificial delaminations have been introduced at 6.25%, 25% and 56.25% area of composite plate by providing Teflon film centrally at mid-plane of the plate during fabrication. After completion of all the layers, again a plastic sheet was covered on the top of last ply by applying polyvinyl alcohol inside the sheet as releasing agent. Again one flat ply board and a heavy flat metal rigid platform was kept at the top of the plate for compressing purpose. The plates were left for a minimum of 48 hours before being transported and cut to exact shape for testing. Figure 4.5 (a-e) shows the fabrication process of delaminated composite plates. All the specimens are tested for free vibration analysis. The geometrical dimensions (i.e. length, breadth, and thickness), ply orientations and percentage of delamination of the fabricated plates are shown in Table-4.2.

All the specimens described in Table 4.2 were tested for its vibration characteristics. To study the effect of boundary condition on the natural frequency of delaminated plates, the plates were tested for three different boundary conditions (B.C) i.e. for four sides simply supported, fully clamped and cantilever. For different boundary conditions, one iron frame was used. Some of the test specimens with different boundary conditions are shown in Figure 4.6 (a-d).

Figure 4.5(a)

Figure 4.5(b)

Figure 4.5(c)

Figure 4.5(d)

Figure 4.5 (e)

Figure 4.5 (a): Application of gel coat on mould releasing sheet, (b) Placing of woven roving glass fiber on gel coat, (c) Removal of air entrapment using steel roller, (d) Teflon foil for artificial introduction of delamination, (e) Set-up for fabrication of delaminated composite plate

Table 4.2: Dimensions of composite plates with and without delamination

Size of plate in meter	No. of layers	% of delamination	Ply orientation	No. of delamination	No. of plates
0.237X0.237X0.003	8	0	$(0/90)_4$	0	5
0.237X0.237X0.003	8	6.25	$(0/90)_4$	1	5
0.237X0.237X0.003	8	25	$(0/90)_4$	1	5
0.237X0.237X0.003	8	56.25	$(0/90)_4$	1	5
0.237X0.237X0.0015	4	0	$(0/90)_2$	0	5
0.237X0.237X0.0015	4	25	$(0/90)_2$	1	5
0.237X0.237X0.0021	6	0	$(0/90)_3$	0	5
0.237X0.237X0.0021	6	25	$(0/90)_3$	1	5
0.237X0.237X0.003	8	0	$[(30/-30)_2]_s$	0	5
0.237X0.237X0.003	8	25	$[(30/-30)_2]_s$	1	5
0.237X0.237X0.003	8	0	$[(45/-45)_2]_s$	0	5
0.237X0.237X0.003	8	25	$[(45/-45)_2]_s$	1	5
0.240X0.240X0.003	8	25	$(0/90)_4$	1	5
0.240X0.120X0.003	8	25	$(0/90)_4$	1	5
0.240X0.160X0.003	8	25	$(0/90)_4$	1	5
0.237X0.237X0.003	8	6.25	$(0/90)_4$	1	5
0.237X0.237X0.003	8	25	$(0/90)_4$	1	5
0.237X0.237X0.003	8	56.25	$(0/90)_4$	1	5

Figure 4.6 (a)

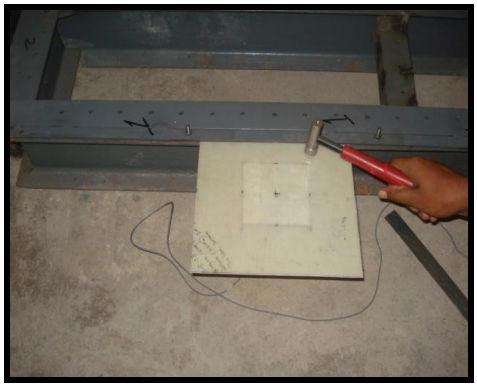

Figure 4.6 (b)

Figure 4.6 (c)

Figure 4.6 (d)

Figure 4.6 (a): Frame for different boundary condition,(b) Cantilever plate, (c) Four sides simply supported plate (d) Four sides clamped plate

4.4.2 Equipments for vibration test

In order to achieve the right combination of material properties and service performance, the dynamic behavior is the main point to be considered. To avoid the typical problems caused by vibrations, it is important to determine natural frequency of the structure and the modal shapes to reinforce the most flexible regions or to locate the right positions where weight should be reduced or damping should be increased. The fundamental frequency is a key parameter. The natural frequencies are sensitive to the orthotropic properties of composite plates and design-tailoring tools may help in controlling this fundamental frequency. Due to the advancement in computer aided data acquisition systems and instrumentation, experimental modal analysis or free vibration analysis has become an extremely important tool in the hands of an experimentalist.

The apparatus which are used in free vibration test are

- Modal hammer (type 2302-5)
- Accelerometer (type 4507)
- FFT Analyzer (Bruel Kajer FFT analyzer type –3560)
- Notebook with PULSE software.
- Specimens to be tested

The apparatus which are used in the vibration test are shown in Figure 4.7 to Figure 4.10.

Figure 4.7: Modal Impact Hammer (type 2302-5)

Figure 4.8: Accelerometer (4507)

Figure 4.9: Bruel & Kajer FFT analyzer

Figure 4.10: Display unit

4.4.3 Procedure for free vibration test

The setup and the procedure for the free vibration test are described sequentially as given below. The test specimens were fitted properly to the iron frame. The connections of FFT analyzer, laptop, transducers, modal hammer, and cables to the system were done. The pulse lab shop version-10.0 software key was inserted to the port of laptop. The plate was excited in a selected point by means of small impact with Impact hammer (Model 2302-5) for cantilever plates. The input signals were captured by a force transducer, fixed on the hammer. The resulting vibrations of the specimens on the selected point were sensed by an accelerometer. The accelerometer (B&K, Type 4507) was mounted on the specimen by means of bees wax. The signal was then processed by the FFT Analyzer and the frequency spectrum was also obtained. Both input and output signals are investigated by means of spectrum-analyzer (Bruel & kajer) and resulting frequency response functions are transmitted to a computer for modal parameter extraction. The output from the analyzer was displayed on the analyzer screen by using pulse software. Various forms of frequency response functions (FRF) were directly measured. However, the present work represents only the natural frequencies of the plates. For FRF, at each singular point the modal hammer was struck five times and the average value of the response was displayed on the screen of the display unit. At the time of striking with modal hammer to the points on the specimen precaution were taken for making the stroke to be perpendicular to the surface of the plates. Then by moving the cursor to the peaks of the FRF graph the frequencies are measured.

4.5 Experimental program for buckling study

4.5.1 Fabrication of specimens

Materials required and fabrication procedure followed for preparation of plates in case of buckling study was same as that used for vibration study. The geometrical dimensions (i.e. length, breadth, and thickness), ply orientations and percentage of delamination, number of delamination and number of the fabricated plates are shown in Table 4.3.The single delamination in composite plates (No of delamination:1) is provided in mid plane only for all number of layers as shown in figure 8.6 of Appendix I. The multiple delamination (No of delamination:3) is provided in 2^{nd}, 4^{th}

and 6th layer of 8 layer composite plates as shown in figure 8.7 of Appendix I. The size of delamination for different percentage of delamination is shown in figure 8.2, 8.3 and 8.4 of Appendix I.

Table 4.3: Dimensions of composite plates with delamination

Size of plate In "mm"	No. of layers	% of delamination	Ply stacking sequence	No. of delamination	No. of plates
240*190*3.5	8	0	$[0]_8$	0	5
240*190*4.5	12	0	$[0]_{12}$	0	5
240*190*6.5	16	0	$[0]_{16}$	0	5
200*150*3.0	8	0	$[0]_8$	0	5
200*150*3.0	8	0	$[30/-30]_{2s}$	0	5
200*150*3.0	8	0	$[45/-45]_{2s}$	0	5
190*160*3.5	8	0	$[0]_8$	0	5
190*120*3.5	8	0	$[0]_8$	0	5
190*80*3.5	8	0	$[0]_8$	0	5
240*190*3.5	8	25	$[0]_8$	1	5
240*190*4.5	12	25	$[0]_{12}$	1	5
240*190*6.5	16	25	$[0]_{16}$	1	5
200*150*3.0	8	25	$[0]_8$	1	5
200*150*3.0	8	25	$[30/-30]_{2s}$	1	5
200*150*3.0	8	25	$[45/-45]_{2s}$	1	5
190*160*3.5	8	6.25	$[0]_8$	1	5
190*120*3.5	8	6.25	$[0]_8$	1	5
190*80*3.5	8	6.25	$[0]_8$	1	5
240*190*3.5	8	6.25	$[0]_8$	1	5
240*190*3.5	8	25	$[0]_8$	1	5
240*190*3.5	8	56.25	$[0]_8$	1	5
240*190*3.5	8	6.25	$[0]_8$	3	5
240*190*3.5	8	25	$[0]_8$	3	5
240*190*3.5	8	56.25	$[0]_8$	3	5

For a plate of size 240mm×190mm with 6.25% delamination, the size of delamination adopted is 60 mm×47.5 mm.

4.5.2 Experimental set-up and procedure for buckling test

To obtain the experimental buckling result, the specimens were loaded in axial compression using INSTRON 1195 machine of 100 KN capacity. The specimen was clamped at two ends and kept free at the other two ends. A dial gauge was mounted at the centre of the specimen to observe the lateral buckling deflection. All specimens were loaded slowly until buckling took place. Clamped boundary conditions were simulated along the top and bottom edges, restraining 2.5cm length. For axial loading, the test specimens were placed between the two extremely stiff machine heads, of which the lower one was fixed during the test, whereas the upper head was moved downwards by servo hydraulic cylinder. All plates were loaded at constant cross-head speed of 0.5mm/minute. The test set up was shown in Figure 4.11 (a & b). As the load was increased the dial gauge needle started moving, and at the onset of buckling there was a sudden large movement of the needle. The load v/s end shortening (displacement) curve was plotted. The displacement is plotted on the X -axis and load is plotted on the Y- axis. The load, at which the initial part of the curve deviated linearity, was taken as the critical buckling load in line with previous studies.

Figure 4.11 (a): Composite plate before buckling

Figure 4.11 (a): Composite plate before buckling

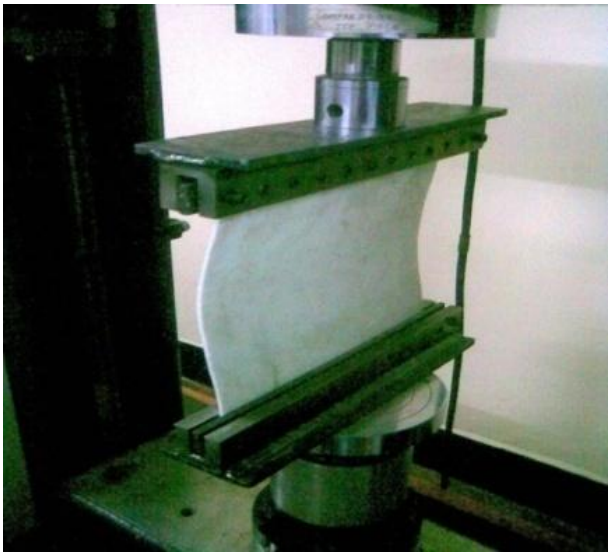

Figure 4.11(b): Composite plate after buckling

CHAPTER 5

RESULTS AND DISCUSSION

5.1 Introduction

The present chapter deals with the determination of interlaminar shear strength, natural frequency, buckling load and excitation frequency of composite plates with delamination. The vibrations, buckling and parametric resonance characteristics of delaminated composite plates are numerically studied by using the formulation given in the Chapter 3. The influence of various parameters like delamination size, number of layers, fiber orientation and aspect ratio on vibration, buckling and parametric resonance characteristics of delaminated composite plates are presented using numerical model. The experimental results on vibration and buckling of industry driven woven fiber glass/epoxy delaminated composite panels are also used to support the numerical predictions. The experimental static results involving the effect of different parameters on interlaminar shear strength (ILSS) of delaminated composite plates are also presented for completeness. The various studies made are presented below.

- **Static analysis**
- **Vibration analysis**
    i. Comparison with previous studies
    ii. Numerical and experimental result
- **Static stability analysis**
    i. Comparison with previous studies
    ii. Numerical and experimental result
- **Dynamic stability analysis**
    i. Comparison with previous studies
    ii. Numerical result

5.2 Static analysis

Delamination is one of the most critical failure modes in composite laminates. Interlaminar shear strength (ILSS) is an important parameter in determining the ability of a composite material to resist delamination damage in laminates. Therefore, there is a need for accurate prediction of the interlaminar shear strength of the delaminated composites in order that they may be properly designed to overcome failure. In the present investigation, ILSS of delaminated woven glass/epoxy laminates are studied at different loading speeds and the results are presented.

The inter laminar shear strength of undelaminated (0 cm), 1 cm, 2.5 cm and 3.5 cm delaminated woven glass/epoxy composite laminates at different loading speeds is presented in Table 5.1. The ILSS values of undelaminated specimen at 2, 50,100, 200 and 500 mm/minute. loading speeds were 27.93**,** 28.34, 28.67, 26.78 and 26.49 MPa; standard deviations (SD) were 0.55, 0.93, 1.05, 0.65 and 0.98 MPa and coefficient of variation (CV) were 1.97%, 3.28%, 3.69%, 2.43% and 3.70% respectively. For the 1 cm delaminated composite laminates the ILSS values at 2, 50,100, 200 and 500 mm/min. loading speed were 26.38, 27.64, 27.93, 25.41 and 24.98 MPa with the coefficient of variation of 2.35%, 1.88%, 1.40%, 2.84% and 2.88% respectively. The standard deviation of the 2.5 cm and 3.5 cm delaminated composite laminates varied from 0.61 to 1.24 MPa and 0.37 to 1.28 MPa respectively. This represents acceptable data correlation within the tests.

The figures 5.1 to 5.5 show the variations of changes-in-inter laminar shear strength of delaminated woven glass/epoxy composite laminates as a function of delamination length at different loading speeds. At 2 mm/minute loading speed, the ILSS value of 1cm delaminated glass/epoxy composite specimen (Figure 5.1) is found to be less than the laminated specimen. But the ILSS value of 2.5cm delaminated composite specimen is more than 1 cm delaminated laminate and 3.5cm delaminated specimen has the least ILSS value. At 50, 100, 200 and 500 mm/minute loading speeds (Figure 5.2, 5.3, 5.4 & 5.5) the change in ILSS values of delaminated specimen gradually decrease with the increase of delamination length. The discrepancy is only observed at 2mm/minute loading speed. The probable reason for this happening may be that at 2mm/minute loading speed the interfacial bonding of 1cm delaminated specimen is

affected by the presence of Teflon ends, which may prematurely nucleate weakening effect. Thus, the change in ILSS value is reduced. However, for 2.5cm delaminated specimen, the increase in the ILSS value may be due to the increase in interfacial bond strength between Teflon, fiber and polymer and subsequently there is an increase in ILSS value. The reduction in ILSS values (averaged over all the loading speeds, Table 5.2) for 1cm and 2.5cm delaminated specimens are 4.23% and 7.24% respectively with respect to control and non significant whereas for 3.5cm delaminated specimen the reduction is significant (12.37%). The present investigation clearly indicates that the change in ILSS value of delaminated specimens gradually decreases with the increase in delamination length.

Table 5.1: Mean, SD & CV in ILSS (MPa) value of glass/epoxy composite laminates at different delamination lengths and loading speeds

Loading speed (mm/min)	Delamination Length(cm)			
	Control (0 cm)	1 cm	2.5 cm	3.5 cm
2 mm				
ILSS	**27.93**	**26.38**	**27.67**	**24.61**
SD	0.55	0.62	1.24	1.18
CV	1.97%	2.35%	4.48%	4.80%
50 mm				
ILSS	**28.34**	**27.64**	**27.44**	**26.51**
SD	0.93	0.52	1.12	1.28
CV	3.28%	1.88%	4.08%	4.83%
100 mm				
ILSS	**28.67**	**27.93**	**24.10**	**22.96**
SD	1.05	0.39	0.61	0.37
CV	3.69%	1.40%	2.53%	1.61%
200 mm				
ILSS	**26.78**	**25.41**	**24.02**	**23.01**
SD	0.65	0.72	0.67	0.40
CV	2.43%	2.84%	2.79%	1.74%
500 mm				
ILSS	**26.49**	**24.98**	**24.96**	**24.03**
SD	0.98	0.72	0.83	0.93
CV	3.70%	2.88%	3.32%	3.87%

Note: SD = Standard deviation, CV = Coefficient of variation

Table 5.2: Percentage reduction in ILSS (MPa) value of 1 cm, 2 cm & 3.5 cm delaminated specimen

Delaminated specimen	Loading speed (mm/minute)						
	2	50	100	200	500	Mean	% reduction
0 cm	27.93	28.34	28.67	26.78	26.49	**27.64**	
1 cm	26.38	27.64	27.93	25.41	24.98	**26.47**	4.23
2.5 cm	27.67	27.44	24.10	24.02	24.96	**25.64**	7.24
3.5 cm	24.61	26.51	22.96	23.01	24.03	**24.22**	12.37*

*indicates significant at 5% probability level

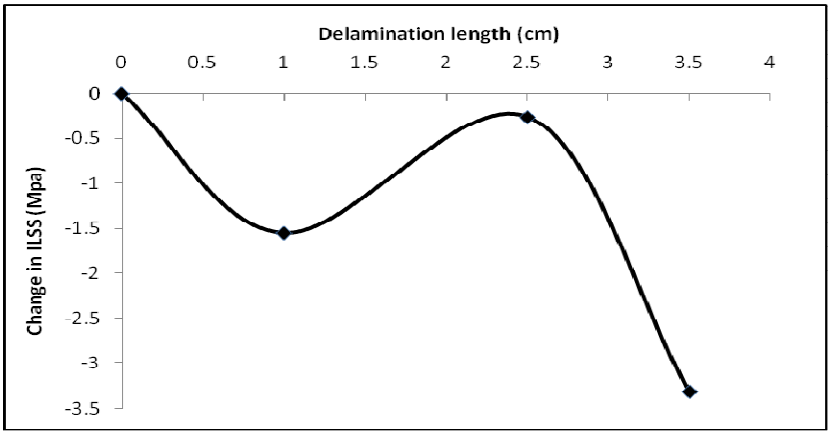

Figure 5.1: Variation of change in ILSS vs. delamination length of glass/epoxy at 2 mm/minute loading speed

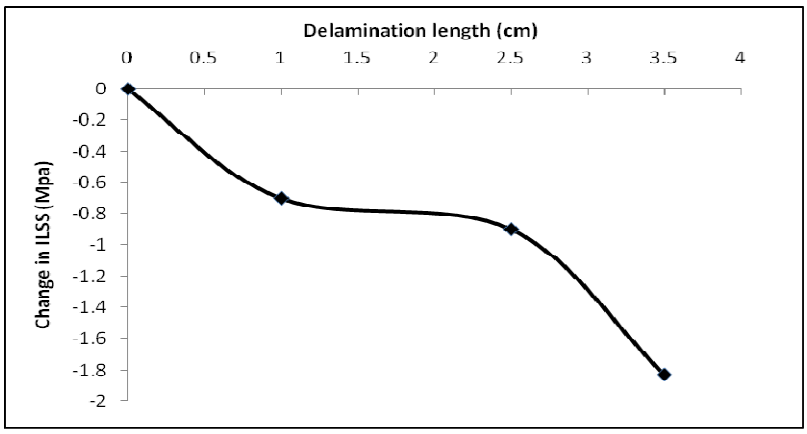

Figure 5.2: Variation of change in ILSS vs. delamination length of glass/epoxy at 50 mm/minute loading speed

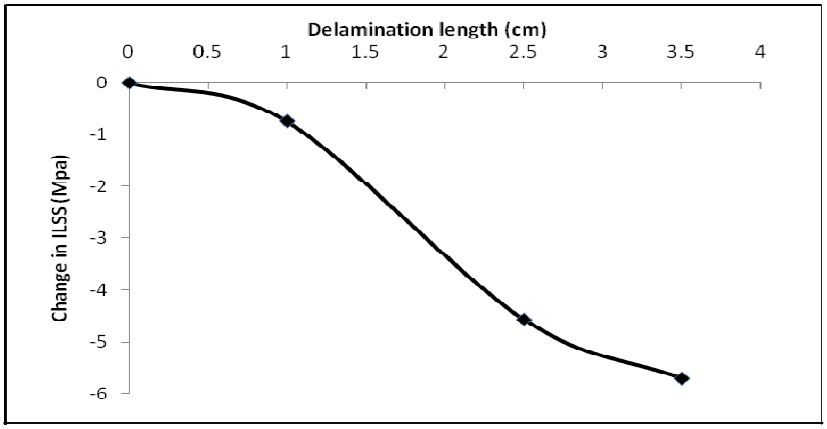

Figure 5.3: Variation of change in ILSS vs. delamination length of glass/epoxy at 100 mm/minute loading speed

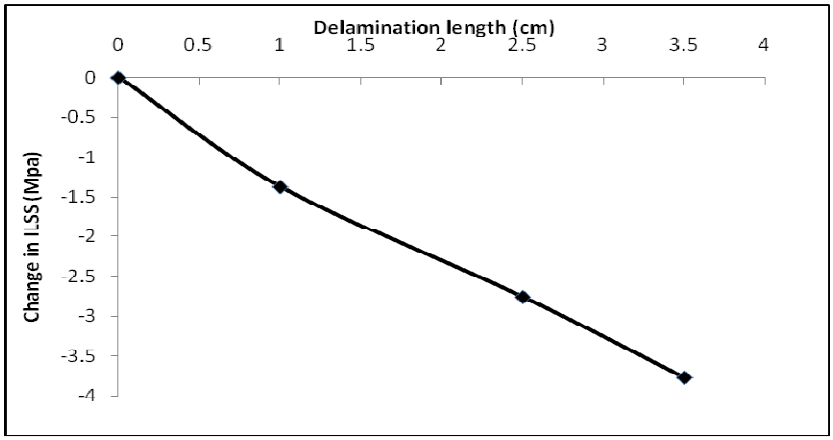

Figure 5.4: Variation of change in ILSS vs. delamination length of glass/epoxy at 200 mm/minute loading speed

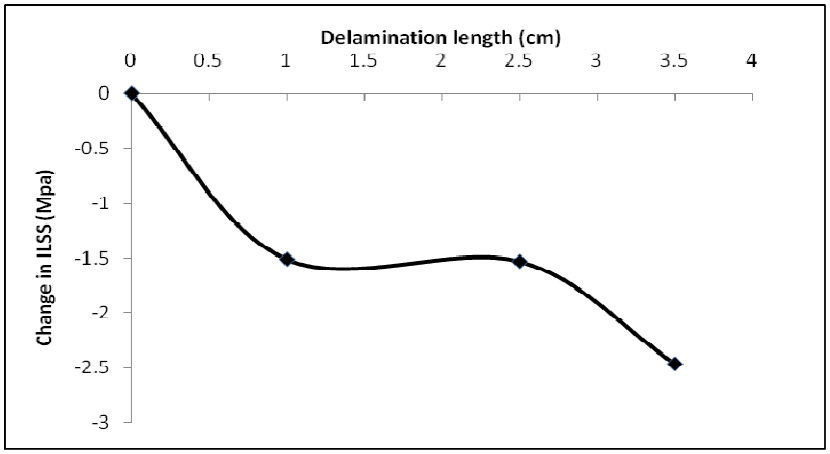

Figure 5.5: Variation of change in ILSS vs. delamination length of glass/epoxy at 500 mm/minute loading speed

Scanning electron microscope test result

The SEM micrographs for glass/epoxy show (Figure 5.6 & 5.7) that matrix cracking, fiber pull out, cohesive failure and interfacial cracking are dominating failure modes that nucleate damage in fractured surface of delaminated composite plates. The cleaner fibers and fiber breakage are prevalent in fractured surface of laminated glass/epoxy composites.

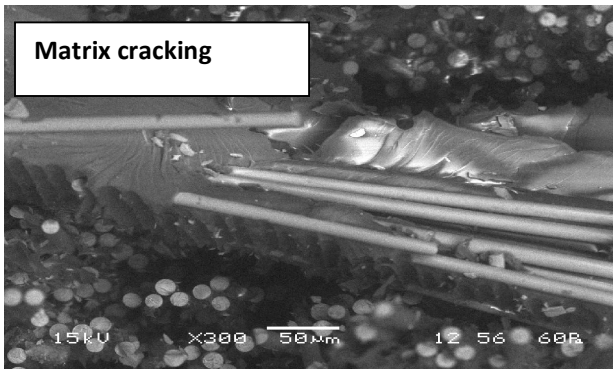

Figure 5.6: Scanning micrograph showing matrix cracking in laminated composites

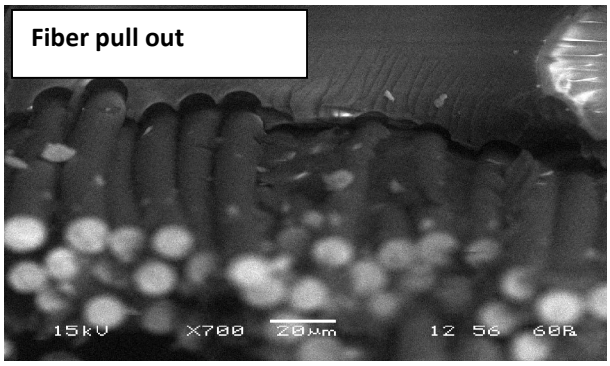

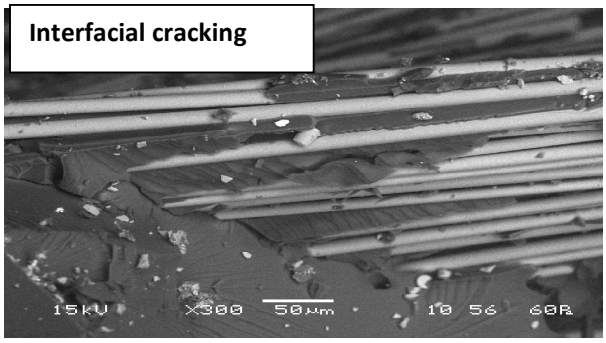

Figure 5.7: Scanning micrograph showing fiber pullout and interfacial cracking in delaminated composites.

5.3 Vibration analysis

Delamination in the composite plates, greatly affect the dynamic behavior of structures. So in the present investigation, natural frequency of delaminated industry driven woven fiber glass/epoxy composite plates were determined both numerically and experimentally. The effects of various parameters like delamination area, boundary conditions, fiber orientation, aspect ratio, number of layers and multiple delaminations were studied critically. Numerical and experimental results are presented for free vibration of delaminated composite plates after comparison with previous investigations.

5.3.1 Comparison with previous study

Based on the finite element formulation and delamination modeling mentioned in Chapter 3, programs are developed as per flow chart (given in appendix) for numerical computations. To validate the programs, the results for free vibration of laminated composite plate obtained by the present finite element formulation are compared with the results of Ju *et al.* (1995). As shown in Table 5.3, it is observed that there is an excellent agreement between two results.

Table 5.3: Comparison of frequency (Hz) for graphite/epoxy composite plates with different boundary conditions

E_{11}=132 GPa, E_{22}=5.35 GPa, G_{12}=2.79 GPa, ν_{12}= ν_{13}=0.291, ν_{23}=0.3, ρ=1446.20 kg/m^3, a=b=0.25m, h=0.00212m No. of layers=8, Lay up = $(0/90/45/90)_2$

Boundary Condition	Mode	Results of Ju *et al.* (1995)	Present FEM result
Four sides simply supported	1st	164.370	163.651
	2nd	404.380	400.918
	3rd	492.290	494.141
	4th	658.400	650.089
Four sides clamped	1st	346.590	342.543
	2nd	651.510	635.641
	3rd	781.060	766.589
	4th	1000.200	963.542
Cantilever	1st	41.350	41.162
	2nd	60.660	60.520
	3rd	221.52	220.461
	4th	258.72	257.709

Similarly the fundamental frequencies for a single delaminated composite cantilever beam, based on the present delamination modelling are compared with the analytical results of Shen and Grady (1992), FSDT results of Hu(1999) and HSDT of Hu (2002). The width of delamination is 12.7mm which is width of beam. As observed in Table 5.4, there exists excellent agreement between the present FEM results with literature.

Table 5.4: Comparison of frequency of cantilever composite beams (127mm × 12.7mm × 1.016mm) with different mid–plane delaminations

E_{11}=132 GPa, E_{22} =10.3 GPa, $G_{12=}$5.0 GPa, ν_{12}= 0.33, ρ =1480 kg/m^3, ply orientation = $((0/90)_2)_s$

Delamination length	Analytical (Shen and Grady 1992)	FSDT (Hu, 1999)	HSDT (Hu, 2002)	Present FEM
Intact	82.042	-	-	82.13
25.4 mm	80.133	-	-	81.97
50.8mm	75.285	76.643	75.369	78.41
76.2mm	66.936	-	-	64.55

Determination of material constants

The composite laminates of eight layers are fabricated to evaluate the material constants. Tensile tests on samples are performed following the procedure described in ASTM D2309/ D2309M (2008) standard and the characteristics of woven fiber glass/epoxy composite plate used for numerical study are presented in Table 5.5**.**

Table 5.5: Material properties of plates used for vibration

Lay-up	N	E_1(GPa)	E_2(GPa)	E_{45}(GPa)	G_{12}(GPa)	ν_{12}	ρ(kg/m^3)
WR	8	7.7	7.7	7.04	2.81	0.17	1661.25

N : - Number of layers, E_{45} :- Tensile modulus obtained in 45° tensile test

E_1, E_2 :- Elastic modulus in longitudinal (1) and transverse direction(2) respectively.

G_{12} :- In-plane shear modulus , ν_{12} :- Poisson's ratio

ρ :- Density

5.3.2 Numerical and experimental results

In the present investigation, both the numerical computation and experimental study are carried out for an eight-layered $(0/90)_4$ woven roving glass/epoxy composite plate. The geometrical dimensions considered for the woven roving composite plates are: length, a = width, b = 0.24m, thickness, h = 0.003m. The material properties of the woven roving glass/epoxy composite plates are considered as given in Table 5.5. Square size delamination was introduced at the mid-plane as shown in Figure 5.8. In this study, the effects of delamination area, boundary conditions, fiber orientations, number of layers and aspect ratio on the natural frequencies are investigated.

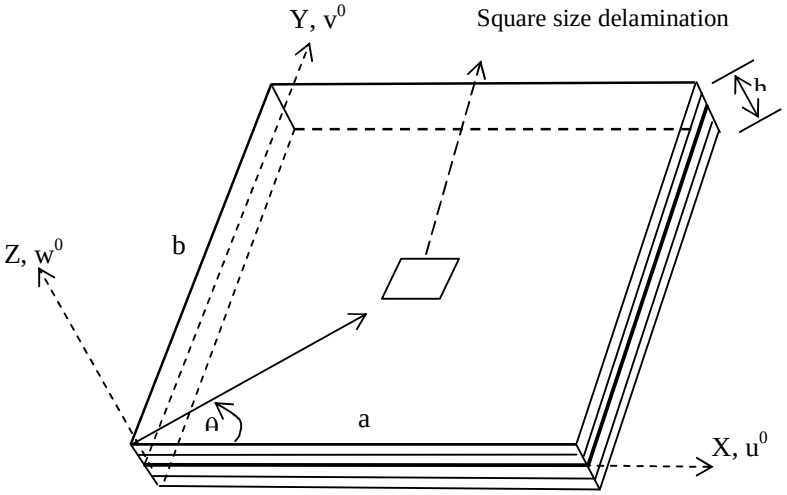

Figure 5.8: Laminated composite plate with mid-plane delamination

5.3.2.1 Effects of delamination area

To study the effects of delamination area on the natural frequencies of an eight layered delaminated plate, square size mid-plane delaminations were introduced at 6.25%, 25% and 56.25% of total plate area. The fundamental natural frequency of the delaminated $(0/90)_4$ plate is depicted in Figure 5.9 as a function of delamination area for a cantilever specimen. The result for natural frequency obtained from numerical analysis is found to be in a good agreement with the experimental result. The experimental fundamental frequencies of 6.25%, 25% and 56.25% delaminated plates

are found to decrease by 10%, 14% and 22 % respectively as compared to the laminated plate. This may be due to reduction in stiffness of the laminates.

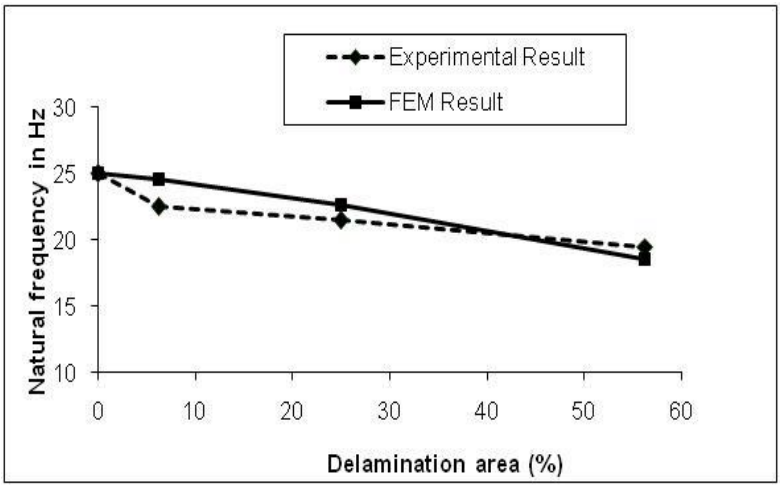

Figure 5.9: Variation of fundamental natural frequency with delamination area of woven fiber cantilever composite plates

The same study was extended to the composite plates with four sides clamped and four sides simply supported boundary conditions, the results of which are presented in Figure 5.10 & 5.11, respectively. The numerical results showed a good agreement with the experimental results for both clamped and simply supported boundary conditions. The experimental fundamental natural frequencies of 6.25%, 25% and 56.25% delaminated plates are found to decrease by 14%, 19.5% and 35 % for four sides simply supported boundary condition and 5.23%, 22% and 32% for four sides clamped condition as compared to the intact plate. This result reveals that at low delamination area (6.25%) the natural frequency of four sides clamped boundary condition is least affected as compared to cantilever boundary condition and four sides simply supported condition.

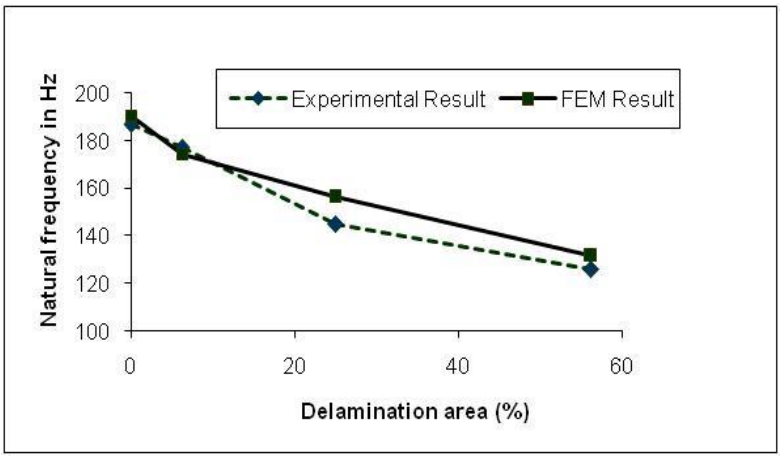

Figure 5.10: Variation of natural frequency with delamination area of four sides clamped woven fiber composite plates

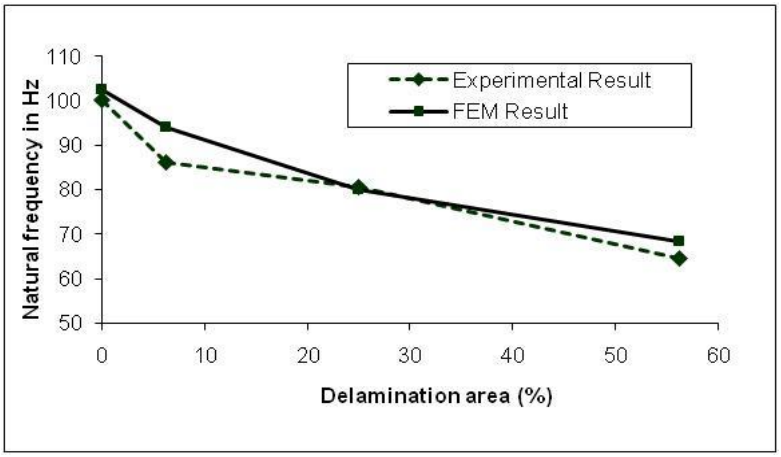

Figure 5.11: Variation of natural frequency with delamination area of four sides simply supported woven fiber composite plate

At high delamination area (56.25%) the natural frequency is least affected for cantilever boundary condition as compared to other two boundary conditions. But relatively large delamination area has considerable effect on the fundamental natural frequency of all the three boundary conditions. From the present investigation, it is noticed that the natural frequency decreases in general with the increase of delamination area invariably for all the three boundary conditions.

5.3.2.2 Effects of boundary condition

To investigate the influence of boundary conditions on natural frequencies of delaminated plates, three types of boundary conditions are considered, namely, S-S-S-S(four edges simply supported),where $u=w=\theta_y=0$, at x=0, a and $v=w=\theta_x=0$, at x=0, a; C-C-C-C (four edges clamped), where $u= v=w= \theta_x= \theta_y=0$, at x=0, a and y=0, b; C-F-F-F (cantilever), where $u= v=w= \theta_x= \theta_y=0$, at x=0. The specimen taken for the study was of eight layered composite plate having stacking sequence of $(0/90)_4$ with 25% of delamination area.

Natural frequencies of 25% delaminated composite plates for experimental and numerical results under different boundary conditions are given in Table 5.6. From this Table it is observed that the numerical and experimental results are in good agreement for all the boundary conditions. The 1st, 2nd and 3rd mode natural frequencies are found to be the least (21.5, 47.0 & 135.7 Hz) for C-F-F-F (cantilever) condition and the highest (145.0, 285.0 & 450.0 Hz) for C-C-C-C (four sides clamped) condition. The experimental fundamental natural frequency of 25% delaminated plate with four sides simply supported and cantilever boundary conditions are decreased by 44.48% and 85.17% respectively with respect to four sides clamped condition.

Table 5.6: Natural frequencies (Hz) of experimental and FEM results for 25% delaminated plate at different boundary conditions

Boundary conditions	Experimental result			FEM result		
	1st mode	2nd mode	3rd mode	1st mode	2nd mode	3rd mode
Four sides clamped	145.0	285.0	450.0	156.4	295.2	471.2
Four sides simply supported	80.5	186.0	330.0	79.9	200.6	349.4
Cantilever	21.5	47.0	135.7	22.7	48.5	128.4

This experimental result implies that the natural frequencies of delaminated plates are greatly dependent on the boundary conditions, i.e. the more strongly the plate is restrained, the greater is the effect of the delamination on the natural frequencies for all the cases.

5.3.2.3 Effects of fiber orientations

In order to know the effect of fiber orientations on natural frequencies of 25% delaminated plate (8-layers), three types of fiber orientations i.e. $[(0/90)_2]_s$, $[(30/-30)_2]_s$, $[(45/-45)_2]_s$ are considered. In this study the changes in the natural frequency as a function of fiber orientation are presented in Figure 5.12 for cantilever boundary condition. The results obtained from free vibration of the plates of both experimental and present FEM analysis are in good agreement. From Figure 5.12, it is observed that the experimental fundamental natural frequency of 25% delaminated plate with 30° and 45° orientation is decreased by 2.32% and 9.30% respectively with respect to the 0° orientation. This reveals that the fundamental natural frequency of delaminated plate decreases with the increase in fiber orientation but the decrease in the fundamental natural frequency is not conspicuous.

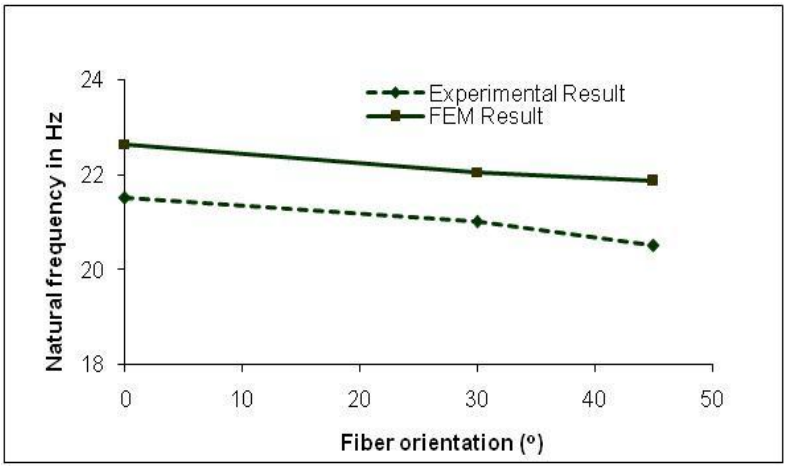

Figure 5.12: Variation of natural frequency with fiber orientation for 25% delaminated woven fiber cantilever composite plate

5.3.2.4 Effects of number of layers of laminate

To examine the effects of number of layers on natural frequency of 25% delaminated $[(0/90)_4]$ plate, three different types of laminate are fabricated, i.e. made

up of 4, 6 and 8 layers, respectively . All the geometrical and material properties of the laminates are same as given in Table 5.5 except the density. The density of the laminates taken for the study was 1402 kg/m^3 and 1599 kg/m^3 for 4 layers and 6 layers respectively. The natural frequencies for free vibration as obtained from experimental study and numerical analysis for cantilever boundary condition show a good agreement as shown in Figure 5.13. The change in natural frequencies as a function of number of layers as depicted in Figure 5.13 reveals that the fundamental natural frequency of delaminated composite plate increases with the increase in number of layers. The increase in the experimental fundamental natural frequency of 25% delaminated plate is 29% and 79% for 6 layers and 8 layers laminate respectively as compared to a 4 layered laminate. This result indicates that relatively more number of layers have considerable positive effect on the fundamental natural frequency of delaminated composite plate.

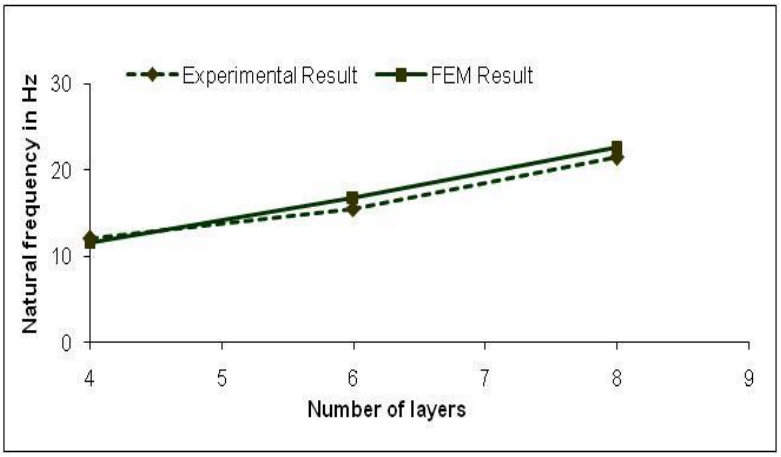

Figure 5.13: Variation of natural frequency with number of layers for 25% delaminated woven fiber composite plate

5.3.2.5 Effects of aspect ratio

To investigate the influence of aspect ratio on natural frequencies of an eight layered 25% delaminated $(0/90)_4$ plate, three different types of aspect ratios i.e. a/b= 1.0, 1.5 and 2.0 are considered. For different aspect ratios, the plate dimension varied, keeping the thickness of the plate (h=0.003m) unchanged. For the aspect ratio of 1.0, a=0.24m and b=0.24m; for 1.5, a=0.24m and b=0.16m; for 2.0, a=0.24m and b=0.12m. The variation in the fundamental natural frequencies as a function of aspect

ratio is given in Figure 5.14 for cantilever boundary condition. A good agreement is observed between numerical and experimental results. The experimental fundamental natural frequency of 25% delaminated plate with 1.5 & 2.0 aspect ratio is found to increase by 2 times and 4 times respectively as compared to 1.0 aspect ratio. This indicates that increase in the aspect ratio increases the natural frequency of a delaminated composite plate.

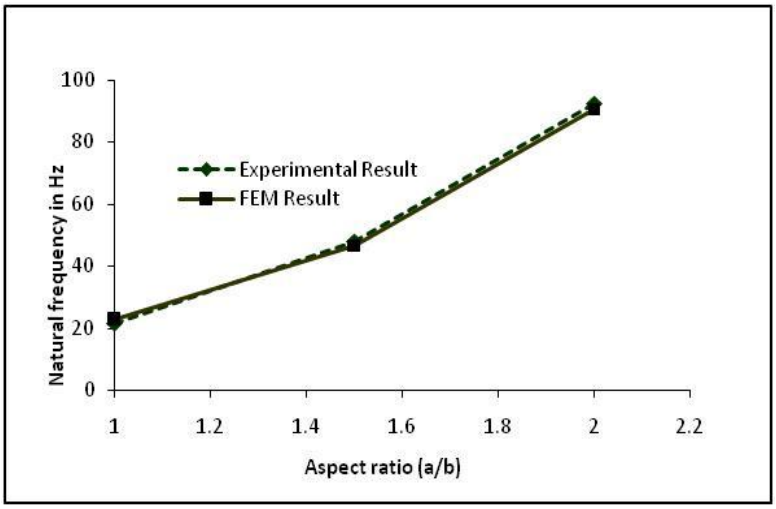

Figure 5.14: Variation of natural frequency with aspect ratio for 25% delaminated woven fiber cantilever composite plates

5.3.2.6 Effects of multiple delaminations

To investigate the effects of multiple delaminations, three types of composites plates with delaminations are considered. Each plate consists of eight layers with a stacking sequence of $(0/90)_4$.The delamination is presumed to be located at 2^{nd} , 4^{th} and 6^{th} layer. The percentage of delamination size is of 6.25%, 25% and 56.25%. The results are found out numerically and are given in Table 5.7 for cantilever boundary condition and four sides clamped boundary conditions.

The variation of natural frequencies with increased percentage of delimitation area for multiple delaminated clamped and cantilever composite plates is shown graphically in Figure 5.15. It is noted that there is a decrease in fundamental natural frequency of multiple delaminated plates with the increase in delamination area as

compared to single delaminated plate for both the boundary conditions. At 6.25 % delamination area the decrease is quite more (28%) for cantilever boundary condition as compared to clamped boundary condition. But at higher delamination area the decrease is more or less same for both the boundary conditions. From the present numerical results (Table 5.7) it is also observed that, in comparison to single delamination, the fundamental frequencies of vibration of delaminated composite plates reduce significantly with multiple delamination.

Table 5.7: Variation of natural frequency for delaminated clamped and cantilever composite plates with different % of delamination area

% of delamination area	mode	Clamped BC (natural frequency in Hz)			Cantilever BC (natural frequency in Hz)		
		Single delamination	Multiple delamination	% reduction in multiple delamination w.r.t control	Single delamination	Multiple delamination	% reduction in multiple delamination w.r.t control
Control (0)	1st	190.54	190.54	--	25.1	25.1	--
	2nd	390.37	390.37		54.8	54.8	
	3rd	576.82	576.82		149.36	149.36	
6.25	1st	174.38	166.74	12.0	24.63	18.26	28.0
	2nd	373.18	358.70		53.15	43.719	
	3rd	556.59	550.35		144.62	107.52	
25	1st	156.38	133.0	30.0	22.65	15.92	36.0
	2nd	295.22	239.25		48.47	38.20	
	3rd	471.24	364.19		128.42	88.06	
56.25	1st	131.64	81.27	57.0	18.55	11.38	56.0
	2nd	258.96	166.45		40.95	29.06	
	3rd	388.35	265.65		107.09	60.79	

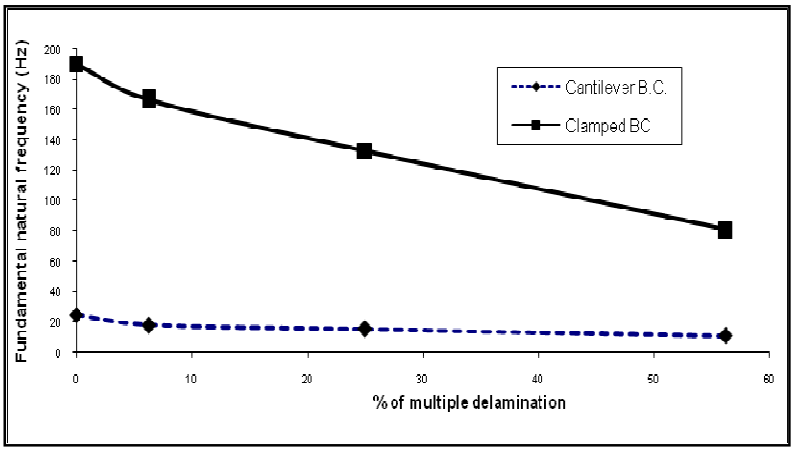

Figure 5.15: Variation of natural frequency of multiple delaminated clamped and cantilever plates with different percentage of delamination area

5.3.3 Pulse report

The Natural frequencies of the free vibration analysis are found out experimentally by using pulse software. Typical pulse reports for the delaminated composite plate (for a/b ratio 1.5, and 25% of delamination) are shown in Figure 5.16 to Figure 5.18. The peaks of the FRF shown in Figure 5.16 give the different natural frequencies of vibration. The coherence shown in Figure 5.17 gives indication of the accuracy of measurement. The variation of the applied force with time (Figure 5.18) gives indication of the magnitude of applied force with time and also number of hits.

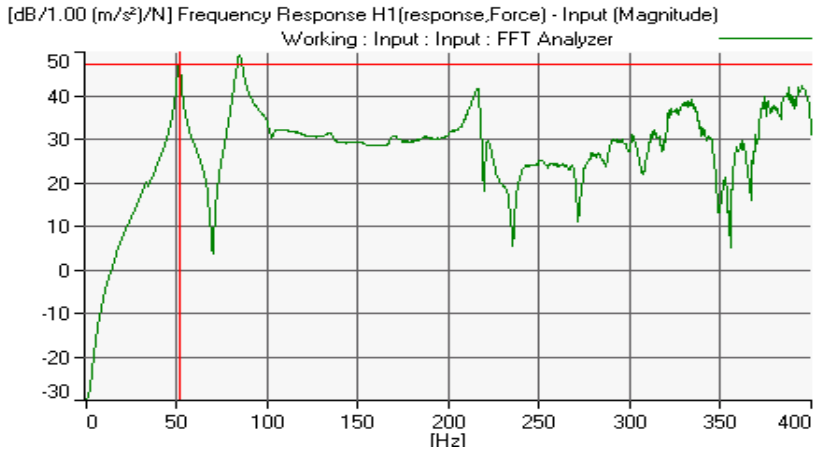

Figure 5.16: Frequency response function spectrum (In X-axis: Frequency in Hz, In Y-axis: Acceleration per force $(m/s^2)/N$)

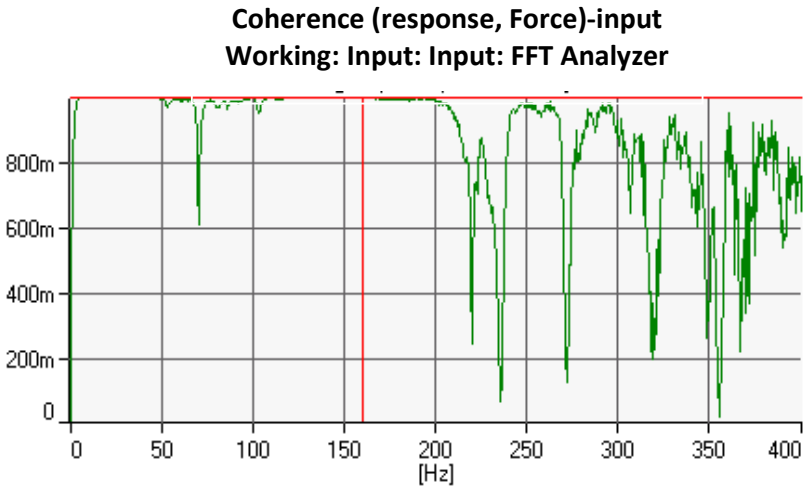

Figure 5.17: Coherence (Response, Force)

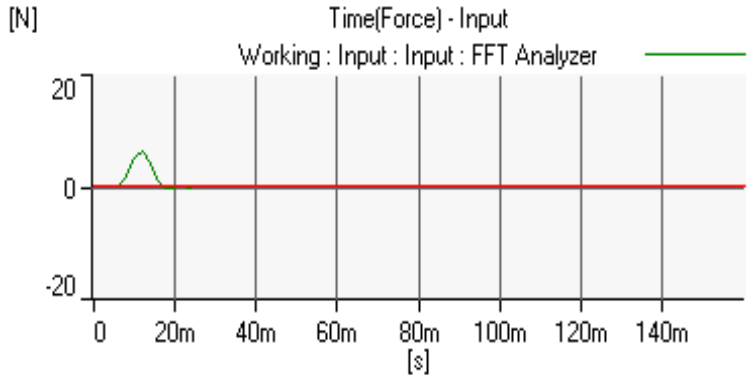

Figure 5.18: Applied force Vs time curve (In X-axis: Time in‘s’, In Y-axis: force in N)

5.4 Buckling/static stability analysis

The presence of delamination may significantly reduce the stiffness and strength of the structures and may affect some design parameters such as the buckling strength of the structure. So in the present investigation the critical buckling load of delaminated glass/epoxy composite plates were determined both numerically and experimentally. The effects of various parameters like delamination area, boundary conditions, fiber orientations, aspect ratio, number of layers and multiple delaminations were studied critically. Numerical and experimental results are presented for buckling load of delaminated composite plates after comparison with previous investigations.

5.4.1 Comparison with previous study

Based on the finite element formulation and delamination modeling, programs are developed for numerical computations. To validate the programs, the results for buckling of laminated composite plate, obtained by the present finite element formulation are compared with the results of Baba (2007) for clamped-free-clamped-free boundary condition. The rectangular plate had eight layers of E-glass/epoxy composites. As shown in Table 5.8, it is observed that there is an excellent agreement between two results.

Table 5.8: Comparison of buckling load (Newton) for laminated C-F-C-F composite plates

E_1 =39.0 GPa, E_2=E_3=8.2 GPa, G_{12}=G_{13}=G_{23}=2.9 GPa , ν_{12}= ν_{23}= ν_{31}=0.29, Length=150 mm, width=25 mm, thickness=1.5 mm

Fiber orientation	Baba (2007)	Present FEM	% error
$[0]_8$	482.42	481.71	0.14%
$[90]_8$	106.33	101.42	4%
$[0/90]_{2s}$	366.52	364.78	0.47%
$[(0/90)_2]_{as}$	290.22	287.46	0.96%

The buckling loads of delaminated composite plate are computed using present formulation and are also compared with those results published by Pekbey and Sayman (2006) for clamped-free-clamped-free boundary condition. The results obtained from both are presented in Table 5.9. The Comparison results show that there exist an excellent agreement between the present FEM and the previously published results of other investigators.

Table 5.9: Comparison of buckling load (Newton/mm) for delaminated C-F-C-F composite plates

E_1 =27.0 GPa, E_2 =21.5 GPa, G_{12} =7.5 GPa, ν_{12}=0.15

Dimension of plate in mm	Fiber orientation	Pekbay and Sayman(2006)	Present FEM
200 x 160 x 1.7	$[0]_8$	6.42	6.919
200 x 160 x 1.	$[30/-30]_{2s}$	5.64	6.251
200 x 160 x 1.7	$[45/-45]_{2s}$	5.38	5.795

5.4.2 Experimental and numerical results

After validating the formulation with the existing literature, both the experimental and numerical results for non-dimensional buckling load (as per Table 5.13) of delaminated composite plates are carried out for the eight-layered $(0/90)_4$ woven roving glass/epoxy composite plate. The material properties (determined by tensile testing of specimens) of the woven roving composite plates which are used for numerical studies are presented in Table 5.10. Square size delamination was provided at the mid-plane. In this study, the effects of delamination area, fiber orientations, number of layers, aspect ratio and multiple delamination on the critical buckling load are investigated under clamped free clamped free boundary condition.

Table 5.10: Material properties of the plate for buckling analysis

Lay-up	N	E_1 (GPa)	E_2 (GPa)	E_{45} (GPa)	G_{12} (GPa)	ν_{12}	ρ (kg/m^3)
WR	8	7.4	7.4	5.87	2.18	0.17	1661.25

5.4.2.1 Effects of delamination area

The variation of non-dimensional buckling load of single delaminated composite plate $(0/90)_4$ with increasing delamination area is shown in Figure 5.19. To study the effects of delamination area on the critical buckling loads of delaminated plates, mid-plane delaminations were introduced at 6.25%, 25% and 56.25% of total plate area of an eight layered laminated plate. The size of plate is taken as 240mm x190mm x3.5mm. Five identical specimens for each specimen design are tested to get an average buckling load. The non-dimensional buckling loads of the delaminated plates are depicted in Figure 5.19 as a function of delamination area for clamped-free-clamped-free boundary condition (B.C). The result for critical buckling loads obtained from numerical analysis is found to be in a good agreement with the experimental result. The experimental critical buckling load of 6.25%, 25.0% and 56.25% delaminated plates decreased by 11%, 28% and 52% respectively from the plate without delamination (Table 5.11). From this study it is observed that for increasing percentage of delamination area there is a decrease in non-dimensional buckling load because of the reduction of stiffness.

Table 5.11: Variation of buckling load (KN) of delaminated CFCF composite plates

% of delamination	Present FEM results	Experimental result	% reduction
0	7.079	7	-
6.25	6.238	6.75	11.0
25	5.079	5.75	28.0
56.25	3.358	3.9	52.0

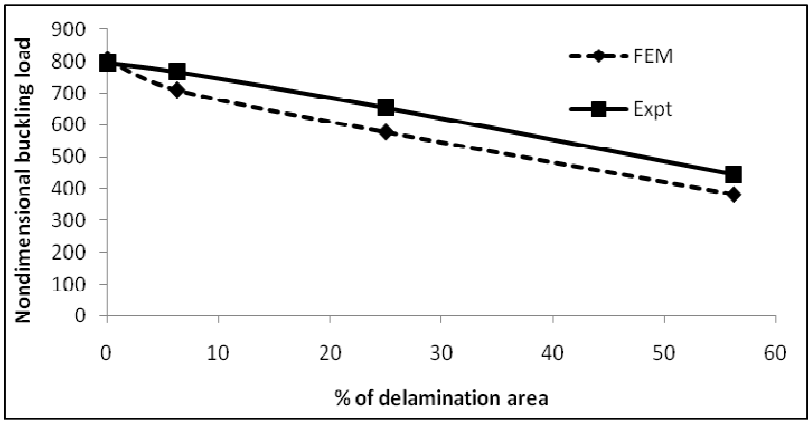

Figure 5.19: Variation of non-dimensional buckling load of single delaminated CFCF composite plate with increasing delamination area

5.4.2 .2 Effects of fiber orientations

Fiber orientation angle is the main parameter for controlling buckling load capacity of composite plates. To investigate the effect of fiber orientations on non-dimensional buckling load of 25% delaminated plate, three types of fiber orientations are considered. i.e. $[0]_{8,}$ $[(30/\text{-}30)_2]_{s,}$ $[(45/\text{-}45)_2]_s$. To orient the fiber in a specified angle, the fabric is initially given a rotation equal to ply orientation and cut to the desired size. The size of plate is taken as 200mm x150mm x3.0mm. The variation of non-dimensional buckling load as a function of fiber orientation for both experiment and numerical solution is presented in Figure 5.20. From this figure it is shown that there is good agreement between experimental and FEM results for 25% delaminated plate. It is observed that as the fiber orientation increases, the non-dimensional buckling load decreases for 25% delaminated plate. It is greatest for fiber orientation angle 0°. The experimental critical buckling load of 25% delaminated plate with 30° and 45° orientation is decreased by 8% and 19% with respect to 0° orientation. So, 25% delaminated plate has a more reliable buckling load when it has $[0]_8$ fiber orientation. It may be observed that, the plates yield highest stability resistance when fibers are aligned along the load direction. From the above results, it is understood that the fiber orientation of the lamina may be used as an index for quality control and a safety factor for the laminated composites.

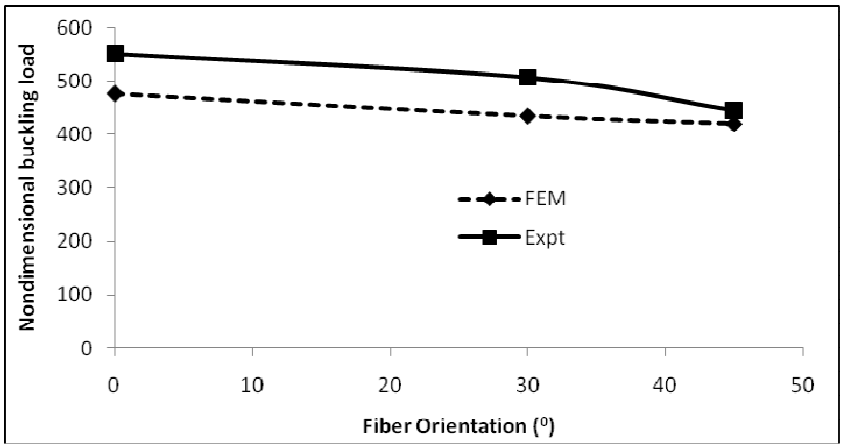

Figure 5.20: Variation of non-dimensional buckling load with fiber orientation for 25% single delaminated woven roving composite plate

5.4.2.3 Effects of number of layers of laminate

To examine the effects of number of layers on 25% delaminated plate with single mid-plane delamination, three different types of laminate are fabricated, which are made up of 8, 12 and 16 layers. The stacking sequence of each plate are $[0]_8$, $[0]_{12}$, $[0]_{16}$. Variation of non-dimensional buckling load with number of layers of composite laminate with 25% delamination (both numerical and experimental results) is graphically presented in Figure 5.21. It is shown that there is good agreement between experimental and FEM results for 25% delaminated plate under clamped-free-clamped-free boundary condition. From Figure 5.21, it is observed that as the number of layers increases the non-dimensional buckling load also increases both experimentally and numerically. The increase in the experimental buckling load of delaminated plate is 2.1 times (108.7%) for 12 layers and 5.91 times (491.3%) for 16 layered laminate as compared to an 8 layered laminate. From this study, it is evident that relatively more number of layers may increase the stability of delaminated composite structures. This result clearly indicates that number of layers had tremendous positive effect on the non-dimensional buckling load of delaminated plate. So this parameter must be considered with due emphasis for safety factor of laminated composite plates with delaminations.

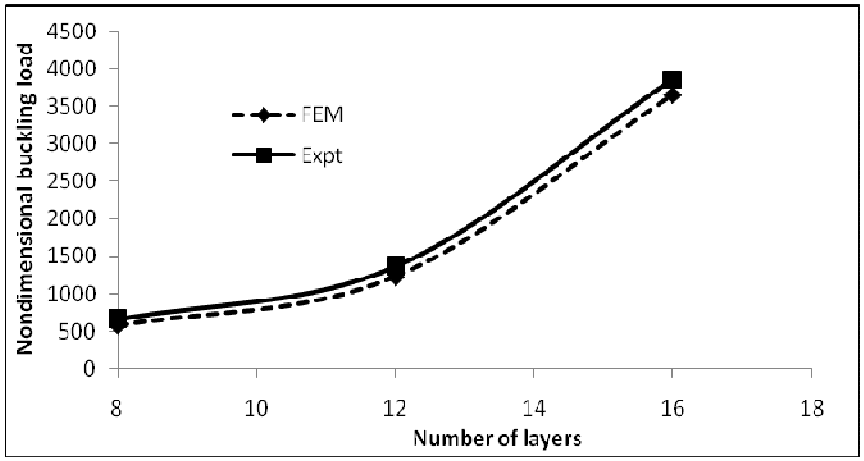

Figure 5.21: Variation of non-dimensional buckling load of 25% single delaminated CFCF cross ply plate with number of layers

5.4.2.4 Effects of aspect ratio

To investigate the influence of aspect ratio on non-dimensional buckling load of an eight layered 6.25% single delaminated $(0/90)_4$ plate, four different types of aspect ratios i.e. a/b = 0.79 (a =190mm and b =240mm), 1.18 (a =190mm and b=160mm), 1.58 (a =190mm and b =120mm) and 2.38 (a = 190mm and b = 80mm) are considered. For different aspect ratios, the plate dimension varied, keeping the thickness of the plate (h=0.0035m) unchanged. The variation of non-dimensional buckling load as a function of aspect ratio is given in Figure 5.22. It is observed that buckling load of delaminated composite plate decreases with the increase in aspect ratio. A good agreement is observed between numerical and experimental results. By increasing the aspect ratio from 0.79 to 1.18, 1.58 & 2.38, the critical buckling load of delaminated plate is found to be decreased by 33.3%, 44.4% and 63.0% respectively. This indicates that increase in the aspect ratio decreases the non-dimensional buckling load of a delaminated plate.

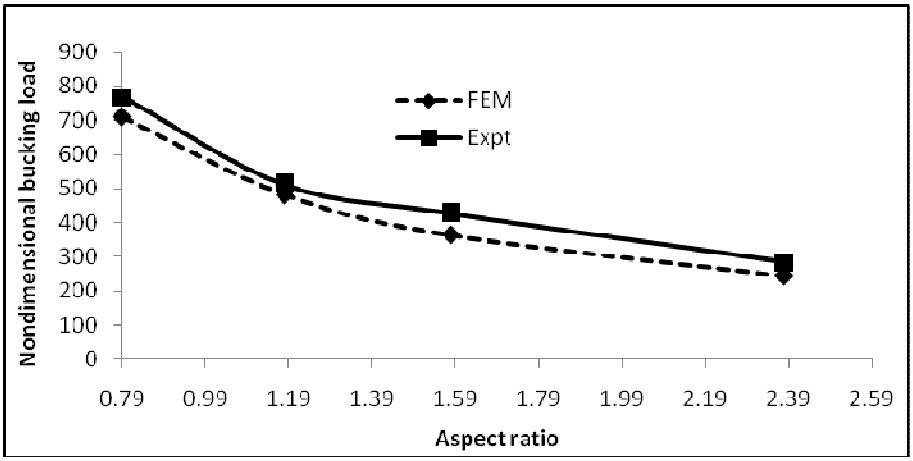

Figure-5.22: Variation of non-dimensional buckling load with different aspect ratios of 6.25% delaminated CFCF woven fiber composite plate

5.4.2.5 Effects of multiple delaminations

To investigate the effect of multiple delaminations, three types of composites plates with delaminations are considered. Each plate consists of eight layers with a stacking sequence of $[0]_{8.}$ The size of plate is taken as 240mm x190mm x3.5mm.The delamination is located at midplane, 2nd and 6th layer. The percentage of delamination is 6.25%, 25% and 56.25%. The results are found out numerically and experimentally. Numerical and experimental results of buckling analysis of composite plate with different % of delamination and without delamination for multiple delaminated composite plates with clamped-free-clamped-free boundary condition are presented in Table 5.12.

Table 5.12: Comparison of numerical and experimental results of buckling load (KN) of delaminated composite plates

% of delamination area	Present FEM result		Experimental result	
	Multiple delaminated plate	Single delaminated plate	Multiple delaminated plate	Single delaminated plate
0	7.079	7.079	7	7.0
6.25	5.672	6.24	6.4	6.75
25	2.746	5.08	3.25	5.75
56.25	1.155	3.36	1.5	5.9

The variation of non-dimensional buckling load of multiple delaminated plates as a function of delamination area is depicted in Figure 5.23 for clamped-free-clamped-free boundary condition. Figure 5.23 shows good agreement between experimental and FEM result for multiple delaminated composite plate. From Figure 5.23 and Table 5.12, it can be seen that the non-dimensional buckling load of multiple delaminated plate decreases as percentage of delamination increases both numerically and experimentally. Also with the increase in the number of delamination from one to three, there is significant decrease in critical buckling load because of the reduction of stiffness. The decrease in critical buckling load is 9%, 45% and 65% from single to multiple delaminated plates with 6.25%, 25% and 56.25% delamination area respectively. So the increase in number and size of delaminations has in general, a deteriorating effect on the stiffness of the plate.

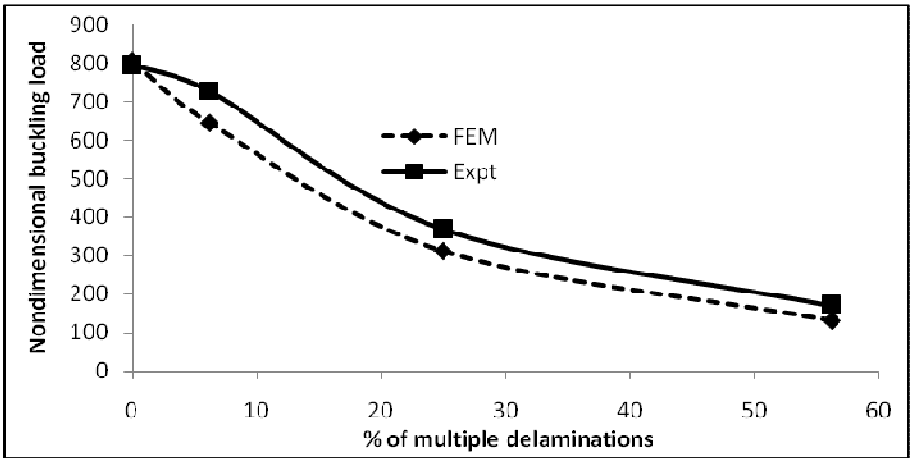

Figure 5.23: Variation of nondimensional buckling load of multiple delaminated CFCF plate with increasing delamination area

5.4.2.6 Effects of boundary conditions

To investigate the influence of boundary conditions on non-dimensional buckling load of delaminated composite plates, three types of boundary conditions i.e. all sides simply supported (SSSS), all sides clamped (CCCC) and two sides clamped two sides free (CFCF) are assumed for numerical analysis. The size of the composite plate assumed is (240x190x3.5) mm^3 with 0%, 6.25%, 25% and 56.25% of delamination and stacking sequence is $[0]_8$. From the Figure 5.24 it is evident that the non-dimensional buckling load of 6.25%, 25% and 56.25% delaminated plates along with the laminated plate (0%

delamination) are highest under all sides clamped boundary condition followed by CFCF boundary condition and the lowest load is observed under simply supported boundary condition. This happens because of the rigidity of the clamped boundary condition as compared to simply supported boundary condition. The critical buckling load of 6.25%, 25% and 56.25% delaminated plates under CCCC boundary condition decreased by 23%, 44% and 63% respectively as compared to laminated plate. In case of CFCF boundary condition the reductions are 11%, 28% and 52% and for simply supported boundary condition the reductions are 19%, 43% and 58% respectively as compared to laminated plate. These results clearly indicate that boundary conditions have immense influence on non-dimensional buckling load of delaminated plates.

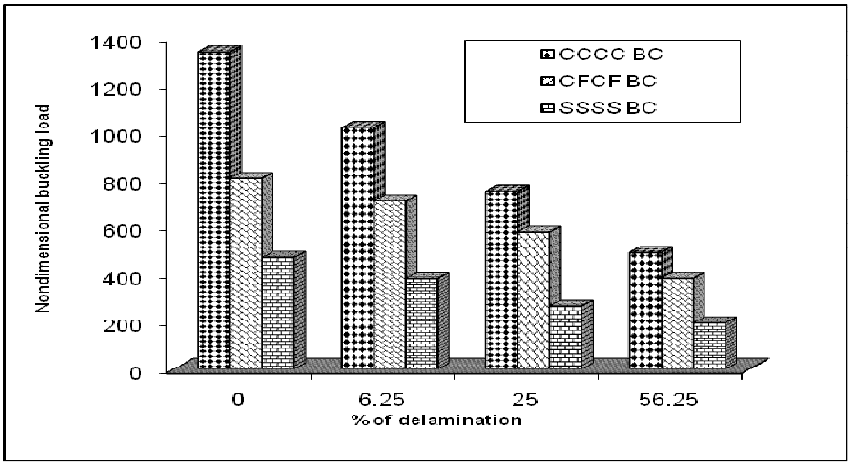

Figure 5.24: Variation of Non dimensional buckling load with different % of delamination for different boundary conditions (BC)

5.4.3 Typical experimental determination of critical buckling load from load v/s end shortening displacement graph

The critical buckling load from buckling analysis of delaminated composite plates is found experimentally by load v/s end shortening displacement graph. The load is plotted in y-axis and end shortening displacement in x-axis. For the determination of critical buckling load, the point where left from the straight line is determined on the graphics and the value of this point on the y axis is called as the critical buckling load. Determination of critical buckling load of a plate with 25% and 56.25% delamination from load v/s end shortening displacement graph is shown in Figure 5.25 and 5.26 respectively.

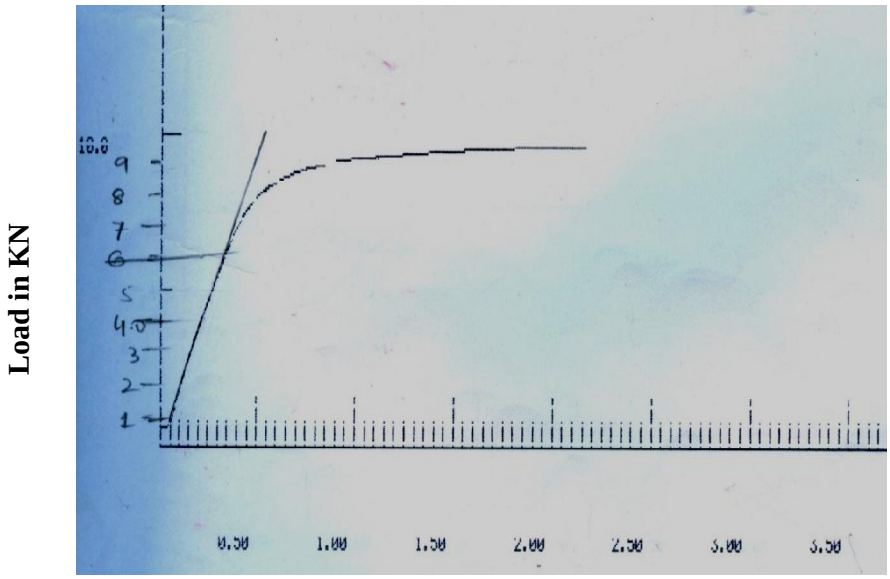

Figure 5.25: Determination of critical buckling load of a plate with 25% delamination from load v/s end shortening displacement graph

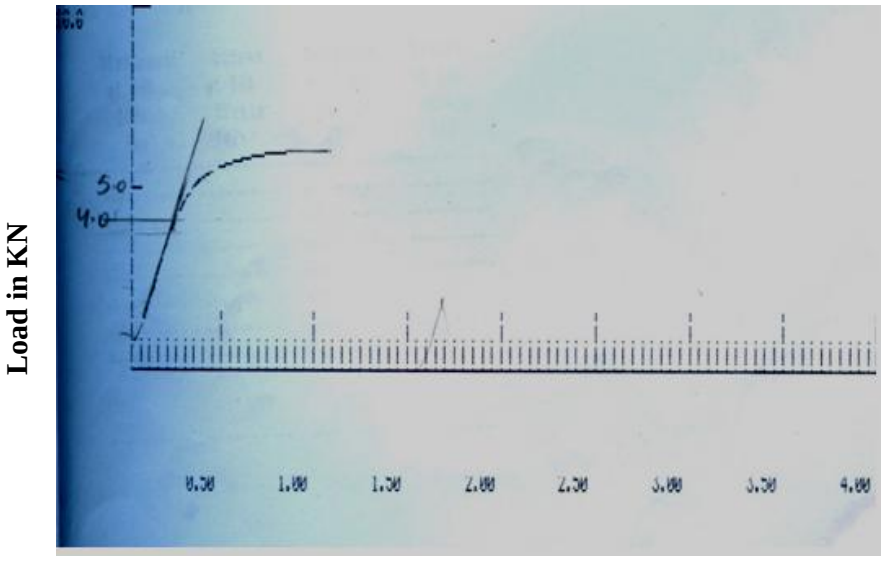

Figure 5.26: Determination of critical buckling load of a plate with 56.25% delamination from load v/s end shortening displacement graph

5.5 Dynamic stability analysis

Dynamic stability analysis is an integral part of most engineering structures. Delaminations reduce the stiffness of the plates. It is therefore important to understand the performance of delaminated composites in a dynamic environment. The subject of predicting the dynamic stability of delaminated structures has thus attracted considerable attention. The dynamic stability of plate structures with delamination is presented by using FEM formulation mentioned in chapter 3. The instability regions are determined for composite plates with and without delaminations. A detailed parametric investigation is carried out to study the influence of delamination area, number of layers, degree of orthotropy, aspect ratio and static in plane load on the parametric resonance characteristics of delaminated cross ply plates.

Boundary conditions

Numerical results are presented for delaminated composite plates with different combination of boundary conditions. Further descriptions of boundary conditions are as follows:

- Simply supported boundary

  v=w=θ_y=0 at x=0, a and u=w=θ_x=0 at y=0, b

- Clamped boundary

  u=v=w=θ_x=θ_y= 0 at x=0, a and y=0, b

- Free edges

Non-dimensionalisation of parameters

Table 5.13 shows the non-dimensional parameters used for vibration, buckling and excitation frequency considered for dynamic stability analysis with the reference to Bert and Birman(1988).

Table 5.13: Non-dimensional parameters of composite plates

No	parameter	Composite plates
1	Frequency of vibration (ω)	$\varpi a^2\sqrt{\rho/h^2 E_2}$
2	Buckling load (λ)	$N_x \frac{b^2}{E_2 h^3}$
3	Frequency of excitation (Ω)	$\overline{\Omega} a^2\sqrt{\rho/h^2 E_2}$

Where ϖ and $\bar{\Omega}$ are in radian.

5.5.1 Comparison with previous study

The numerical validation of the governing equation is performed by solving the corresponding free vibration and buckling eigenvalue problems. The natural frequency and critical buckling load results are compared with the results available in the existing literature. To validate the program, the natural frequency for mid-plane delaminated plate is already compared with the result by Shen and Grady (1992) as shown in Table 5.4. The results on buckling with different delamination length of cross-ply composite plates due to dynamic load is compared with results by Radu and Chattopadhyay (2002) using higher order shear deformation theory and are shown in Table 5.14. It is observed that there is good agreement between the two results.

Table 5.14: Comparison of buckling load for different mid plane delamination length of the cantilever rectangular plates

E_{11} =134.4 GPa, E_{22} =10.34 GPa, G_{12} = G_{13} =4.999 GPa, ν_{12}=0.33, ρ=1600 kg/m^3 ,a=127 mm, b=12.7 mm, h=1.016 mm, stacking sequence = $(0/90)_{2s}$, a/h=125

Delamination length (mm)	Critical buckling load (N)	
	Radu & Chattopadhyay (2002)	Present FEM
0	16.336	16.3296
25.4	16.068	15.8292
50.8	15.054	14.9085

After validation of the present formulation, investigation is performed on the dynamic instability characteristics of the composite plates. The present study is carried out considering graphite/epoxy rectangular plates made out of eight identical plies with material properties: E_{11} =134.4 GPa, E_{22} = 10.34 GPa, G_{12} = G_{13} =4.999 GPa, ν_{12}=0.25, ρ=1600 kg/m^3 ; length a= 127 mm, width b=12.7 mm, thickness t=1.016 mm, stacking sequence= (0/90/0/90/90/0/90/0). Where E_{11} and E_{22} are Young's modulus, G_{12} and G_{13} are Shear modulus and ν_{12} is Poisson's ratio. The effects of various parameters like delamination area, number of layers, degree of orthotropic, static load factor, length-thickness ratio and aspect ratio on the dynamic instability characteristics are studied.

In this study, the boundary condition in one of the short edge is fixed and opposite edge is loaded with dynamic buckling force. The non-dimensional excitation frequency Ω (= $\bar{\Omega}a^2\sqrt{\rho/h^2 E_2}$) is used throughout the dynamic instability studies. Where $\bar{\Omega}$ is the excitation frequency in radian /second. Instability regions are plotted in the plane having non-dimensional excitation frequency as abscissa and dynamic load factor as ordinate.

5.5.2 Numerical results for dynamic stability

5.5.2.1 Effects of delamination size

To study the effect of delamination size on the dynamic instability region (DIR), single mid-plane delaminated graphite/epoxy plates with different delamination sizes like 0%, 6.25%, 12.5% and 25% of total plate area are considered. Taking the lower and upper boundary of primary instability region the graph is depicted in Figure 5.27 for length to thickness ratio L/t =125. From the Figure it is observed that the onset of instability occurs earlier with the increase in delamination size from 0% to 6.25%. But the introduction of 6.25% delamination has no remarkable effect in lowering the non-dimensional excitation frequency. Further increase in delamination from 6.25% to 12.5% and from 12.5% to 25%, the instability region is found to shift to a lower and lower excitation frequency. This result reveals that with the increase in delamination size, the non-dimensional excitation frequency decreases and therefore the dynamic instability regions (DIR) are shifted to lower excitation frequencies.

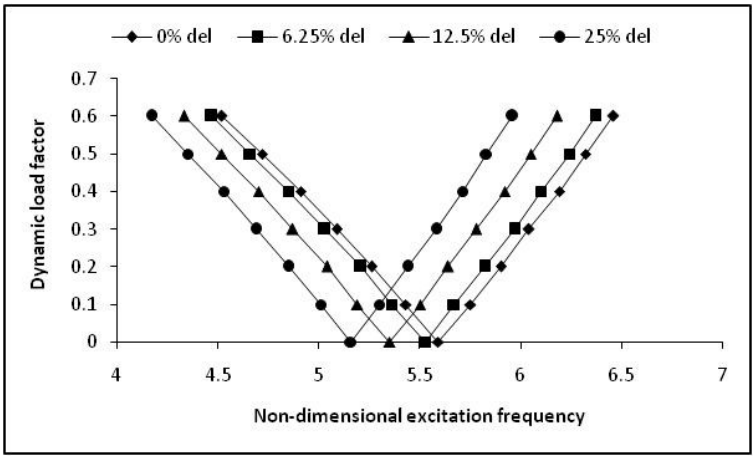

Figure 5.27: Variation of instability region of $[(0/90)_2]_s$ cross- ply plate with different percentage of delamination for L/t =125

5.5.2.2 Effects of number of layers

The variation of instability region of 2-layer (0/90) delaminated (0%, 6.25%, 12.5% and 25%) composite plates with length to thickness ratio L/t =125 is shown in Figure 5.28. From the Figure it is observed that, the dynamic instability occurs at 3.238, 3.214, 3.147 and 2.962 non-dimensional excitation frequency for 0%, 6.25%, 12.5% and 25% delaminated plates respectively. Instability occurs later for the laminated plate than the delaminated plates. Up to 12.5% delamination the decrease in excitation frequency is not so conspicuous like 25% delamination.

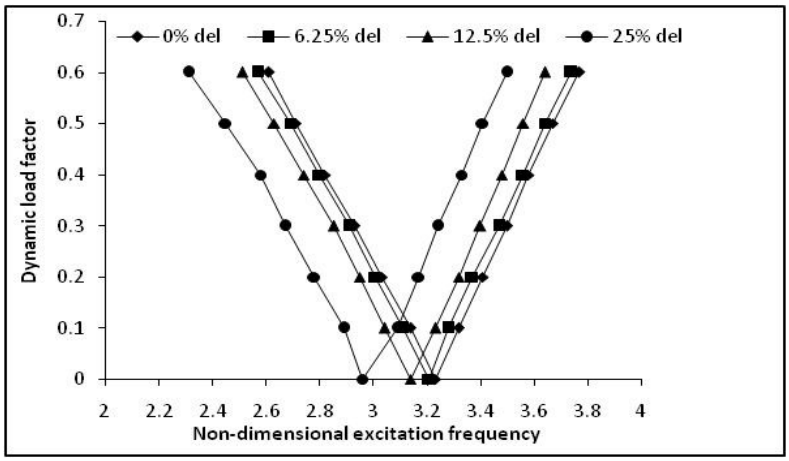

Figure 5.28: Variation of instability region of 2-layer (0/90) composite plate with different percentage of delamination

The variation of instability region of 4-layers $(0/90)_s$ composite plate with different percentage of delamination (0%, 6.25%, 12.5% and 25%) is shown in Figure 5.29. Dynamic instability regions (DIR) are plotted for 4- layers cross-ply rectangular plate with length to thickness ratio L/t =125. It is noted that the dynamic instability of 6.25%, 12.5% and 25% delaminated plates having 4-layers starts at 4.396, 4.211 and 3.974 instead of at 3.214, 3.147 and 2.962 non-dimensional excitation frequency as in case of 2-layer composite plates with 6.25%, 12.5% and 25% delamination respectively. The results reveal that by increasing the number of layers of the delaminated plates the instability regions occur at higher excitation frequencies. The observed behavior is attributed due to the effect of bending-stretching coupling for the case of delaminated composite plates. This indicates that the delaminated plates with more number of layers may impart better structural stability and safety.

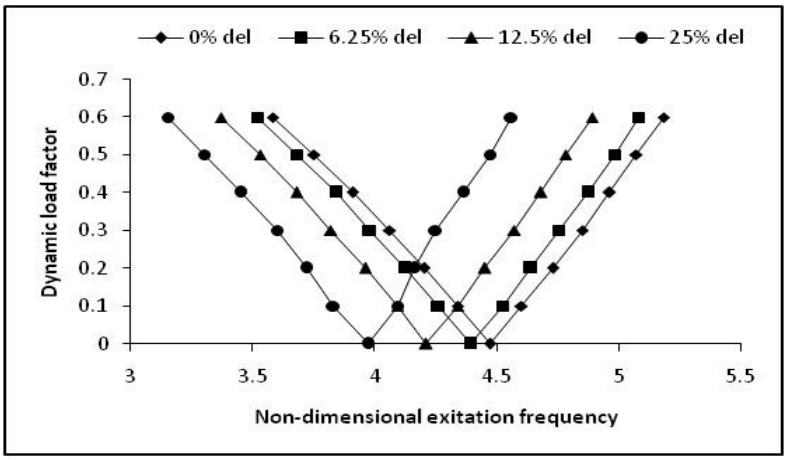

Figure 5.29: Variation of instability region of 4-layer $(0/90)_s$ composite plate with different percentage of delamination

5.5.2.3 Effects of degree of orthotropy

The effects of degree of orthotropy on dynamic instability region (DIR) of single mid-plane delaminated graphite/epoxy plates with delamination sizes 0%, 6.25%and 25% is studied for E_{11}/E_{22}=40 and 20 keeping other material parameters constant. Figure 5.30 shows the variation of instability region for the degree of orthotropy, $E11/E_{22}$ = 40 of composite plate with different percentage of delamination. For the intact plate (0% delamination) instability starts at a higher

excitation frequency. The introduction of 6.25% delamination in laminated plate induces instability at a lower excitation frequency. Further increase in delamination from 6.25% to 25% causes instability earlier. This indicates that the dynamic instability occurs earlier for 25% delaminated plates than 6.25% delaminated plates.

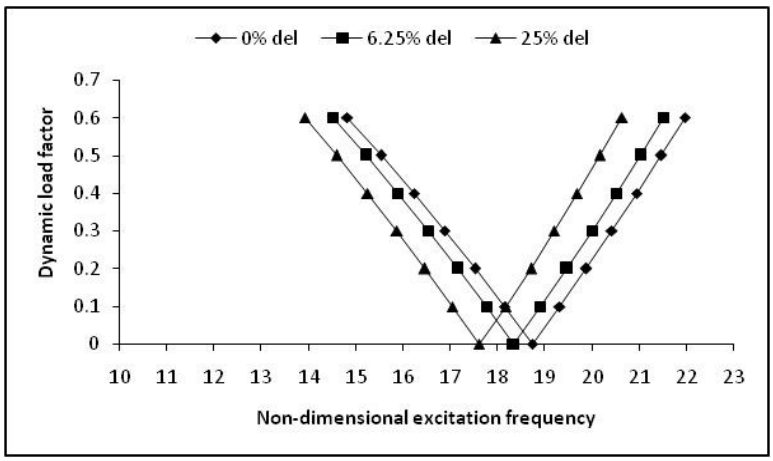

Figure 5.30: Variation of instability region for the degree of orthotropy (E_{11}/E_{22} =40) of composite plate with different percentage of delamination

Variation of instability region for the degree of orthotropy (E_{11}/E_{22} =20) of composite plate with different percentage of delamination is shown in Figure 5.31. As expected, the onset of instability of composite plates with the degree of orthotropy $E11/E_{22}$ = 20 occurs earlier with the introduction of delamination from 0% to 6.25%. With further increase of delamination from 6.25% to 25%, the excitation frequency reduces significantly. Comparison of Figure 5.30 and Figure 5.31 reveals that the effect of delamination is more pronounced for the composite plates with lower degree of orthotropy (E_{11}/E_{22} = 20) than the plates with higher degree of orthotropy (E_{11}/E_{22} = 40). These results indicate that with the increase in degree of orthotropy of delaminated plates, the excitation frequency increases and thus the instability regions shifted to a higher frequency due to increase in stiffness.

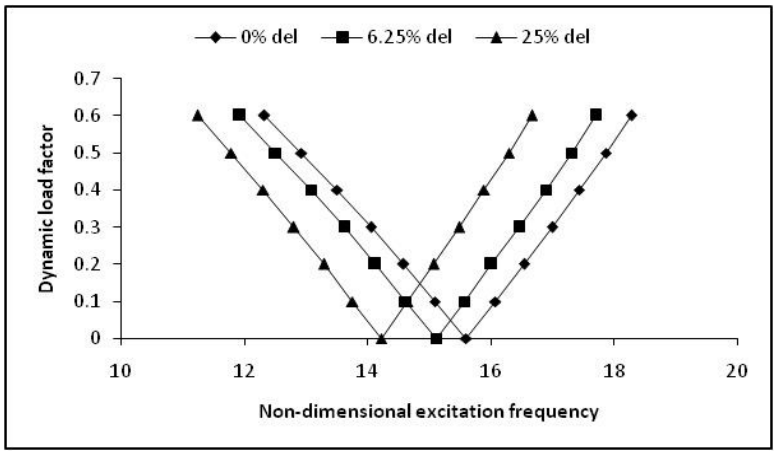

Figure 5.31: Variation of instability region for the degree of orthotropy (E_{11}/E_{22} =20) of composite plate with different percentage of delamination

5.5.2.4 Effects of aspect ratio

Figure 5.32 shows the variation of instability region of 0% delaminated simply supported cross ply plate (L/t =10, E_{11}/E_{22}= 25) for different aspect ratio (a/b = 0.5, 1.0 and 1.5) on the dynamic instability characteristics. For the laminated plate with a/b = 0.5, the instability occurs at a lower non-dimensional frequency (11.069). By increasing the aspect ratio from 0.5 to 1.0 and from 1.0 to 1.5 the instability regions are shifted to a higher and higher excitation frequency.

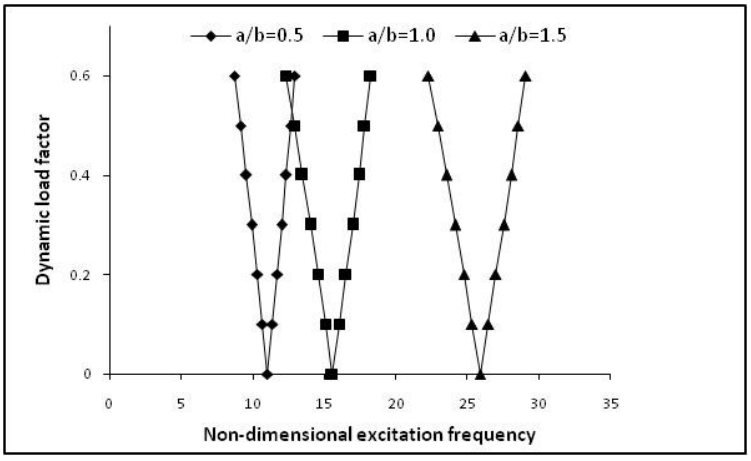

Figure 5.32: Variation of instability region of 0% delaminated cross ply plate with different aspect ratio

The variation of instability region of 25% delaminated simply supported cross ply plates (L/t =10, E_{11}/E_{22}= 25) with different aspect ratio is shown in Figure 5.33**.** In case of 25% delaminated plate, the onset of dynamic instability occurs much later for a/b = 1.5 and earlier for a/b = 0.5 and the width of the instability region increases from a/b = 0.5 to a/b = 1.5. The comparative study of both the Figures 5.32 & 5.33 reveals that with the introduction of 25% delamination in the intact plates with a/b = 0.5, a/b = 1.0 and a/b = 1.5 the excitation frequency is found to shift from 11.069 to 9.992, from 15.062 to 14.225 and from 26.931 to 23.794 respectively. This indicates that in the presence of delamination in a composite laminate for a particular aspect ratio, instability occurs at a lower excitation frequency than the intact plate and by increasing the aspect ratio of the delaminated plates the region of instability may be shifted to a higher excitation frequency.

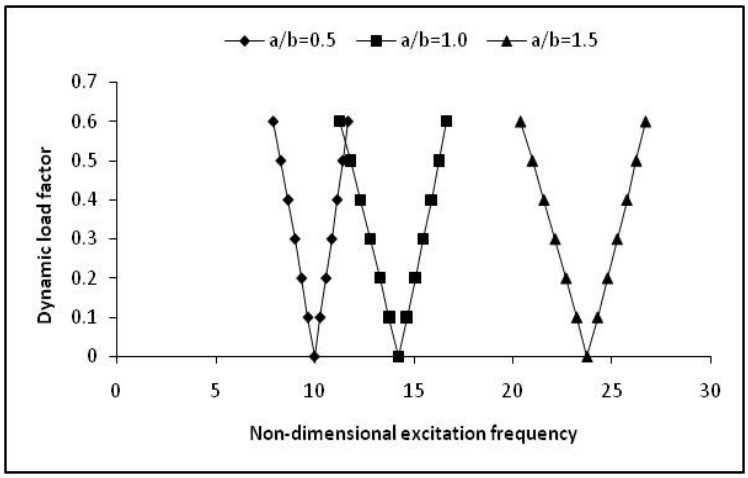

Figure 5.33: Variation of instability region of 25% delaminated cross ply plate with different aspect ratio

5.5.2.5 Effects of static loads

The effect of static component of load (for α = 0.0, 0.2 and 0.4) on the dynamic instability region of a 6.25% delaminated cross ply rectangular plate with clamped-free-clamped-free boundary condition is demonstrated in Figure 5.34. The instability occurs earlier for higher static load factor (α = 0.4) and later for lower static

load factor ($\alpha = 0.0$). This study reveals that with the increase in static in-plane load, the lowest natural frequency decreases and the instability regions occur at a relatively lower excitation frequency. The width of the instability zone also increases with the increase in static in-plane load.

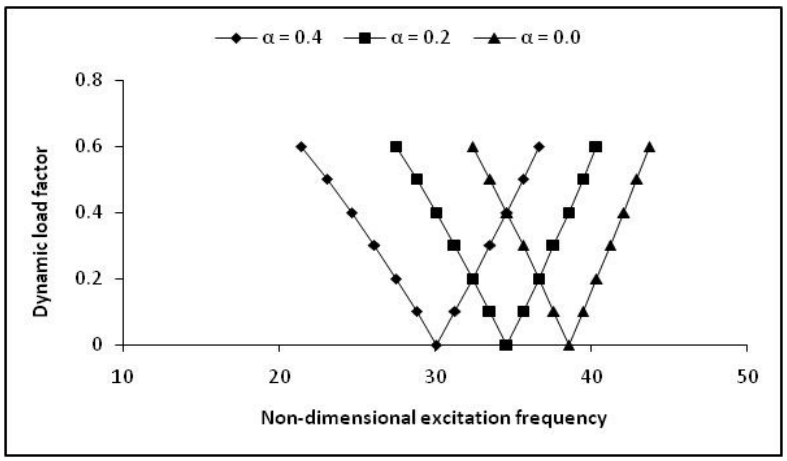

Figure 5.34: Variation of instability region of 6.25% delaminated rectangular plate with different static load factor

CHAPTER 6

CONCLUSION

6.1 Introduction

The present work deals with the study of the vibration, buckling and parametric resonance characteristics of delaminated composite plates. The formulation is based on the first order shear deformation theory. A finite element procedure using an eight-node isoparametric quadratic plate element is employed in the present analysis with five degrees of freedom per node. The development of regions of instability arises from Floquet's theory developed by Bolotin (1964) and the boundaries of the primary instability regions have been determined to study the effect of various parameters on the dynamic instability regions of the delaminated composite plates.

Results are presented for the interlaminar shear strength (ILSS), free vibration, buckling and parametric resonance characteristics of delaminated composite plates. The effects of various geometrical parameters like delamination size, boundary conditions, number of layers, fiber orientations, aspect ratios, degree of orthotropy and static load factor on the free vibration and stability characteristics of delaminated composite plates have been analysed. The conclusions drawn in respect of different studies are presented below.

6.2 Static analysis

Effects of different delamination lengths on interlaminar shear strength of woven fiber glass/epoxy woven fiber composite plates at different cross head velocities are investigated experimentally. Three point bending tests are also conducted to assess the interlaminar shear strength of the laminates. Following conclusions are drawn from the present research work.

- The ILSS decreases with the increase in delamination length.
- The ILSS of delaminated glass/ epoxy composite plates decreases with the increase of crosshead velocities unlike the plates without delamination.

- SEM test result reveals that the variations of delamination length and crosshead velocity might have strong influence in changing the predominating mode of failure of glass/epoxy laminates.

6.3 Vibration analysis

The main thrust of the present study is the modal analysis of delaminated composite plates, because of its inherent link with stability analysis. The effect of different parameters on the frequencies of vibration are observed and compared with numerical prediction using FEM. The conclusions are summarized as given below.

- There is a good agreement between the experimental and numerical results.
- The frequencies of vibration decrease with introduction and further increase of size of delamination in woven fiber composite plates.
- Numerical and experimental results show that the effect of delaminations on the modal parameters of delaminated composite plates is dependent not only on the size but also on the boundary conditions i.e. the more strongly a plate is restrained along its edges, the greater the effect of delmination on the modal parameter.
- The natural frequencies of delaminated plates also vary with different ply orientation. For cantilever boundary condition, there is a decrease in natural frequency with increase in the orientation angle.
- It is observed that natural frequency increases with increase in number of layers and aspect ratios for delaminated plate.
- Variation of natural frequency is observed for number of multiple delaminations. The fundamental natural frequency reduces with increasing number of delaminations. Thus increase in the number and sizes of delaminations have a deteriorating effect on the plate dynamic stiffnesses. The effect of multiple delaminations on the natural frequencies of delaminated plate is also greatly dependent on boundary conditions as observed in single delamination.

6.4 Buckling analysis

The present study includes numerical and experimental study of buckling analysis of delaminated composite plates with clamped-free boundary condition. The finite element analysis allowed the mechanics of delamination to be investigated and understood more easily than would be possible from experimental data alone. The influences of various parameters like effects of delamination area, ply orientation, number of layers, aspect ratio, multiple delaminations and different boundary condition on the buckling load of woven roving delaminated plates are studied. The experimental buckling load is in good agreement with the predictions using FEM. Main sources of discrepancy differ between finite element analysis and experimental results are imperfect in specimen geometry, specimen material and experimentally achieved boundary conditions. The conclusions are summarized as given below.

- For delaminated composite plate, with the increase of percentage of delamination area, the non-dimensional buckling load decreases as the stiffness decreases. The rate of decrease of buckling load is not uniform for increase in percentage of delamination.
- The different fiber orientation angles affected the non-dimensional buckling load. When the fiber orientation angle increases, the non-dimensional buckling load decreases. So the delaminated composite plate with $[0]_8$ layup has highest buckling load and with $[45/-45]_{2s}$ layup has lowest buckling load.
- For delaminated composite plate, with the increase of number of layers, the non-dimensional buckling load also increases.
- With the increase in aspect ratio of delaminated composite plates the non-dimensional buckling load decreases.
- For multiple delaminated composite plates, with the increase of percentage of delamination area compared to single delaminated plate the buckling load decreases more because of the reduction in stiffness of composite plate.
- The effect of boundary condition on buckling load of composite plates is studied numerically. The clamped boundary conditions show the highest

buckling load in the context of considered edge conditions. This can be explained by the rigidity of clamped boundary conditions. The buckling loads for delaminated composite plates under clamped free and simply supported boundary conditions are much lower than those under clamped boundary condition.

6.5 Dynamic stability analysis

A first order shear deformation theory based on finite element model has been developed using Bolotin's approach for studying the instability region of mid-plane delaminated composite plate. The results of dynamic stability studies are summarized as follows:

- The onset of instability occurs at lower excitation frequency with the increase in delamination size.
- With the increase in number of layers of delaminated plate, the dynamic instability occurs at higher excitation frequency.
- The dynamic instability region is shifted to a lower excitation frequency with decrease of degree of orthotropy of delaminated composite plates.
- The onset of instability occurs at higher excitation frequency with increase of aspect ratio and width of the instability region increase with increase of aspect ratio for delaminated cross ply plate.
- With increase of static load factor the instability region tends to shift to lower excitation frequencies and become wider showing destabilizing effect on the dynamic stability behaviour of delaminated composite plate.

The significant contributions on the behavior of delaminated composite plates are:

A general formulation dealing with vibration, buckling and dynamic stability of multiple delaminated composite plates is presented. Suitable finite element formulations for single and multiple delaminations are presented using eight noded isoparametric element. A program is developed in MATLAB environment to compute

the natural frequency, critical buckling load and instability regions of delaminated composite plates. From the results, it is clear that delamination causes the reduction of natural frequency and critical buckling load. It also shifts the dynamic instability region of composite materials to a lower excitation frequency. The presence of one or more delamination reduces the stiffness of the structure from the point of view of buckling behavior and causes early resonance due to reduction in natural frequency. So, delaminations play a critical role on the vibration behavior of the structures. The instability behavior of delaminated plates is influenced by the geometry, material, ply lay-up, ply orientation, boundary conditions, the type and position of loads and size of delamination. So the designer has to be careful while dealing with structures subjected to in-plane periodic loading. This can be used to the advantage of tailoring during design of delaminated composite structure. Finally the figures dealing with the variations in natural frequency, buckling load and instability regions can be used as design aids for delaminated composites subjected to in plane loads.

The parametric resonance characteristics of the delaminated composite plates can be used as a tool for structural health monitoring for identification of delamination location and extent of damage in composites and also helps in assessment of structural integrity of composite structures.

6.6 Further scope of research

The present investigation has been confined on free vibration, buckling and dynamic stability of delaminated composite plates. This can be further extended for force vibration and stability studies.

- The present study deals with square delamination. This may be extended for different shapes of delamination.
- For single delaminated plate, the delamination is considered here at the mid plane. So arbitrary location may be taken into account for further extension.
- Dynamic stability of multiple delaminated shell can be studied.

- The present study is based on linear range of analysis. It can also extend for nonlinear analysis.
- Dynamic stability of composite plates with circular, elliptical, triangular shaped delamination can be studied.
- The effects of damping on instability regions of delaminated composite plates and shells can be studied.
- The effects of piezo electric system in delaminated composites can be studied.

REFERENCES

Abadi, F. and Poro, A. (2003): Modified short beam shear test for measurement of interlaminar shear strength of composites, *Journal of Composite Materials*, Vol. **37**, pp. 453-464.

Acharya, A.K., Chakraborty, D. and Karmkar, A. (2007): Free vibration of delaminated composite cylindrical shell roofs, Vibration Problems ICOVP - 2007. Publisher Springer Netherlands.

Agrawal, P. and Prasad, R.C. (2005): Influence of environment on the mechanical properties of carbon/epoxy composite, *CORROSION*, April 3 - 7, 2005 , Houston, Tx ; Copyright 2005. NACE International.

Aran, A.G., Moslemian, R. and Arefmanesh, A. (2009): Compressive behaviour of glass/epoxy composite laminates with single delamination, *Journals of Solid Mechanics***,** Vol.**1**, pp. 84-90**.**

Aslan, Z. and Sahin, M. (2009): Buckling behaviour and compressive failure of composite laminates containing multiple large delaminations, *Composite Structures*, Vol.**89**, pp.382-390.

Aslan, Z. and Alnak, Y. (2010): Characterization of ILSS of laminated woven E/glass epoxy by four bend shear test, *Polymer Composite*, Vol.**31**, pp. 359-368.

ASTM D 2344/ D 2344M (2006): Standard test method for short-beam strength of polymer matrix composite materials and their laminates, Annual Book for ASTM Standards, American Society for Testing and Materials.

ASTM D 3039/D 3039 M (2008): Standard Test Method For Tensile Properties Of Polymer Matrix Composite Materials.

Azouaoui, K., Ouali, N., Ouroua, Y., Mesbah, A. and Boukharouba, T. (2007): Damage characterization of glass/polyster composite plates subjected to low energy impact fatigue, *Journal of Sound and Vibration*, Vol. **308**, pp. 504-513.

Baba, B.O. (2007): Buckling behavior of laminated composite plates, *Journal of Reinforced Plastics and Composites*, Vol.**26**, pp1637-1655.

Bert, C.W. and Birman, V. (1987): Dynamic instability of shear deformable antisymmetric angle-ply plates, *International Journals of Solids & Structures*, Vol.**23**, 1053-61.

Biswas, S., Datta, P.K. and Kong, C.D. (2011): Static and dynamic instability characteristics of curved laminates with internal damage subjected to follower loading, *Mechanical Engineering Science*, Vol.**225**, pp 1589-1599.

Bolotin, V.V. (1964): The Dynamic stability of elastic systems. Holden-Day, San Francisco.

Brandinelli, L. and Massabo, R. (2003): Free vibration of delaminated beam type structures with crack bridging, *Composite Structure*, Vol.**61**, pp.129-142.

Bruno, D. and Grimaldi, A. (1989): Delamination failure of layered composite plates loaded in compression, *International Journal of Solids Structure*, Vol. **26(3)**, pp.313-330**.**

Cappello, F. and Tumino, D. (2006): Numerical analysis of composite plates with multiple delaminations subjected to uniaxial buckling load, *Composites Science and Technology*, Vol. **66**, pp. 264–272.

Chai, H., Babcock, C.D. and Knauss, M. (1981): One dimensional modelling of failure of laminated plates by delamination buckling, *Journal of Solids and Structures*, Vol. **17**, pp. 1069-1083**.**

Chakrabarti A. and Sheikh, A.H. (2005): Analysis of laminated sandwich plates based on interlaminar shear stress continuous plate theory. *Journal of Engrg Mech,* Vol.**131**(4), pp. 377-384.

Chakrabarti, A. and Sheikh, A.H. (2010): Dynamic instability of composite and sandwich laminates with interfacial slips, *International Journal of Structural Stability and Dynamics*, Vol.**10(2)**, pp. 205–224.

Champanelli R.W. and Engblom, J.J. (1995): The effect of delaminations in graphite/PEEK composite plates on modal dynamic characteristics, *Composite Structure*, Vol. **31**, pp. 195-202.

Chandrashekhara, K. (1989)**:** Free vibrations of anisotropic laminated doubly curved shells, *Computers and Structures*, Vol.**33** (2), pp.435-440.

Chang, T.P., Hu, C.Y. and Jane, K.C. (1998): Vibration of delaminated composite plates under axial load, *Mech. Structure,* Vol. **26**, pp. 195-218.

Chattopadhyay, A. and Radu, A.G. (2000): Dynamic instability of composite laminates using a higher order theory, *Computer and Structure*, Vol. **77**, pp. 453–460.

Chattopadhyay, A., Radu, A.G. and Dragomir-Daescu, D. (2000): A high order theory for dynamic stability analysis of delaminated composite plates, *Comput. Mech*., Vol. **26**, pp. 302-308.

Chattopadhyay, L. and Murthy, S.S. (2011): Analytical and finite element modeling and simulation of buckling and post buckling of delaminated orthotropic plates, *International Journal of Modelling and Scientific Computting*, Vol.**2**, pp. 97-104.

Chen, L.W. and Yang, J.Y. (1990): Dynamic stability of laminated composite plates by the finite element method. *Computer and Structure*, Vol.**36**:845–851.

Christensen, R.M. and Teresa, S.J. (2003): Delamination failure investigationfor out-of-plane loading in laminates, Article submitted to the Conference on Composite Materials, *ICCM-14, San Diego, CA*, July 14-19.

Costa, M.L., de Almeida, S. F. M. and Rezende, M.C. (2001): The influence of porosity on the interlaminar shear strength of carbon/epoxy and carbon/bismaleimide, *Composites Science and Technology*, Vol.**61**, pp. 2101-2108.

Cox, J.R. and Wilson, C.D. (2008): Apparent interlaminar shear strength of a graphite/epoxy composite with carbon nano fiber reinforcement, *49th AIAA Structural Dynamics and Material Conference*, 1770.

Damghani, M., Kennedy, D. and Featherston, C. (2011): Critical buckling load of delaminated composite plates by using exact stiffness analysis, *Computers & Structures*, Vol. **89,** pp. 1286-1296.

Das, B., Sahu, S.K. and Ray, B.C. (2007): Effect of loading speed on the failure behaviour of FRP composites, *Aircraft Engineering and Aerospace Technology*, Vol. **79(1)**, pp. 45-52.

Della, C.N. and Shu, D. (2007): Vibration of delaminated composites: A Review, *Applied Mechanics Review* , Vol. **60**, pp. 1-20.

Deolasi, P.J. and Datta, P.K. (1995): Parametric instability of rectangular plates subjected to localized edge compressing (compression or tension), *Computer and Structure*, Vol. **54**, pp.73–82.

Dey, P. and Singha, M.K. (2006): Dynamic stability analysis of composite skew plates subjected to periodic in-plane load, *Thin-walled Structures*, Vol. **44**, pp. 937-942.

Esfahani, M.M., Ghasemnejad, H. and Barrington, P.E. (2010): Experimental and numerical analysis of delaminated hybrid composite beam structures, *Applied Mechanics and Materials*, Vol.**24-25**, pp.393-400.

Fazilati, J. and Ovesy, H.R. (2010): Dynamic instability analysis of composite laminated thin-walled structures using two versions of FSM, *Composite Structures*, Vol. **92(9)**, pp. 2060–2065.

Ganapathi, M., Varadan, T.K., and Balamurugan, V. (1994): Dynamic instability of laminated composite curved panels using finite element method, *Computers and Structures*, Vol. **53**(2), pp. 335-342.

Gim, C.K. (1994): Plate finite element modeling of laminated plates, *Composite Structure*, Vol. **52**, pp.157-168.

Gu, H. and Chhatopadhya, A. (1999): An experimental investigation of delamination buckling and post buckling of composite plates, *Composites Science and Technology*, Vol. **59**, pp. 903-910**.**

Hadi, N.H. and Ameen, K.A. (2011): Nonlinear free vibration of cylindrical shells with delamination using high order shear deformation theory: A finite element approach, *American Journal of Scientific and Industrial Research*, Vol. **2 (2)**, pp.251-277.

Hallet, S.R., Ruiz, C. and Harding, J. (1999): The effect of strain rate on the interlaminar shear strength of a carbon/epoxy cross-ply laminate: comparison between experiment and numerical prediction, *Composite Science and Technology*, Vol.**59,** pp.749-758.

Hein, H. (2006): Vibration of composite beams with multiple delaminations, *III European Congress on Computational Mechanics Solids, Structures and Coupled Problems in Engineering*, pp. 1-11.

Hong-Yan, Z., Dong-Xing, Z., Bao-Chang, Wu. and Yu-Yang, C. (2009): Influence of voids on inter laminar shear strength of carbon epoxy fabric laminates, *Transactions of Nonferrous Metals Society of China*, Vol. **19**, No. Sp. Iss. 2.

Hou, J.P. and Jeronimidis, G. (1999): Vibration of delaminated thin composite plates, *Composites, Part A*, Vol. **30**, pp. 989-995.

Hu, N.(1999) Buckling analysis of delaminated laminates with consideration of contact in buckling mode, *International Journal for Numerical methods in Engineering*, Vol **44**(10), pp 1457-1479.

Hu, N., Fukunaga, H., Kameyama, M., Aramaki, Y. and Chang, F.K. (2002): Vibration analysis of delaminated composite beams and plates using a higher order finite element, *International Journal of Mechanical Science*, Vol.**44**, pp. 1479-1503.

Hu, N., Fukunaga, H., Sekine, H. and Ali, K.M. (1999): Compressive buckling of laminates with an embedded delamination, *Composite Science and Technology*, Vol.**59**, pp. 1247-1260

Hutt, J.M. and Salam, A.E. (1971): Dynamic stability of plates by finite element method, *Journal of Engineering Mechanics ASCE*, Vol. **3**, pp. 879–899.

Hwang, S.F. and Liu, G.H. (2002): Experimental study for buckling and post buckling behaviours of composite materials with multiple delaminations, *Journals of Reinforced Plastics and Composites,* Vol. **21**, pp. 333-349.

Hwang, S.F. and Mao, C.P. (2001): Failure of delaminated carbon/epoxy composite plates under compression, *Journal of Composite Materials,* Vol.**35**, pp.1634-165**.**

Jaeschke, P., Kern, M., Stute, U., Haferkamp, H., Peters, C. and Herrmann, A.S. (2011): Investigation on interlaminar shear strength properties of disc laser machined consolidated CF-PPS laminates, *Express Polymer Letters*, Vol.**5 (3)**, pp. 238–245.

Jagdish, K.S. (1974): The dynamic stability of degenerate systems under parametric excitation, *Ingenieur-Archive*, Vol.**43**, pp. 240–246.

Jones, R.M. (1975): Mechanics of Composite Materials, McGraw Hill, New York.

Ju, F., Lee, H.P. and Lee, K.H. (1995): Finite element analysis of free vibration of delaminated composite plate, *Composite Engineering*,Vol. **5**, pp. 195-209.

Kang, C., Han, Z., Lu, G. and Zhang, S. (2011): Compressive buckling of composite plates with delamination, *Advanced Materials Research*, Vol. **150-151**, pp. 235-238.

Karmkar, A., Roy, H. and Kishimoto, K. (2006): Free vibration analysis of delaminated composite pretwisted shells, *Aircraft Engineering and Aerospace Technology*, Vol. **77**, pp.486-490.

Kessler, S.S., Spearing, S.M., Attala, M.J. and Cesnik, E.S. (2002): Damage detection in composite materials using frequency response method, *Composites, Part B*, Vol.**33**, pp. 87-95.

Kharazi, M. and. Ovesy, H.R. (2008): Post buckling behaviour of composite plates with through-the-width delaminations, *Thin Walled* Structures, Vol.**46**, pp. 939-946.

Khashaba, U.A. and Seif, M.A. (2006): Effect of different loading conditions on the mechanical behaviour of (0/+45/90)s, woven composites, *Composite Structures*, Vol.**74**, pp. 440-448.

Kim, R.Y. and Donaldson, S.L. (2006): Experimental and analytical studies on the damage initiation in composite laminates at cryogenic temperatures, *Composite Structures*, Vol.**76**, pp. 62-66.

Kim, H.J. and Hong, C.S. (1997): Buckling and postbuckling behaviors of composite laminates with a delamination, *Composites Science and Technology*, Vol.**57**, pp. 557-564.

Kim, H.Y. and Hwang, W. (2002): Effect of debonding on natural frequencies and frequency response function on honey comb sandwich beam, *Composites Structure* Vol.**55**, pp. 51-62.

Kong, Z.X. and Wang, J.H. (2009): Interlaminar shear strength of glass fiber reinforced dially phthalate laminates enhanced with nanoclays, *Advanced Materials Research*, Vol. **79 - 82**, pp. 1779-1782.

Kotek, J., Glogar, P. and Cerny, M. (2001): Interlaminar shear strength of textile reinforced carbon-carbon composite, *39th International Conference June 4-6, Tabon Czech Republic.*

Krawezuk, M., Zak, A. and Ostachowicz, W. (1997): Dynamics of cracked composite material structure, *Comput. Mech*., Vol. **20**, pp. 79–83.

Kucuk, M. (2004): An investigation on buckling behaviour of simply supported woven steel reinforced thermoplastic laminated plates with lateral strip delamination, *Journals of Reinforced Plastics and Composites*, Vol. **23**, pp.209-216.

Kutlu, Z. and Chang, F.K. (1992): Modelling compression failure of laminated composites containing multiple through-the-width delaminations, *Journal of Composite Materials*, Vol. **26**, pp. 350-387.

Kwon, Y. W. (1991): Finite element analysis of dynamic instability of layered composite plates using a high-order bendingtheory, *Computer and Structure*, Vol.**38**, pp. 57–62.

Lee, S.Y. (2010): Finite element dynamic stability analysis of laminated composite skew plates containing cutouts based on HSDT, *Composite Science & Technology*, Vol.**70(8)**, pp.1249–1257.

Lee, S., Park, T. and Voyiadjis, G.Z. (2003): Vibration analysis of multidelaminated beams, *Composites, Part B*, Vol.**34**, pp**.** 647-659.

Lee, Sang-Youl , Park, Dae-Yon. (2007): Buckling analysis of laminated composite plates containing delaminations using the enhanced assumed strain solid element, *International Journal of Solids and Structures*, Vol. **44(24)**, pp. 8006-8027.

Liao, C.L. and Cheng, C.R. (1994): Dynamic stability of stiffened laminated composite plates and shells subjected to in-plane pulsating forces, *International Journal of Numerical Methods in Engineering*, Vol. **37**, pp. 4167-83.

Lopes, C.S., Joris Remmers, J.C. and Gürdal, Z. (2008): Influence of porosity on the interlaminar shear strength of fibre-metal Laminates, *Key Engineering Materials,* Vol. **383**, pp. 35-52.

Luo, H. and Hanagud, S. (1996): Delamination modes in composite plates, *Journal of Aerospace Engineering,*Vol. 9, pp. 106-113.

Mohsen, F. and Amin, S. (2010)**:** Analysis of delamination buckling and post buckling of composite structures by generalised differential quadrature method, *International Journal of advanced Engineering Sciences and Technologies*, Vol. **1**, pp. 030 – 037.

Moorthy, J., Reddy, J.N. and Plaut, R.H. (1990): Parametric instability of laminated composite plates with transverse shear deformation, *International Journals of Solids & Structures,* Vol.**26**, pp.801-811.

Nancy, J., Fang, J. and Chou, T.W. (2005): Characterization of interlaminar shear strength of ceramic matrix composites, *Journal of the American Ceramic Society*, Vol.**76(10)**, pp. 2539-2548.

Obdrzalek, V. and Vrbka, J. (2010): Buckling of a plate with multiple delamination, *Engineering Mechanics*, Vol.**17**, pp. 37-47.

Oh, J., Maenghyo, C. and Kim, J.S. (2005): Dynamic analysis of composite plate with multiple delaminations based on higher-order zigzag theory, *International Journal of Solids and Structures*, Vol.**42**, pp. 6122-6140.

Okutan, B. (2002): The effects of geometric parameters on the failure strength for pin loaded multi directional fiberglass epoxy laminates, *Composites, part B*, Vol. **32**, pp. 567-578.

Olsson, R., Donadon, M.V. and Falzon, B.G. (2006): Delamination threshold load for dynamic compact of an plates, *International Journal of solids and Structures*, Vol. **43**, pp.3124-3141.

Ostachowicz, W. and Krawczuk, M. (1994): Dynamic analysis of delaminated composite beam, *Mech. Vibration*., Vol. **3**, pp.107-116.

Othman, A.R. and Barton, D.C. (2008): Failure initiation and propagation characteristics of honeycomb sandwich composites, *Composite Structures*, Vol. **851**, pp. 26-38.

Parhi, P.K., Bhattacharyya, S.K. and Sinha, P.K. (2000): Finite element dynamic analysis of laminated composite plates with multiple delaminations, *Journal of Reinforced Plastics and Composites*, Vol. **19**, pp. 863-882.

Park and Lee. (2009): Parametric instability of delaminated composite spherical shells subjected to in-plane pulsating forces, *Composite Structures*, Vol. **91**, pp. 196–204.

Park, T., Lee, S. and Voyiadjis, G.Z. (2004): Recurrent single delaminated beam model for vibration analysis of multidelaminated beams, *Journal of Engineering Mechanics* Vol. **130**, pp.1072-1082.

Patel, S.V., Datta, P. K. and Sheikh, A.H. (2009): Parametric study on the dynamic instability behavior of laminated composite stiffened plate, *Journal of Engineering Mechanics ASCE,* Vol.**135(11)**, pp.1331–1341.

Pavier, M.J. and Chester, W.T. (1990): Compression failure of carbon fiber reinforced coupons containing central delaminations, *Composites*, Vol.**21**, pp. 23-31.

Pekbey,Y. and Sayman, O. (2006): A numerical and experimental investigation of critical buckling load of rectangular laminated composite plates with strip delamiantion, *Journal of Reinforced Plastics and Composites*, Vol. **25**, pp.685-697.

Pinho, S.T., Davilla, C.G. and Camanho, P.P. (2005): Failure models and criteria for FRP under in-plane or three-dimensional stress states including shear non-linearity, *In NASA Technical Memorandum 213530. National Aeronautics and Space Administration (NASA), USA.*

Piotrowski, G.B. and Lucas, B. (2006): Interlaminar shear strength of a woven E-glass reinforced PMC, *On Board Techonology*, pp.12-15.

Radu, A.G. and Chattopadhyay, A. (2002): Dynamic stability analysis of composite plates including delaminations using a higher order theory and transformation matrix approach, *International Journals of Solids & Structures*, Vol.**39**, pp.1949–1965.

Ramkumar, R.L., Kulkarni, S.V. and Pipes, R.B. (1979): Free vibration frequencies of delaminated beam, *34th Annual Technical Conferences proceedings, Reinforced/Composite Institute, Society of plastic Industry,* Section 22-E, pp**.** 1-5.

Ray, B.C. (2004): Effects of crosshead velocity and sub-zero temperature on mechanical behaviour of hygrothermally conditioned glass fiber reinforced epoxy composite, *Material Sciences & Engineering*, Vol. **379**, pp. 39-44.

Ray, B.C. (2005): Thermal shock and thermal fatigue on delamination of glass-fiber-reinforced polymetric composites, *Journal of Reinforced Plastics and Composites*, Vol. **24(1)**, pp. 111-116.

Roy, T. and Chakraborty, D. (2008): Delamination in FRP laminates with holes under transverse impact, *Materials and Design*, Vol. 29, pp. 124-132.

Ruiz, C. and Xia, Y.R. (1991): The significance of interfaces in impact response of laminated composites, *Composite Material Technology*, 161-166.

Sahu, S.K. and Datta, P.K. (2007): Research Advances in the dynamic stability behaviour of plates and shells, 1987-2005, *Applied Mechanics Reviews, ASME,* Vol.**60**, 65-75.

Sahu, S.K., and Datta, P.K. (2003): Dynamic stability of laminated composite curved panels with cutouts, *Journal of Engineering Mechanics*, ASCE, Vol.**129(11)**, pp.1245-1253.

Sallam, S. and Simitses, G.J. (1985): Delamination buckling and growth of flat cross-ply laminates, *Composite Structures*, Vol. **4**, pp. 361-381**.**

Sancho, J. and Miravete, A. (2006): Design of composite structures including delamination studies, *Composite Structures*, Vol. **26**, pp. 283-290.

Sanders, J.L. (1963): Nonlinear theory of thin shells. *Quarterly Applied Mathematics*, Vol.**21**, 21-36.

Shen, M.H.H. and Grady, J.E. (1992): Free vibrations of delaminated beams, *AIAA Journal*, Vol. **30**, pp.1361-1370.

Shiau, L.C. and Zeng, J.Y. (2010): Free vibration of rectangular plate with delaminations, *Journal of Mechanics*, Vol. **26(1)**, pp. 87-93.

Shu, D. and Della, C.N. (2004): Free vibration analysis of composite beams with two non overlapping delaminations, *International Journal of Mech. Sci.*, Vol. **46**, pp.509-526.

Simitses, G.J. (1987): Instability of dynamically loaded structures, *Applied Mechanics Review*, Vol.**40 (10)**, pp.1403-1408.

Srinivasan, R.S. and Chellapandi, P. (1986): Dynamic stability of rectangular laminated composite plates, *Computer and Structure*, Vol. **24**, pp. 233–238.

Srivastava, A.K.L., Datta, P.K. and Sheikh, A.H. (2003): Dynamic instability of stiffened plates subjected to non-uniformharmonic edge loading, *Journal of Sound and Vibration*, Vol. **262**, pp.1171–1189.

Suemasu, H. (1993): Effects of multiple delaminations on compressive buckling behaviors of composite panels, *Journal of Composite Materials*, Vol. **27**, pp 1172-1192.

Suzuki, K., Kimpara, I. and Kageyama, K. (2004): Non-linear vibration and damping characterization of delaminated composite laminates by using multilayered finite element, *ICAS, 24th International Congress of the Aeronautical Sciences, pp. 1-10.*

Teresa, S.J., Freeman, D.C. and Groves, S.E. (2004): The Effects of through-thickness Compression on the interlaminar shear response of laminated fiber composites, *Journal of composite materials,* Vol. **38**, pp.681-697.

Thornburg, R.P. and Chattopadhyay, A. (2003): Combined delamination and matrix cracking in adaptive composite laminates. *Proceedings of the 44th AIAA/ASME/ASCE/AHS/ASC structures, Structural dynamics and materials conference, Norfolk*,VA,7-10 April, pp.3395-3405.

Tsai, S.W. and Hahn, H.T. (1980): Introduction to composite materials, *Technomic*, Stanford, Connecticut, 1980.

Tsouvalis, N.G. and Garganidis, G.S. (2011): Buckling strength parametric study of composite laminated plates with delaminations, *Ships and Offshore Structure*, Vol. **6**, pp. 93-104.

Tumino, D., Cappello, F. and Rocco, D. (2007): 3D buckling analysis of delaminated composite specimens, *Science and Engineering of Composite Materials*, Vol.**14**, pp. 181-188.

Walter, T.R, Subhash , G., Sankar , B.V. and Yen, C.F. (2010): Monotonic and cyclic short beam shear response of 3D woven composites, *Composites Science and Technology* , Vol.**70**, pp. 2190–2197.

Wang, S. and Dawe, D.J. (2002): Dynamic instability of composite laminated rectangular plate and prismatic plate structures, *Computer Methods & Applied Mechanics Engineering*, Vol.**191**, pp. 1791-1826.

Xu, D., Hoa Suong, V. and Ganesan, R. (2006): Buckling analysis of triaxial woven fabric composite structures, *Composite Structures*, Vol.**72**, pp. 236-253.

Yam, L.H., Wei, Z., Cheng, L. and Wong, W.O. (2004): Numerical analysis of multi-layer composite plates with internal delamination, *Computers and Structures*, vol.**82**, pp. 627-637.

Yamaki, N. and Nagai, K. (1975): Dynamic stability of rectangular plates under periodic compressive forces. Report of the Institute of High Speed Mechanics. Technical report, Tohoku University, Japan.

Yeh, M. and Tung, K. (2006): Dynamic instability of delaminated composite plates under parametric excitation, *Key Engineering Materials*, Vol. **326-328**, pp. 1765-1768.

Yeh, M.K. and Tan, C.M. (1994): Buckling of elliptically delaminated composite plates, *Journal of Composite Materials*, Vol.**28**, pp. 36-52.

Yokoyama, T. and Nakai, K. (2006): Evaluation of interlaminar shear strength of unidirectional carbon/epoxy laminated composites, *J. Phys. IV France*, Vol.**134**, pp. 797-804.

Yuan, W.C., Zhou, L. and Yuan, F.G. (2008): Wave reflection and transmission in composite beams containing semi-infinite delamination, *Journal of Sound and Vibration*, Vol. **313**, pp.676-695.

Zak, A., Krawezuk, M. and Ostachowicz, W. (2001): Vibration of a laminated composite plate with closing delamination, *Journal of International Material Systems and Structures,*Vol. **12**, pp. 545-551.

Zhang, C., Hoa, S.V. and Ganesan, R. (2002): Experimental characterization of interlaminar shear strengths of graphite/epoxy laminated composites, *Journal of Composite Materials*, Vol.**36 (13)**, pp. 1615-1652.

Zhang, Y.T and Fu, Y. B. (2000): A micro mechanical model of woven fabric and its application to the analysis of buckling under uniaxial tension, Part I: The micro mechanical model, *Inernational Journal of Engineering Science*, Vol.**38 (17)**, pp. 1895-1906.

Zhang, Z., Shankar, K., Tahtali, M. and Morozov, E.V. (2010): Vibration modeling of composite laminates with delamination damage, *ICA, 20th International Congress on Acoustics*, pp.1-8.

Zhu, J.F., Gu, Y. and Tong, L. (2005): Formulation of reference surface element and its application in dynamic analysis of delaminated composite beams, *Composite Structures*, Vol.**68**, pp.481-490.

Zor, M. (2003): Delamination width effect on buckling loads of simply supported woven fabric laminated composite plates made of carbon/epoxy, *Journals of Reinforced Plastics and Composites*, Vol. **22**, pp. 1535-1546.

Zor, M., Sen, F. and Toygar, M. E. (2005): An investigation of square delamination effects on buckling behaviour of laminated composite plates with a square hole by using three-dimensional FEM analysis, *Journal of Reinforced Plastics and Composites*, Vol.**24**, pp. 1119-1130.

APPENDIX- I

Multiple delamination modeling

For Single mid-plane delamination and multiple delaminations including the mid plane with different sizes like 0, 6.25%, 25%, 56.25% of the total plate area is considered. The delamination sizes are assumed to increase from the centre of the laminate and can be located anywhere along the thickness of the laminate. In case of three delaminations (multiple delamination), the delamination interfaces are located after 2^{nd}, 4^{th} and 6^{th} ply in a 8 layered laminate. The composite plates with different percentage of delamination, single and multiple delaminations are shown in Figure 8.1 to 8.7.

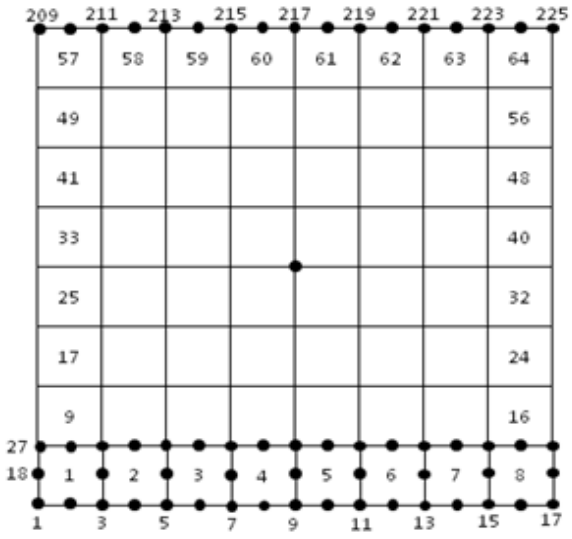

Figure 8.1: 64 Elements, 225 nodes Plate with no delamination

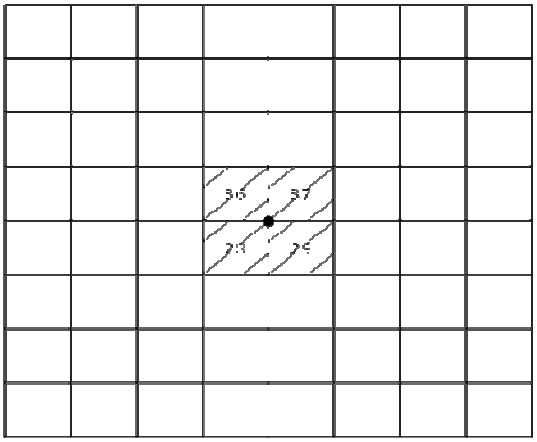

Figure 8.2: 6.25% central delamination

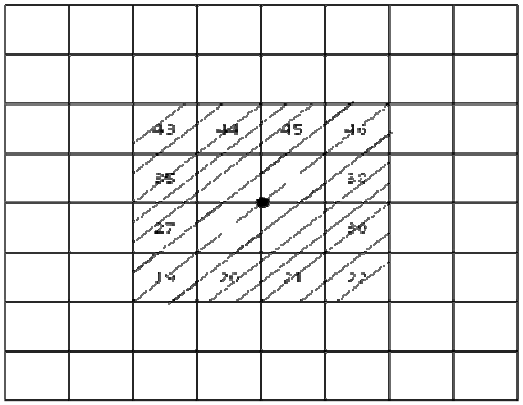

Figure 8.3: 25% central delamination

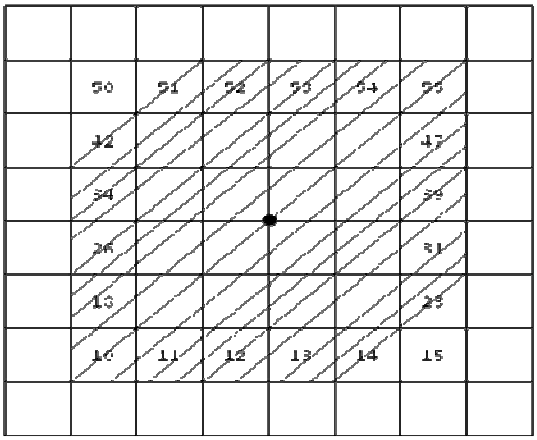

Figure 8.4: 56.25% central delamination

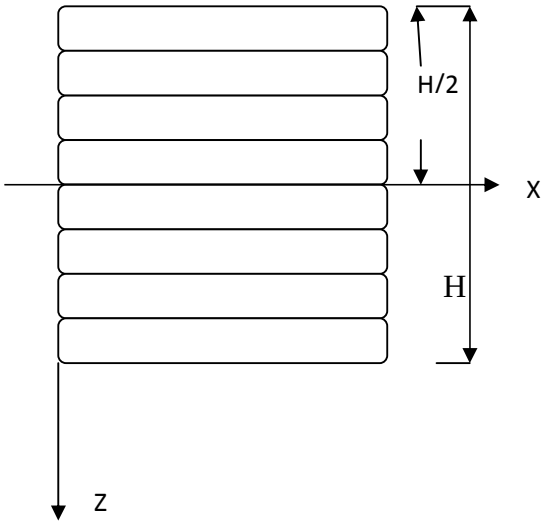

Figure 8.5: Eight layered laminate without delamination

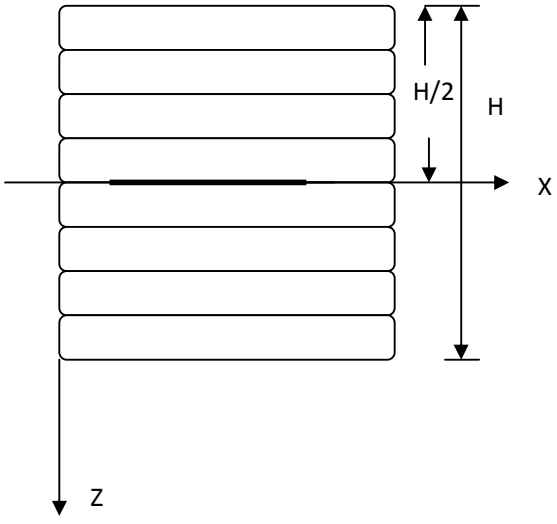

Figure 8.6: Midplane delamination

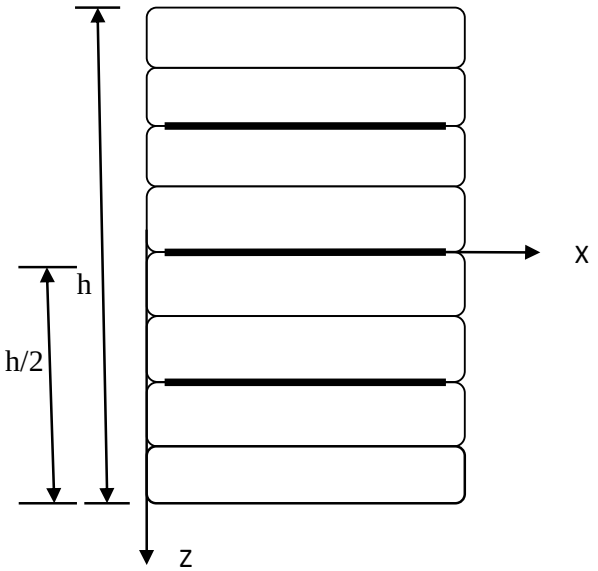

Figure 8.7 Eight layered laminate with three delaminations

APPENDIX- II

Program Features and Flow Charts

For the present analysis, codes are developed in MATLAB environment for vibration, buckling and dynamic stability analysis of delaminated composite panels using the present formulation. The codes consist of a main program and several functions. The finite element procedures involve three basic steps for computation in line with the formulation which may be termed as:

- Preprocessor
- Processor
- Post Processor

The different functions of these steps are elaborated as below.

Preprocessor

This module of the program reads the necessary information about the geometry i.e. length, breadth and thickness of the panels including percentage of delamination, mesh divisions, material properties, boundary conditions, static and dynamic load factors in case of instability analysis. The nodal connectivity is generated out of the dimensions of the panels and mesh divisions by discretization of the structures through automatic mesh generation. This also identify the elements undergone delamination based on the percentage of delamination and the scheme of delamination. The nodal coordinates of each element is generated and each degrees of freedom is identified for imposing boundary conditions.

Processor

This module of the program performs the following tasks:

- Generation of constitutive matrices for both laminated and delaminated elements using the online and offline stiffness of lamina
- Generation of strain displacement matrices from the shape function derivatives

- The element elastic stiffness matrices are generated for both laminated and delaminated elements using both constitutive matrix and strain displacement relations after identification of delaminated elements.
- The element mass matrix is generated using the density parameters and shape function of the element
- Generation of geometric stiffness matrix from the in plane stress distribution using
- All the element elastic stiffness, mass and geometric stiffness are assembled to form global or overall stiffnesses.
- Determination of eigenvalues using inbuilt 'eigen' function in MATLAB i.e natural frequencies, critical load for the vibration and buckling analysis of delaminated composite panels.
- The lowest critical load is taken as a reference load and static and dynamic load as input parameters, the different points of instability regions are computed as a eigenvalue problem as in equation

POST PROCESSOR

In this part of the program, all the input data are echoed to check for their accuracy. The output data is subsequently processed to get the frequency in Hz and also non-dimensionalised wherever desired. The results are stored in a series of output files for each category of problems and these are used to prepare tables and graphs. The flow charts used in this study are presented below.

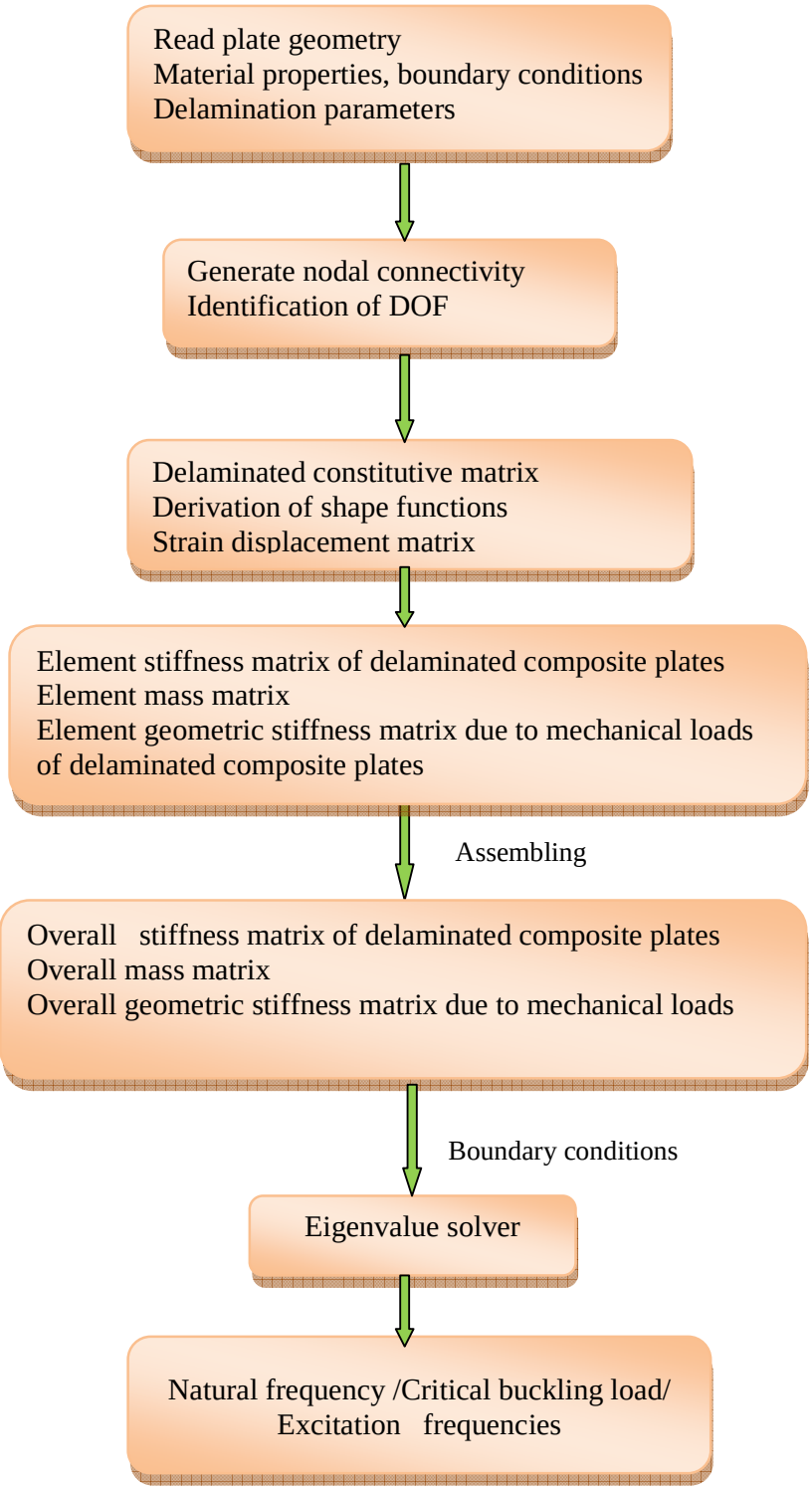

Flow chart of program in MATLAB for instability of delaminated composite plates subjected to in-plane periodic loading